PONTIFICIA UNIVERSIDAD CATOLICA DE CHILE

ESCUELA DE INGENIERIA

SOLAR GEOTHERMAL HYBRID POWER PLANT ANALYSIS

IGNACIO A. MIR FERNANDEZ

Thesis submitted to the Office of Research and Graduate Studies in partial fulfillment of the requirements for the Degree of Master of Science in Engineering.

Advisor:
RODRIGO ESCOBAR

Santiago de Chile, August 2010

PONTIFICIA UNIVERSIDAD CATOLICA DE CHILE
ESCUELA DE INGENIERIA

SOLAR GEOTHERMAL HYBRID POWER PLANT ANALYSIS

IGNACIO A. MIR FERNANDEZ

Members of the Committee:

RODRIGO ESCOBAR

JULIO BERTRAND

JULIO VERGARA

JOHN SELTERS

FERNADO RODRIGUEZ

Thesis submitted to the Office of Research and Graduate Studies in partial fulfillment of the requirements for the Degree of Master of Science in Engineering.

Santiago de Chile, August 2010

A mis papás y hermanos

ACKNOWLEDGMENTS

First I would like to recognize the support and the guidance of my advisor Rodrigo Escobar from Pontificia Universidad Católica de Chile throughout this process. In the same line, I would like to acknowledge the supervision and the assistance of Julio Bertrand from ENAP, who was an external advisor and without his expertise this work could not be done.

I would like to acknowledge the patience and support of my parents and family who encourage me the whole time.

Also, I want to thank the contributions of the members of our office: Teresita, Alberto, Fernando, Cristián, Alan, Sebastien and in particular to my friend Matías.

I would like to formally thank to the Pontificia Universidad Católica de Chile and its administrative personnel for keeping a great program and also to ENAP for support and promote investigation on national key matters.

I am indebted to all the members of the committee for their conscious review and valuable input to this thesis.

I finally want to express my gratitude to all my friends, each in his own way, supported and helped me carry out this project.

TABLE OF CONTENTS

LIST OF FIGURES

LIST OF TABLES

RESUMEN

Esta investigación analiza los distintos aspectos de la generación híbrida de energía eléctrica basada en energía solar y energía geotérmica, y las sinergias que se producen al integrar ambas fuentes de energía, mediante un análisis termodinámico y un análisis económico de esta forma de generación bajo dos estrategias de operación de la planta: 1. Producir el máximo de energía utilizando ambas fuentes de energía, y 2. Utilizar la energía solar para reducir el consumo de recursos geotérmicos manteniendo estable la potencia de salida de la planta.

Se desarrolló un modelo térmico utilizando el *software* EES para un año tipo, en base horaria, utilizando información meteorológica obtenida del *software* Meteonorm y otros datos obtenidos de la literatura. Con los resultados termodinámicos se simuló la operación de la planta durante una vida útil de 30 años mediante el *software* Excel y se obtuvo el desempeño económico realizando supuestos basados en las condiciones de mercado y en las proyecciones entregadas por diversas instituciones.

Los resultados teóricos muestran que se puede aumentar hasta en un 29,9% la energía producida por un pozo geotérmico y se pueden lograr ahorros de hasta un 13.4% en el consumo de recursos geotérmicos. Los resultados del modelo económico muestran un aumento en el valor presente del proyecto para el caso en que se aplica la estrategia de operación 1. Para el caso en que se aplica la estrategia de operación 2, el desempeño económico del proyecto muestra una dependencia frente al comportamiento del reservorio sujeto a permanentes cambios en el flujo másico de extracción. De acuerdo al modelo económico, si se logra disminuir la tasa de decaimiento del reservorio lo suficiente, el proyecto puede aumentar su valor al disminuir la cantidad de pozos de extracción necesarios para su funcionamiento, siendo necesario realizar estudios más profundos en el tema.

De acuerdo con los resultados obtenidos, es recomendable acoplar la energía solar a la energía geotérmica cuando la localización lo permita, aprovechando sinergias y contrapesando debilidades conjuntamente.

ABSTRACT

This research analyzes different aspects of hybrid electric power generation based on solar and geothermal energies, and the synergies that occur when both energy sources are simultaneously exploited. This study is divided in a thermodynamic and economic analysis under two different plan operation strategies: 1. Maximize energy production using both energy sources and 2. Use solar energy to reduce geothermal resources consumption while maintaining stable the power plant output.

The processes that occur within the hybrid plant were modeled and the plant operation computationally simulated for a typical year in hourly basis using weather information obtained from Meteonorm software and other data. The results were used to simulate the operation of the plant in a 30 years life period, to obtain the economic performance under different assumptions based on market conditions and projections.

The results show that the energy produced by a geothermal well can be increased up to 29.9% and achieve savings of up to 13.4% in the use of geothermal resources. The economic results show an increase in the net present value of the project case 1. For case 2, the economical performance of the project depends on the behavior of the reservoir when it is subject to permanent changes in the extraction mass flow rate. According to this economic model the project increase its net present value by reducing the amount of make-up drilling if the decline rate decreases enough. In this sense it is necessary to make further studies on the subject.

According to the results, it's recommended to couple solar energy with geothermal energy wherever possible, to take advantage of synergies and to mitigate weaknesses.

1 Introduction

1.1 The climate change

The global climate system faces a serious crisis with potentially catastrophic consequences. Several studies state with a very high level of confidence that human activity since the beginning of the fossil fuel era with the industrial revolution in 1750, has caused an increase in the world's average temperature. This is due to the emission of greenhouse gases (GHG) into the atmosphere (IPCC, 2009) (Hansen et al, 2006) (Chen & Funke, 2010).

GHG are gases with special characteristics. They are transparent to incoming radiation from the sun, but they absorb and reflect back the infrared (long wave) radiation emitted from the surface of the earth (so when sunlight hits the atmosphere, it passes through without difficulty, but, when the earth warms up and tries to radiate energy back into space as infrared radiation, the GHG barrier in the atmosphere trap this energy and returns it back to the earth). This is the effect generated by the glass or plastic on the roofs of the greenhouses, increasing the temperature inside by keeping the heat inside. The main GHGs are carbon dioxide (CO_2) and methane (CH_4), and nitrous oxides (NO_x). CO_2 is a mayor combustion product. CH_4 and NO_x are of more complex origins.

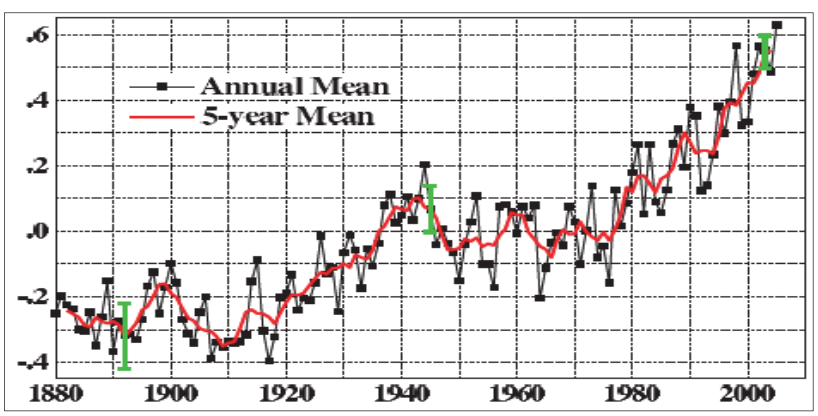

Figure 1.1 Global anual mean anomalies relative to 1951–1980 from surface air measurements at meteorological stations and ship and satellite measurements (Hansen et al, 2006).

The combustion of fossil fuels generates large amounts of CO_2. Fossil fuels are originally confined in underground reservoirs result of the fossilization of organic material over millions of years. However, since the industrial revolution, fossil fuels have been the main source of energy driving society development by enabling benefits of modern life, but the cost we must pay are the consequences of emitting carbon dioxide into the atmosphere.

Most scientist and institutions agree on the anthropogenic origin of climate change (United States National Academy of Sciences, 2008) (Academia Brasiliera de Ciências et al, 2006) (Oreskes, 2004). The largest organization that groups thousands of scientists around the globe is the Intergovernmental Panel on Climate Change (IPCC), It reviews and assesses the most recent scientific, technical and socio-economic information produced worldwide relevant to the understanding of climate change.

The projected trends in the most pessimistic scenarios show an increase in global average temperature up to 6.4 °C by 2100, with devastating consequences for all ecosystems in the world (IPCC, 2009).

The repercussions of this phenomenon include increased sea level, affecting coastal settlements, displacing such population to higher lands, variations in rainfall regimes around the world, weather systems with an increased number of catastrophic weather events such as floods, storms or periods of drought, the ocean currents system will change due to a decrease in the salinity levels caused by the melted ice on the poles, changing the marine habitats and the ability of the ocean to drive climate, periods of floods and droughts more frequent and prolonged, food shortages due to loss of arable land, political conflicts caused by the lack of resources and the people relocation, among many others.

The annual global CO_2 emissions grew by 80% between 1970 and 2004, raising atmospheric concentrations of the major GHG (CO_2, 379 ppm and CH_4, 1774 ppb in

2005) significantly exceeded the natural concentration range of the past 650,000 years (IPCC, 2009).

The atmospheric CO_2 concentration has increased steadily in the past years. Measurements began in 1958 and the atmospheric concentration of this gas have remained above of what is considered a safe level of 350 ppm since 1988 (McGee, 2010). Figure 1.2 shows the atmospheric concentration of CO_2 over the past 50 years.

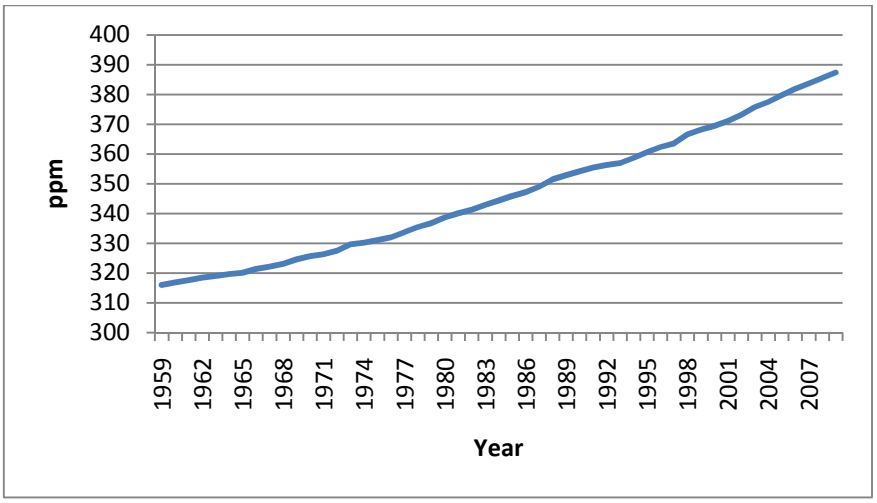

Figure 1.2 Concentration of Atmospheric CO_2 (McGee, 2010)

1.2 World's Energy System and the Energy Revolution

During 2007, the world produced 12.029,27 Mtoe of energy, of which 81.4% came from burning fossil fuels, emanating 28.9 Gton of CO_2. The electricity sector represents 17% of final energy consumption of which 68% is produced from fossil fuels (IEA, 2009).

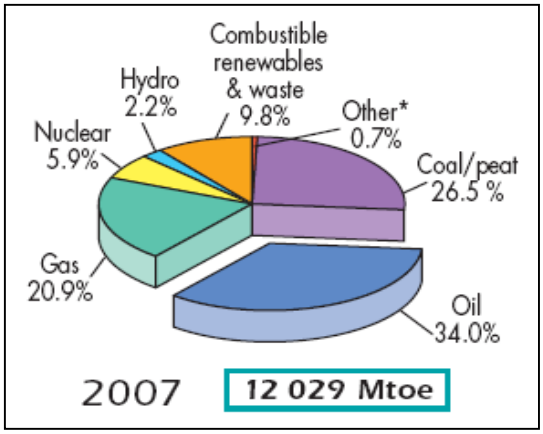

Figure 1.3 2007 World Energy supply shares *other includes geotermal, solar, wind, etc. (IEA, 2009)

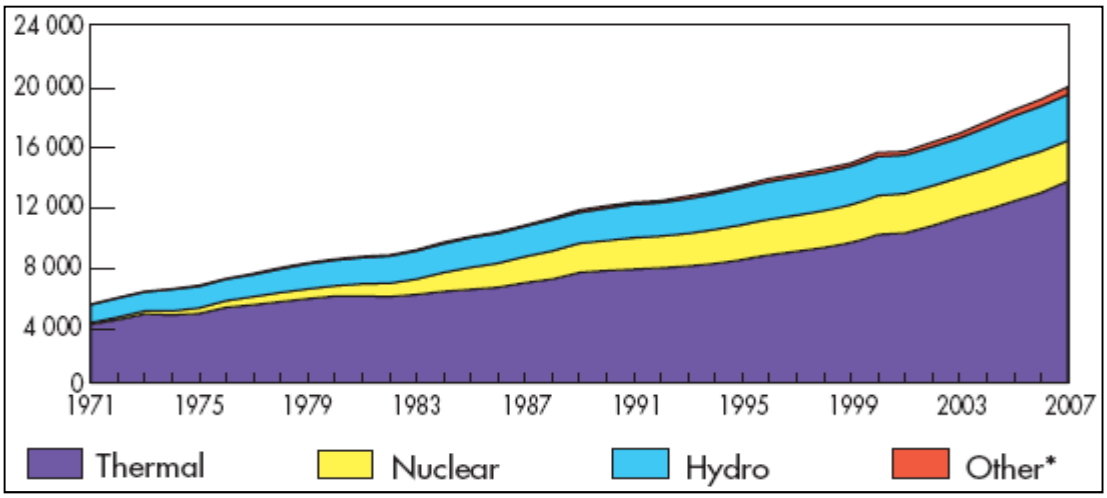

Figure 1.4 Evolution from 1971 to 2007 of world electricity generation by fuel (TWh) *Other includes geothermal, solar, wind, combustible renewables & waste, and heat. (IEA, 2009)

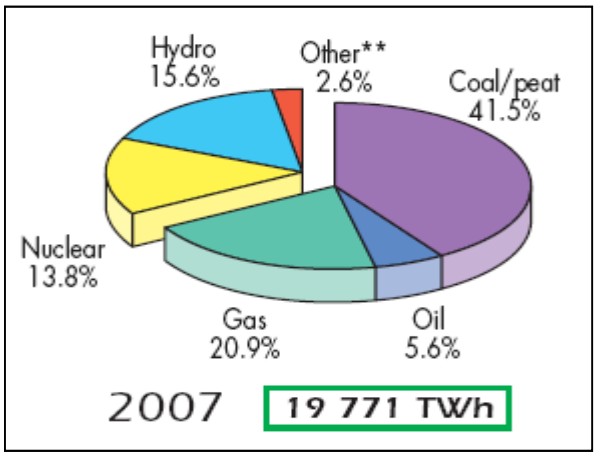

Figure 1.5 2007 Fuel Shares of World Electricity Generation (IEA, 2009)

Most of our energy systems are based on fossil fuels. Our society depends on this abundant and relatively inexpensive source of energy. However, negative consequences for the future of society are evident.

Then, the problem and the causes are assumed to be well defined, but the solution is complex and it requires the participation of all actors involved and a serious commitment to address global climate change.

One way to address the problem of global warming and their consequences is to reduce GHG emissions to the atmosphere. This requires a reduction on the consumption of fossil fuels or the use carbon capture and sequestration techniques, not yet commercially available. A solution based on emission reduction might seem simple, however, it requires attacking the problem from different angles and a *energy revolution* is required reduce reliance on fossil fuels and achieve to transform the global energy architecture into an efficient and environmentally friendly system.

Replacing fossil fuels in the global energy matrix is difficult. There are interest groups, regions that oppose the replacement of fossil fuels because there are their sources of wealth and it requires developing a strong global political action to redefine the energy system.

Currently, there are several alternatives to generate electricity with low GHG emission levels: nuclear energy, hydropower, solar, wind, tidal, geothermal, biomass, among others technologies.

Apparently we have at our disposal plenty of options to substitute fossil fuels, but there are important reasons why such technologies have not been able to compete with and replace fossil power generation. In the case of solar and wind energy, its intermittent nature inevitably makes them dependent on other source of energy to support the production and match the demand. Other technologies, such as wave and tidal are still on an early stage of development and there are no commercial applications to harvest this sources of energy in the short term. The hydropower

technology is a renewable source of energy but requires specific geographic conditions to be exploited and in general, the largest hydraulic resources are already being used to generate electricity. Geothermal energy is similar to hydropower, requires specific conditions to be exploited and in general, the resources available in the world are already being harvested for energy production.

Nuclear power has proven to be a safe, efficient and environmentally friendly as long as nuclear waste is treated responsibly, despite this, remain in the collective memory some accidents happened decades ago, leading to popular rejection of this energy source. Due to the fact that nuclear fuel production technologies is similar to that required for nuclear weapons, fuel production for electric power generation requires safeguards and international monitoring to local national institutions. Moreover, nuclear fuel, under the production cycle scheme that is used at present, is scarce and only allows its use for a limited period of time, so it does not solve the main problem: to create a reliable, efficient and low GHG emissions power supply that is sustainable in the long term.

The overall goal is to reduce the concentration of GHG in the atmosphere and to achieve this, quotas are established and emissions reduction programs based on historical emissions from each country, established on the Kyoto protocol (UNFCCC, 2008), consequently, solutions to reduce emissions should be local and be adapted to the capabilities and resources of each country.

1.3 Energy in Chile

In Chile a large part of the energy mix for electricity production is composed by renewable resources. In 2008, 42% of the electricity produced in the country came from hydropower. However, from the total energy consumed in the country during that year, 71.3% came from fossil fuels, obtained almost entirely from abroad (CNE, Balance Nacional Energético 2008, 2009). This situation places the country in a complex situation from the energy point of view, because not only is intensive in the

use of fossil fuels but also strongly depends on international markets, putting the country in a energy dependence and vulnerability situation, exposed to decisions made by the countries exporting these energy resources. The consequences of this situation have been proven to be shocking, e.g. during the gas crisis in 2007 where many industries where cut off from the gas supply system from Argentina, or the rise in international oil prices hitting hard the Chilean economy in 2008.

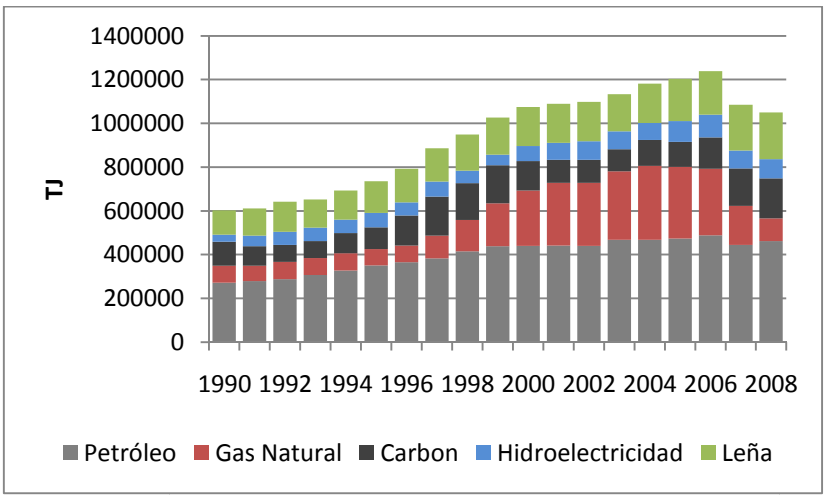

Figure 1.6 2008 Gross Energy Consumption Shares in Chile, Tera Joules (CNE, Balance Nacional Energético 2008, 2009)

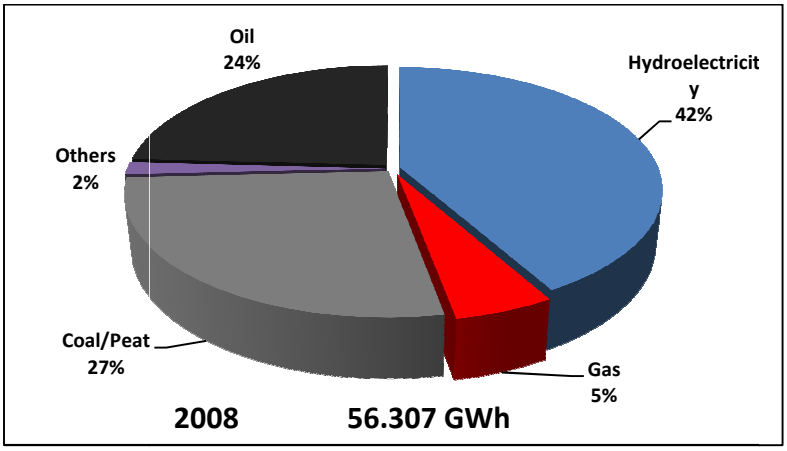

Figure 1.7 2008 Electricity Generation Shares in Chile

Chile does not have an energy policy aimed to reduce GHG emissions; however it is necessary to diversify the national energy matrix in order to use native energy resources to limit dependence on foreign resources.

In this regard there have been some government policies that increase incentives to use renewable energy for electricity generation, besides demanding a share of generation with this type of energy to electricity generators companies (Chilean electric law number 19.940 and 20.018 (Ley Corta I, 2004) (Ley Corta II, 2005)).

Another important change in the energy field that has occurred in Chile in the past few years is the legislation on geothermal resources, providing a clear set of rules where companies and government interact to benefit from this type of energy, abundant in the country but has not been exploited yet.

This new regulatory framework has had an immediate impact on the energy industry, where several national and international companies have expressed interest in participating in the electricity generation market based on geothermal energy. Up to now, some exploration tasks are already being carried out.

From a scientific standpoint, the challenge is huge but inspiring; to find new ways to transform energy sources, using environmentally clean, efficiently and economically viable technologies to lead the energy revolution that we all need.

This paper aims to provide a new form of power generation, more efficient, clean and environment friendly, using the characteristics of solar and geothermal energy to create a hybrid power plant that combines the best of both worlds based the fact that a lot of geothermal concession areas are in the Atacama Desert, the driest in the world, where large amounts of solar radiation are available.

It is therefore necessary to know more about these energy sources, their characteristics and development status.

1.4 Chapter Summary

Global Warming is a fact and the most important institutions around the globe agree that the human activities are responsible for it, specifically the release of huge amounts of GHG into the atmosphere are the driving motor for the climate change and its repercussions could be catastrophic for the human civilization as soon as 100 years from now. The solution is in our hands, to initiate a global energy revolution that changes our energy consumption matrix into an efficient, environmentally friendly and low level of GHG emissions system.

2 Solar and Geothermal Energy

2.1 Introduction

Both Geothermal and solar energy are natural and low GHG emission sources of energy. Although solar energy industry is at an earlier stage of development than geothermal industry, both technologies are economically competitive with other energy sources and have commercial power plants currently operating in several countries. This chapter explains the different technologies used in solar and geothermal industries and their stages of development up to the date of this study.

2.2 Solar Energy

The sun constantly radiates heat as a product of nuclear fusion reactions that occur inside its core. This energy strikes Earth's atmosphere at an average rate of 1367 W/m^2 (Duffie & Beckman, 1980). The amount of solar energy that actually impacts the earth's surface however, depends on atmospheric conditions and geographical position.

There are two main approaches for converting solar radiation into useful energy, photovoltaic technology and thermal technology.

In this investigation, the thermal application of solar energy is employed, using the sun’s radiation as a heat source.

The heat can be used in various ways for different applications, including water heating for household use, cooking, air heating/cooling or to produce electricity.

The production of electricity from solar energy is done in a similar way than on a regular fossil fuel power plant, replacing the boiler by an array of solar collectors or a radiant boiler is used as a heat source through a power cycle. For the transformation of energy to be efficient, it is necessary to reach high temperatures and to do so with a

solar field, different configurations are used to concentrate solar radiation and thus achieve higher temperatures.

Among the solar concentrating technologies, there are three main types of configurations, with advanced levels of development, including pilot power plants: a) parabolic dishes that concentrate solar radiation in the focus point, b) solar towers that use mirrors to concentrate solar radiation in a central point up in a tower and c) parabolic trough concentrators that concentrate solar radiation on a focus line.

Figure 2.1Concentrating Solar Technologies: Up Left: Parabolic Dish. Up Right: Solar Concentrating Tower. Down: Parabolic Trough (Abengoa Solar, 2007)

The hybrid power plant will use a parabolic trough type of solar collectors, because of their highest stage of development, with commercial plants producing electricity in the USA. This creates a competitive market for their components. While the cost of electricity generated by such technologies is still higher than fossil alternatives and it relays in economic incentives to being profitable, its costs are expected to fall about 25% to 5 USD ¢/kWh, by 2020. [Assessment of parabolic trough and tower solar technology cost and performance forecast, NREL, 2003]

The United States and Spain have led the solar technology innovation, with investigation centers and pilot plants that have develop the solar industry to its present stage. The largest solar installation in the world is in the Mojave Desert in California and consists of nine generating units totaling 354 MW of installed capacity using parabolic trough mirrors.

A more detailed description of the operation of parabolic trough concentrating mirrors technology is found in chapter 6.

2.3 Geothermal Energy

Geothermal energy is the energy emanating from the core of the Earth in the form of heat, transported mainly by conduction to the outer layers of the planet. This energy is generated by the nuclear decay of radioactive particles..

The rate at which this energy finally reaches Earth's surface depends on the geological conditions of each location. The Earth’s crust is divided into different plates. In general, is at the junction of these plates, where the underlying magma is closer to Earth's surface, thus providing a shortcut to the energy to reach the surface.

Figure 2.2 shows every volcano location around the world. Volcanoes are the result of the collision between tectonic plates and are a sign that magma is closer to the surface. In this matter and from a geothermal point of view, Chile is privileged, since it is part of what is known as the Pacific Ring of Fire.

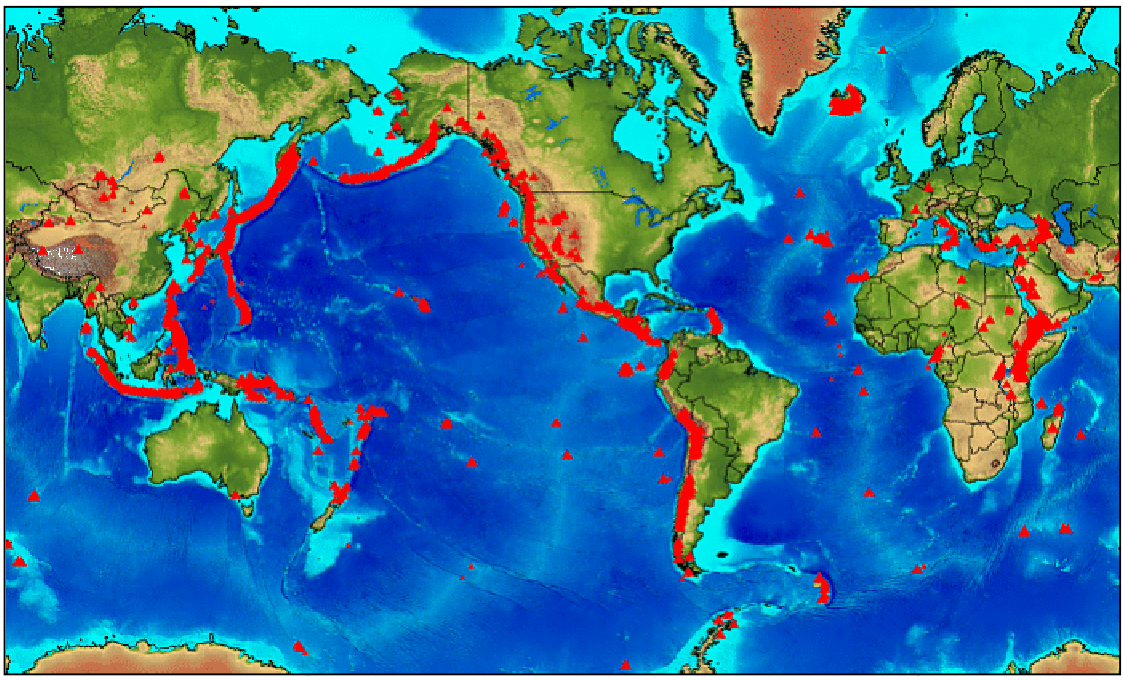

Figure 2.2 World's Volcanoes Map (Smithsonian, 1994)

The Pacific Ring is a horseshoe shaped plates junction line, which contains the greatest number of volcanoes and the largest seismic activity on the planet. This area is formed mainly by all the Pacific Ocean's shores covering several countries. The ring is formed by the subduction line (relative tectonic plate movement in the contact region, Fig 2.3) of several tectonic plates. In Chile it is formed mainly by the subduction of the Nazca plate under the South American plate. This phenomenon, besides forming volcanoes and earthquakes, keeps magmatic bodies near the surface, providing a source of energy.

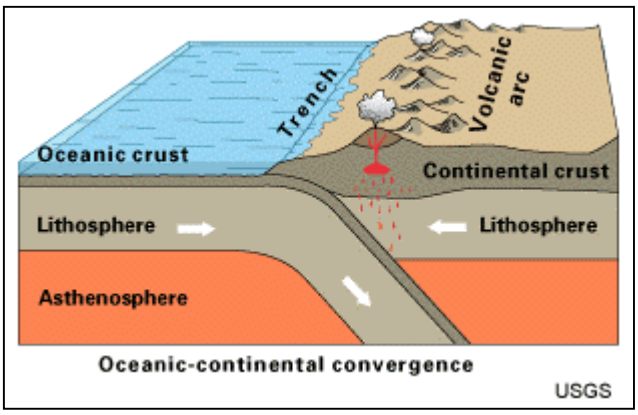

Figure 2.3 Subduction of Tectonic Plates (USGS, 2010)

However, having a magmatic body near to the surface is not a sufficient condition to harness geothermal energy; a driving element is needed to gather and extract heat at a feasible rate. Natural water bodies are used for energy accumulation.

Water from rainfall, snowmelt and underground water travels down the ground through cracks and underground conduits reaching great depths, then, heat from the magma heats the water, in many cases exceeding 300 °C. If the right geological conditions are present, hot pressurized water would be contained in underground reservoirs, made of porous rock surrounded by impermeable rock layers forming natural underground pools, known as geothermal reservoirs (Fig 2.4).

These reservoirs can be found using a set of specific techniques. They often present surface manifestations such as hot springs, fumaroles or geysers. Once a reservoir is found, it is possible to estimate its size and temperature, and then production wells are drilled to extract the steam and hot water, which can be used in various applications, including electricity production and heating.

In geothermal power plants different technologies are used to generate electricity from the geothermal resources depending on temperature and other characteristics of the geo-fluid down at the reservoir. In all cases, the extracted fluids are injected back into the reservoir to maintain its internal pressure. Thus the only emissions from geothermal power plants is the steam emanating from the condensers without

generating any pollution In some cases, the geothermal reservoir contains small amounts of CO_2 and other non condensable gases that are released into the atmosphere or treated according to local regulation, because they cannot be pumped down to the reservoir. These emissions are minimal and in no way comparable to the emissions of a fossil burning power plants.

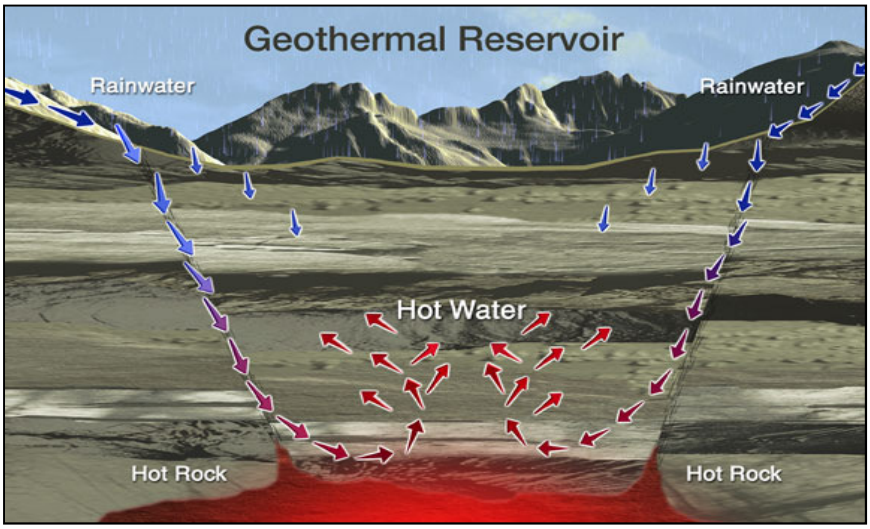

Figure 2.4 Geothermal Reservoir (GEO, 2008)

A distinctive characteristic of geothermal energy is that it provides base load electrical supply, unlike most renewable energy. Another advantage of geothermal energy is its adaptability to any land type, existing geothermal plants installed on the mountains, deserts, forests or in the middle of croplands, without being a threat to its surroundings in any way.

Geothermal energy benefits local economies and reduces fuel imports and dependency on volatile fossil fuels markets. For Chile, this feature is important because it allows diversifying the energy matrix while decreasing reliance on foreign fossil fuels, contributing on the solution of key issues of the Chilean electricity market.

Globally, during the year 2000, 4207 GWh of geothermal energy was used for direct use applications, mostly for heating, while for the year 2005 there were 9064 MW

installed electric power capacity worldwide, producing approximately 67.500 GWh. 2544 MW of the total are installed in USA (IGA, 2009).

According to the Ministry of Mining, geothermal power potential in Chile is 3350 MW (Aravena, 2006), But this source of energy still has not been tapped in the country, mainly because of the high risk associated with exploration and exploitation of this resources and the lack of government policies for the development of the geothermal energy, essential for this industry as one can tell from the international experience.

This situation begun to change in recent years with the creation of the Chilean law number 19.657 on Geothermal Energy Concessions to, where geothermal resources are declared public property and to regulate the exploration and exploitation concessions giving rights and obligations to the awarded companies. Under this new regulatory framework 50 exploration concessions and 7 exploitation concessions have been awarded to different companies up to July, 2010 (SERNAGEOMIN, 2010).

2.4 Geothermal Solar Hybrid Power Plant

There are many advantages and disadvantages in both solar and geothermal energies technologies, some of their disadvantages could be reduced if operated combined, this research explores the benefits of exploiting both energy sources together, based in the fact many of the areas with high geothermal potential in Chile are located in the Atacama Desert, where high levels of solar radiation is available.

At the time of this study there are no geothermal-solar hybrid power plants operating in the world, which is why this study becomes pertinent to evaluate the feasibility whether to develop geothermal resources together with solar energy where they both met jointly.

There have been done studies in Mexico and El Salvador (Lentz & Almaza, 2003) (Handal, Alvarenga, & Recinos, 2008) that examined the possibility of increasing the enthalpy of the geothermal wells using solar energy but in both studies, the solar energy collected was used to generate more steam directly from the geothermal brine, what has two main inconvenient: first, taking out more water from the brine causes more minerals to scale, specially inside the heat exchanger and second, using a high exergy resource such as concentrated solar energy to produce a lower exergy product is a loss of second law efficiency , i.e. using a high temperature resource to produce saturated steam and keeping its temperature on the same level as it was before, represents a loss of an opportunity to improve the power cycle thermal efficiency. These studies present no economic studies in the subject and there are no studies on how to attach a solar field at a geothermal plant. Appendix A discusses different possibilities for coupling these technologies as well as the advantages and disadvantages of this approach.

2.5 Chapter Summary

In this chapter, we reviewed the basic operating principles of the technologies that are involved in the operation of our hybrid plant. We have identified the main indicators of the generation markets worldwide for these technologies providing an idea of the size of the industry and its stage of development.

At this point we have a general idea of the global energy situation, the main problems facing the energy markets and the challenges proposed by the world's energy future. In the next chapters we will look more deeply in to our hybrid plant, both from a thermodynamic and from the operational point of view.

3 Objectives.

The objective in this thesis was to evaluate the thermal and economic performance of a geothermal-solar hybrid power plant in three different scenarios.

Specific Objectives are:

- To analyze different coupling options between these technologies in order to find the best option possible.
- To formulate thermodynamic models that allow interpret the operation of a single flash and double flash geothermal power plant under different operation conditions.
- To develop a thermodynamic model to simulate the operation of a parabolic trough solar field for any climatic condition.
- To hybridize a single flash and double flash geothermal power plant with a parabolic trough solar field and formulate the thermodynamic model that describes its operation.
- To study the operation of the hybrid power plant in order to decrease resource consumption by replacing geothermal energy with solar energy while maintaining constant output power.
- To study the operation of the hybrid power plant increasing the output power from the power plant during the daylight hours using solar power without increasing consumption of geothermal resources.
- To perform an economic evaluation of the models proposed and obtain parameters for comparing the models on a common economic base to determine the advisability of conducting such projects.
- To determine the optimal economic and thermodynamic of geothermal-solar hybrid power plant and analyze their specific applications in Chilean power generation market.

4 Understanding the Geothermal Thermodynamic Process.

4.1 Introduction

This chapter explains the thermodynamic processes that occur in a geothermal cycle, starting with the hot water inlet down at the reservoir and following the cycle up to the power house, where the energy conversion takes place, to finally go down back to the reservoir, explaining all the physical and thermodynamic changes along the way.

The objective of this chapter is to document the basic phenomena involved in a geothermal power plant to operation.

4.2 Reservoir-Geothermal Well System.

The starting point of the geothermal power cycle is the water extraction from the reservoir, which is at high pressure and temperature, assuming liquid water dominated reservoir. As water moves within the reservoir and reaches the intake of the well, it has lost some pressure due to friction through a porous medium, described by Darcy's law. This drop in pressure is a direct function of the velocity of the fluid so by increasing the mass flow from the reservoir, increases the pressure drop from the reservoir to the entrance of the well.

While the water flow moves up through the well, pressure losses occur due to four reasons: a) hydrostatic column drop, b) flux acceleration, c) friction against the well walls and d) singularities such as sudden well diameter changes.

As the mass flow moves up, pressure is reduced. At some point it reaches saturation pressure, evaporating part of the fluid, creating steam bubbles. This point is called Flashing Point.

The distance from the wellhead to the flash point is called flash horizon. The flash horizon lowers as the mass flow rate increases, because the inlet pressure decreases and the flow moves faster increasing pressure losses inside the well, therefore

saturation pressure is reached sooner. For higher mass flow rates or very high reservoir temperatures, the flash horizon can even reach the reservoir. In this study it will be assumed that the flash horizon never reaches the reservoir.

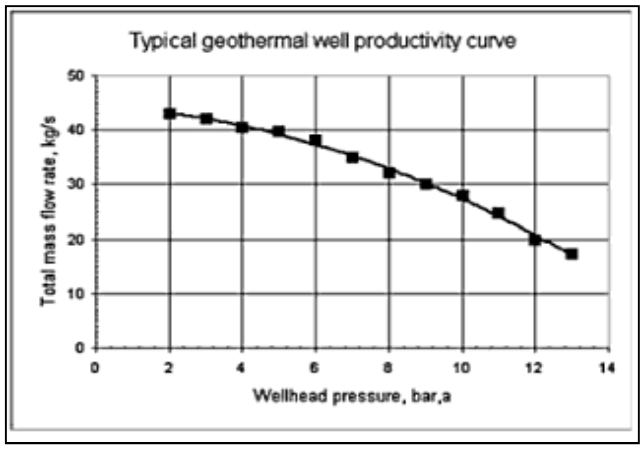

Figure 4.1 Typical Geothermal Productivity Curve (DiPippo, 2008)

Every geothermal well has a production curve, which relates the mass flow extracted to the wellhead outlet pressure. The production curve is the result of the reservoir's local conditions and well's structural characteristics. This curve is finally determined from experimental data.

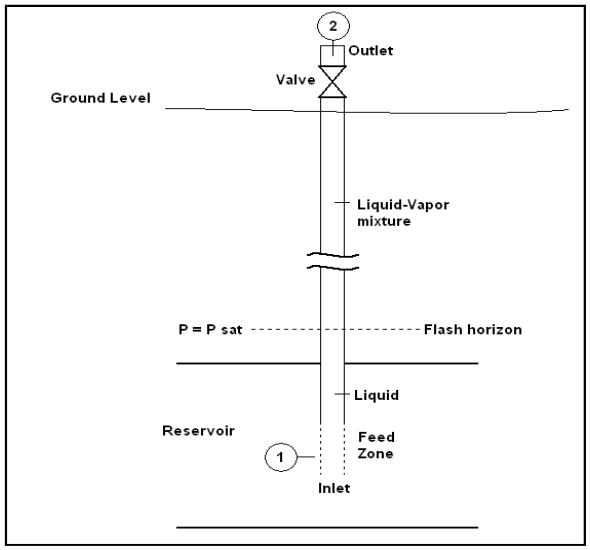

Figure 4.2 Geothermal Well Diagram

4.3 Reservoir enthalpy.

It is assumed, without loosing generality, that water enthalpy at the reservoir depends only on temperature for a wide range of pressure due water incompressibility. According to this, only the reservoir temperature is needed in order to obtain the enthalpy. We can use water thermodynamical properties tables to evaluate enthalpy at any pressure bigger or equal to the water saturation pressure at reservoir temperature, in this analisis, saturation pressure will be used to obtain the enthalpy of the liquid at the reservoir.

$$h_1 = enthalpy\big(Water, T = T_r, P = P_{sat}(T_r)\big) \quad (4.1)$$

Where h_1 represents the enthalpy of the liquid at the reservoir, T_r represents the temperature of the reservoir and $P_{sat}(T_r)$ is the water saturation pressure at reservoir temperature.

4.4 Flashing Process.

The saturated liquid stream partially vaporizes when it undergoes a reduction in pressure, as it moves up the well. This process occurs steadily, because when the liquid vaporizes, the mixture temperature drops due to energy transfer to the vaporized gas particles, lowering the saturation pressure sustaining a thermodynamic equilibrium at a specific depth. As the mixture moves up in the well, the pressure decreases forcing more liquid to evaporate to maintain thermodynamic equilibrium. If we neglect any change in kinetic and potential energy, and assume that the process is adiabatic (no heat exchange between the well and its surroundings), we may describe the process as isenthalpic.

$$h_2 = h_1 \quad (4.2)$$

Where h_2 is the enthalpy of the liquid vapor water mixture at the outlet of the geothermal well.

Numerical simulations of the complete process from the reservoir to the surface, accounting for all physical and thermodynamical effects occurring inside the geothermal well show enthalpy variations close to 3% of the value at the reservoir (Cardemil, 2006). In this thesis we will neglect them for simplicity.

4.5 Gathering System

A typical 30 MW geothermal plant has 5 to 6 production wells and 2 to 3 injection wells (DiPippo, 2008) which may be drilled wide apart from each other to harvest different parts of the reservoir or may be drilled all together using directional drilling techniques. In any case, an adequate gathering system is required to transport the geofluids to the power house. The liquid steam mixture from the wells must be separated in order to be used at the power plant, so a phase separator is needed. A geothermal separator is usually a cylindrical pressure vessel oriented vertically where the phases disengage due to their density difference in density using gravity as driving force. Separators may be located at each well head or could be grouped in a central separator receiving mixture from several wells. In this thesis, pressure loses due to friction and potential energy change occurring on the gathering system will be neglected.

Figure 4.3 Geothermal power plant separator unit in Leon, Nicaragua (UNEP, 2005)

4.6 Separation Process

The separation is modeled as a constant pressure process without energy exchange with the surroundings, i.e., as an isobaric and adiabatic process, hence, the dryness fraction or quality of the mixture entering the separator may be found from the thermodynamic lever rule:

$$x_2 = \frac{h_2 - h_3}{h_4 - h_3} \quad (4.3)$$

Where x_2 is the dryness fraction of the mass flow from the wellhead, h_3 stands for the enthalpy of the saturated liquid at separator pressure and h_4 is the enthalpy of the saturated steam at separator pressure.

4.7 Temperature-entropy Diagram.

A thermodynamic process is usually best viewed in a thermodynamic state diagram where the fluid temperature is shown in the ordinate and the fluid specific entropy is plotted in the abscissa. For pure water, the diagram is separated in three mayor areas, the liquid only area, the steam only area, and the liquid vapor area, the boundary between these areas form a bell shaped line. The temperature-entropy (T-s) diagram for pure water is shown in figure 1.3 where the general flashing process is represented.

4.8 Single Flash Power Plant

The single flash plant is one of the simplest technologies to transform geothermal energy in electricity. Consist in expanding the pressurized steam exiting the separator in a steam turbine to produce work. The turbine axis is connected directly to an electric generator producing electric power.

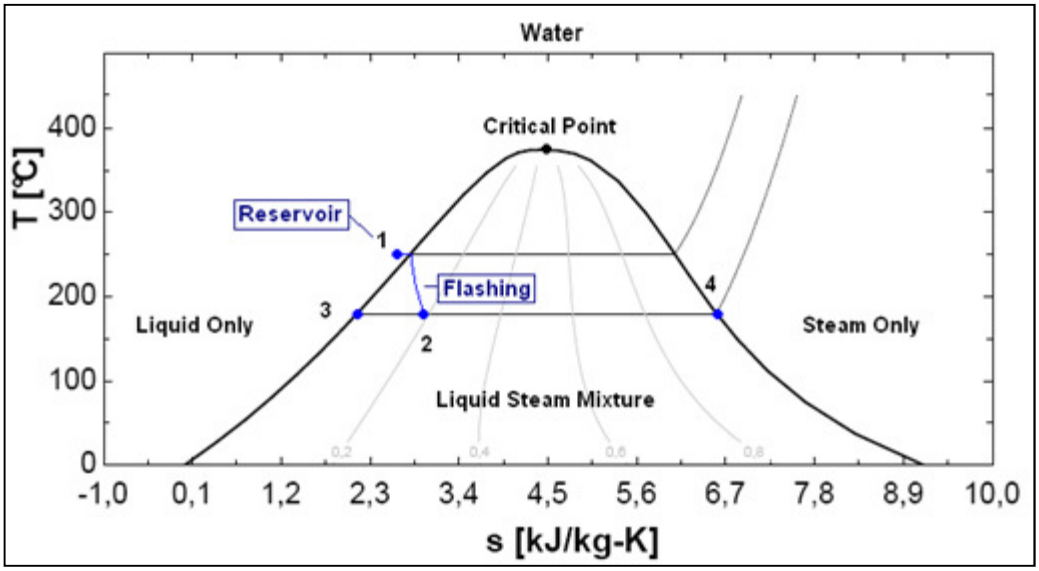

Figure 4.4 T-s Diagram for pure water showing the reservoir and flashing process

The steam stream from the total mass flow from the wells is simply calculated:

$$\dot{m}_{steam} = x_2 \cdot \dot{m}_{total} \quad (4.4)$$

The specific power from the turbine is obtained as:

$$w_t = h_4 - h_5 \quad (4.5)$$

Where h_5 stands for the enthalpy at the turbine outlet.

If we assume an ideal turbine, meaning that no heat is transferred to the environment, the steam expansion would be thermodynamically reversible, i.e. it works adiabatically and isentropically then we will have the ideal work produced by the turbine. Thus, we define the isentropic efficiency as the fraction between the real work produced by the turbine and the ideal work at the same conditions.

$$\eta_t = \frac{h_4 - h_5}{h_4 - h_{5s}} \quad (4.6)$$

Where η_t is the turbine isentropic efficiency and h_{5s} is the isentrópic enthalpy at the turbine outlet.

Figure 4.5 shows a T-s diagram for the entire single flash thermodynamic process.

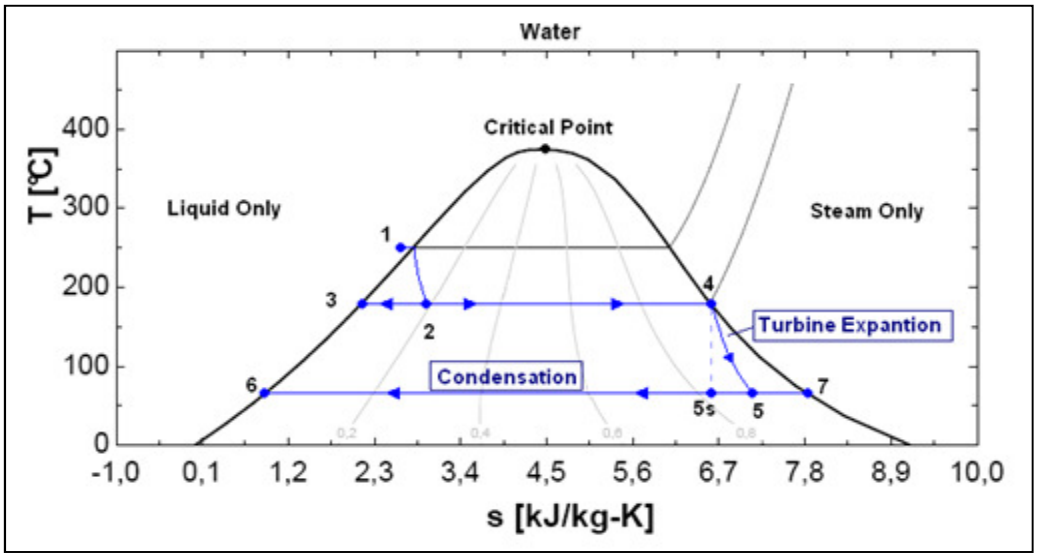

Figure 4.5 T-s Diagram for a Single Flash Power Plant

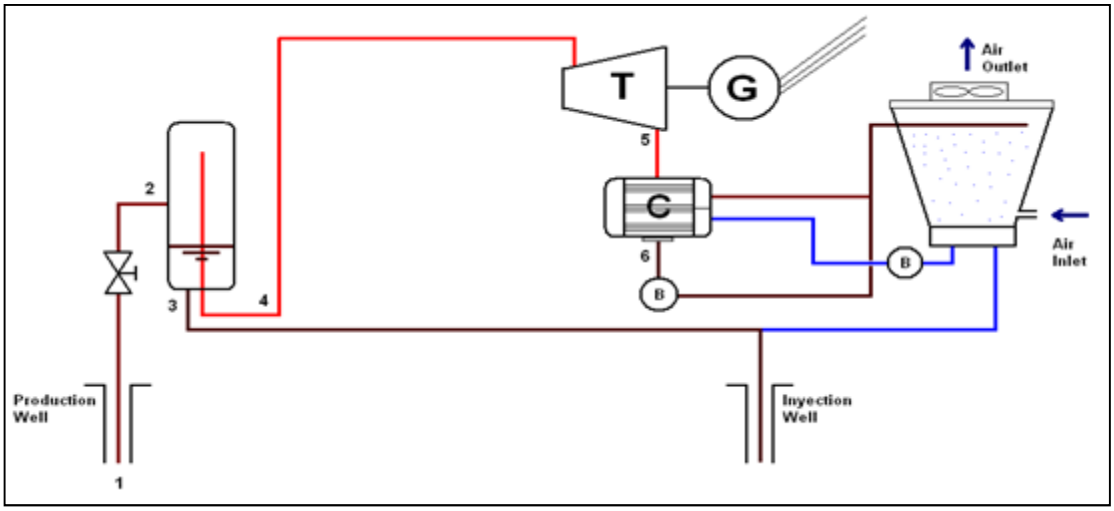

Figure 4.6 Single Flash Plant Diagram.

Numbers in Fig 4.6 match the T-s Diagram. T, C and G stands for Turbine, Condenser and Electric Generator respectively.

Before we can set a value to the isentropic efficiency it must be recognized that the turbine efficiency is affected by the moisture level present in the steam during expansion. The larger the moisture present, the smaller the turbine efficiency would

be. This effect can be quantified using the Baumann rule (Leyzerovich, 2005) which proposes that 1% average moisture causes roughly a 1% drop in turbine efficiency. Adopting the Baumann's rule, the isentropic efficiency is given by:

$$\eta_t = \eta_{td} \cdot \frac{x_4 + x_5}{2} \quad (4.7)$$

Where η_{td} represents the turbine isentropic efficiency working with dry steam. x_4 is the dryness fraction at the turbine inlet, assumed to be equal to one, and x_5 is the dryness fraction at the turbine outlet.

For the purpose of this study the turbine isentropic efficiency for dry steam is assumed to be constant and equal to 85%.

$$\eta_{td} = 0.85 \quad (4.8)$$

Dryness fraction at turbine outlet is calculated using the leverage rule.

$$x_5 = \frac{h_5 - h_6}{h_7 - h_6} \quad (4.9)$$

Where h_6 y h_7 are the enthalpies of saturated liquid and saturated vapor at condenser pressure respectively.

It is clear from figure 4.5 that the dryness fraction at the turbine outlet depends on the isentropic efficiency, so in order to determine the thermodynamic state at point number five it is required to determine the specific work done by the turbine, equations 4.6 to 4.9 must be solved simultaneously.

The mechanical power produced by the turbine is then calculated as:

$$\dot{W}_t = \dot{m}_{steam} \cdot w_t \quad (4.10)$$

The net power results from subtracting the parasitic loads to the energy produced by the turbine. In our calculations we will assume the generator efficiency to be equal to one and the parasitic loads to be negligible to the total power produced.

Thus:

$$\dot{W}_{net} = \dot{W}_t \quad (4.11)$$

Where $\dot{W}_{net}$ is the net power produced by the geothermal power plant.

The heat rejected by the condenser after the expansion at the turbine is calculated as:

$$\dot{Q}_{cond} = \dot{m}_{steam} \cdot (h_5 - h_6) \quad (4.12)$$

4.9 Single Flash Optimization.

From section 4.1, we know that the production curve relates the mass flow produced by a geothermal well with the pressure at the well head. Then the arising question is what outlet pressure should be chosen? There are two approximations to solve this problem; the first one is to maximize the amount of energy extracted from each unit extracted from the reservoir, this procedure is known as maximizing the utilization efficiency. The second approach is to maximize the total output power produced by the power plant.

$$Max\,\{x_2 \cdot (h_4 - h_5)\} \quad (4.13)$$

Equation 4.13 shows the maximization problem to be solved when the objective is to maximize the resource utilization.

$$Max\,\{\dot{m}_{total} \cdot x_2 \cdot (h_5 - h_6)\} \quad (4.14)$$

Equation 4.14 shows the maximization problem to be solved in order to find the operational point that maximizes the plant output power.

In both cases a well head pressure and therefore a total mass flow is obtained as optimal operational conditions.

Without having certain information about the well and the expected reservoir behavior, it is impossible to take a decision about what operation point must be chosen. Therefore, we assume that the reservoir is not going to be depleted and that the well is going to behave stably during the time horizon analyzed. Under these assumptions, it's logical to operate the power plant in order to obtain the most energy out from the reservoir during the exploitation time, so the equation 4.14 will be used to find the optimal operational point. These assumptions are based in general reservoir behavior (DiPippo, 2008).

4.10 Double Flash Power Plant.

Double flash plant technology is an evolution on the single flash technology. Double flash plants can produce up to 20% extra energy out of the same resource compared to a single flash plant (DiPippo, 2008), but this technology is more expensive and complex. Therefore, it is harder to operate and more maintenance is needed.

The wells and gathering system along with the main separators are essentially the same as those used in a single flash power plant. The only difference between the single and double flash technology is that the saturated liquid exiting the separator, reinjected in the single flash technology, is expanded to an intermediate pressure where a second flash evaporation process takes place (number 6 in Fig. 4.7). The liquid gas mixture is then conducted to a new phase separator where the gas phase is incorporated to the main stream in a multiple inlet turbine or could be expanded in a separated low pressure turbine, either way extra power is then produced by the same resource.

Figure 4.7 shows a T-s diagram for a double flash power plant thermodynamic process. Figure 4.8 represents an idealized Diagram of a double flash power plant.

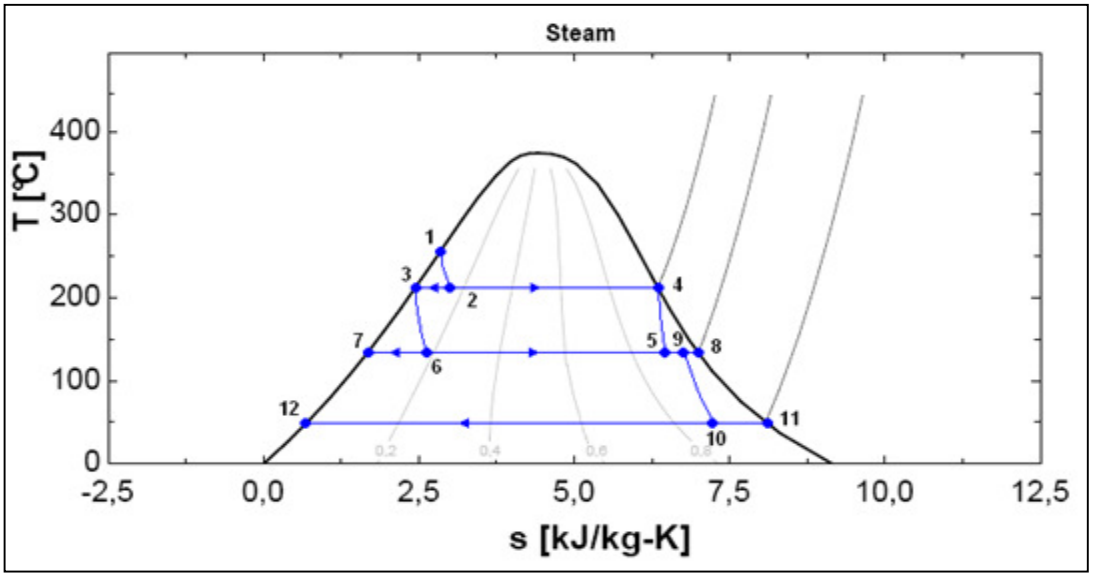

Figure 4.7 T-s Diagram for a Doble Flash Power Plant

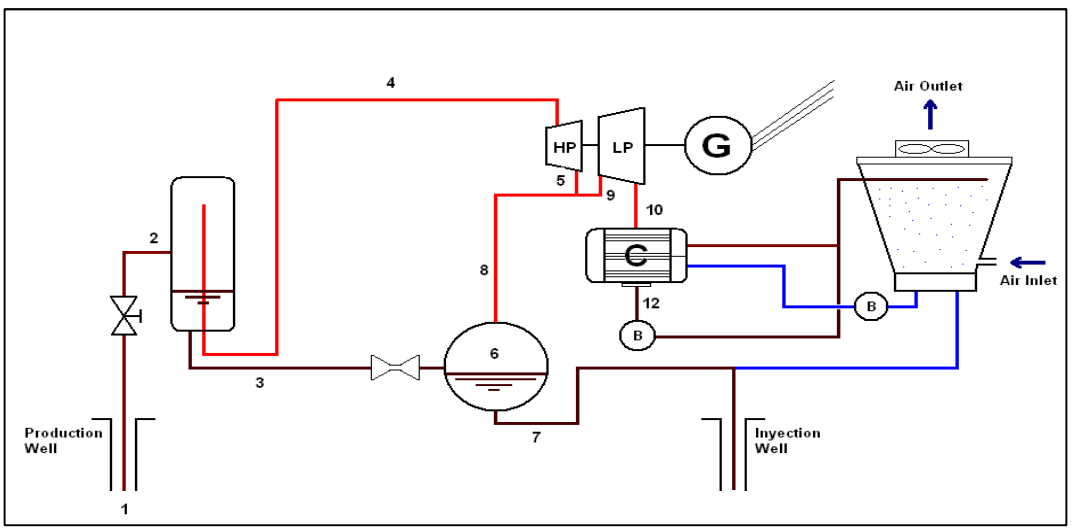

Figure 4.8 Doble Flash Power Plant Diagram

Numbers match Fig 4.7 Diagram. HP, LP, C and G stands for High Pressure Turbine, Low Pressure Turbine, Condenser and Electric Generator Respectively.

To calculate the output power generated by the plant, equations 4.1 to 4.4 must be solved in the same way we did for the single flash plant from the reservoir to the separator. The steam stream exiting the main separator calculated in eq. 4.4 named before as $\dot{m}_{steam}$ will be renamed $\dot{m}_{steam\ 5}$.

The high pressure turbine (HP) power is calculated similarly to the turbine on the single flash plant, consequently, thermodynamic conditions at point 5 are found.

$$w_{HP} = h_4 - h_5 \quad (4.15)$$

$$\eta_{t,HP} = \frac{h_4 - h_5}{h_4 - h_{5s}} \quad (4.16)$$

$$\eta_{t,HP} = \eta_{td,HP} \cdot \frac{x_4 + x_5}{2} \quad (4.17)$$

$$\eta_{td,HP} = 0.85 \quad (4.18)$$

$$x_5 = \frac{h_5 - h_7}{h_8 - h_7} \quad (4.19)$$

Where the pressure in both separators is known. h_3, h_4, h_7, h_8 are calculated directly from steam tables using adequate pressure and saturated liquid or steam condition as appropriate. h_{5s} is easily calculated using point 4 entropy and secondary separator pressure. x_4 is assumed to be 1. With this, the equation system formed by eqs. 4.15 to 4.19 is ready to be solved and thermodynamic conditions at point 5 together with the specific work done by the HP turbine are found.

The second flash process is modeled as adiabatic and isenthalpic due to the fact that happens very fast, with no work involved and no heat transfer to the surroundings. Thus the enthalpy at point 6 is assumed to be the same than point 3.

$$h_6 = h_3 \quad (4.20)$$

Then, to find the steam mass flow exiting the second separator, we need to calculate the dryness fraction after the flash evaporation.

$$x_6 = \frac{h_6 - h_7}{h_8 - h_7} \quad (4.21)$$

Then, the steam mass flow from the second flashing process, in terms of total mass flow is written as

$$\dot{m}_{steam\,6} = (1 - x_2) \cdot x_6 \cdot \dot{m}_{total} \quad (4.22)$$

Following the second flashing process, two different steam streams are mixed together, they have the same pressure but different thermodynamic conditions, on one hand, we have the wet steam coming from the HP turbine defined by point 5 and in the other hand we have the dry steam separated from the second flash process defined by point 8. Mass and energy equilibrium equations are needed in order to find the enthalpy and dryness fraction of the mixture represented by point 9 in the T-s diagram in fig. 4.7.

$$\dot{m}_{steam\,9} = \dot{m}_{steam\,6} + \dot{m}_{steam\,5} \quad (4.23)$$

$$\dot{m}_{steam\,9} \cdot h_9 = \dot{m}_{steam\,6} \cdot h_6 + \dot{m}_{steam\,5} \cdot h_5 \quad (4.24)$$

$$x_9 = \frac{h_9 - h_7}{h_8 - h_7} \quad (4.25)$$

Now we have the thermodynamic properties at the entrance to the low pressure (LP) turbine stage. The same process we did for the HP turbine is repeated to find the specific power generated by the LP turbine.

$$w_{LP} = h_9 - h_{10} \quad (4.26)$$

$$\eta_{t,LP} = \frac{h_9 - h_{10}}{h_9 - h_{10s}} \quad (4.27)$$

$$\eta_{t,LP} = \eta_{td,LP} \cdot \frac{x_9 + x_{10}}{2} \quad (4.28)$$

$$\eta_{td,LP} = 0.85 \quad (4.29)$$

$$x_{10} = \frac{h_{10} - h_{12}}{h_{11} - h_{12}} \quad (4.30)$$

Finally the total power produced by the double flash geothermal power plant is found multiplying the specific work on each turbine by its respective steam mass flow rate.

$$\dot{W}_t = \dot{m}_{steam\,5} \cdot w_{HP} + \dot{m}_{steam\,9} \cdot w_{LP} \quad (4.31)$$

The total heat rejection rate in the condenser is

$$\dot{Q}_{cond} = \dot{m}_{steam\,9} \cdot (h_{10} - h_{12}) \quad (4.32)$$

4.11 Double Flash Optimization

Optimization process for a double flash power plant is more complex than the previous case due to the fact that now we have two degrees of freedom. For each main separator pressure, the pressure in the secondary separator may vary from the condenser pressure to the well head pressure. One can found the pressure in this range that gets the most power out of the resource. Repeating this procedure we end up with a set of pairs of wellhead pressure and its respective optimal second flashing pressure. Among these pairs, there is one that maximizes the output power for the plant.

It is not difficult to program the set of equations that allows us find the total power produced by the plant in terms of each separator's pressure and locate the optimal point of operation using computational tools.

4.12 Chapter Summary

In this chapter all the processes involved in a power cycle based on geothermal energy were covered, we also made some assumptions for the operation of the power plant.

Under the assumptions made, we are able to model the performance of the geothermal component of our hybrid plant for any operational condition. The next chapter explains the solar component of our hybrid power plant to understand and to be able to mathematically model the performance of the solar field that will be attached to the geothermal power plant.

5 Solar Field

5.1 Introduction

The solar field consists in a set of parabolic trough mirrors array that concentrate solar irradiation onto a heat collector element. This collector element is a tube with an external absorber surface. In the inside runs a heat transfer fluid (HTF) carrying the heat absorbed through the solar field into the power house. Figure 5.1 shows a parabolic trough collector Diagram. Figure 5.2 shows a parabolic trough profile.

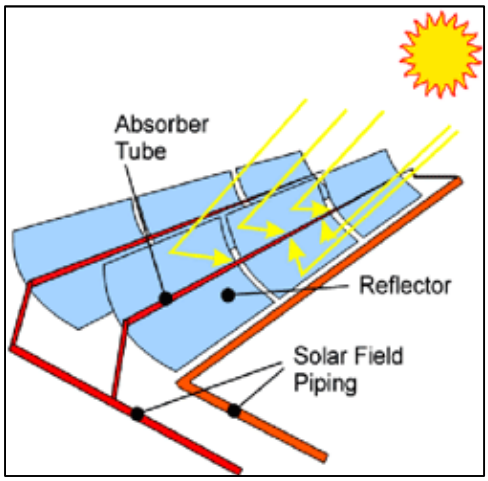

Figure 5.1 Solar Colector Assembly (NREL, National Renewable Energy Laboratory, 2009)

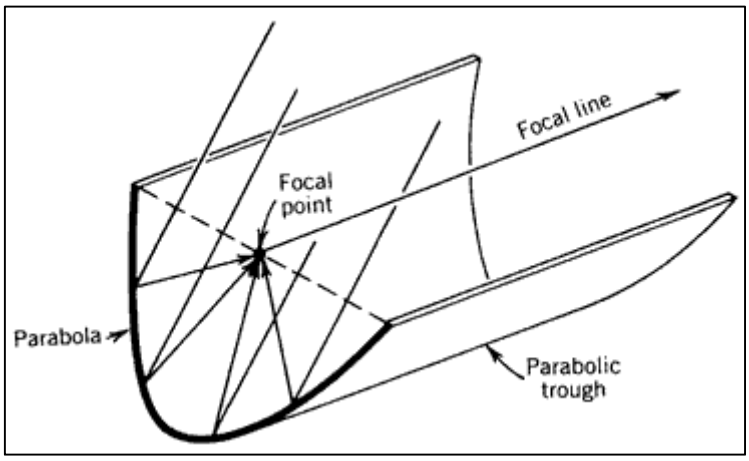

Figure 5.2 Parabolic Trough Profile (Stine & Harrigan, 1985)

Seen from the side, the trough has a parabolic profile allowing all radiation incoming parallel to the parabola axis radiation to be concentrated in the focus line where the receiver is located.

Given this geometric characteristic, the incoming radiation needs to be always parallel to the parabola axis for the system to work. A solar tracking system is needed to keep the mirrors aligned while the sun changes its position in the sky. This type of solar concentrators needs only one axis tracking system, and the solar field can be installed with a north-south or east-west alignment. In this work we will assume a north-south alignment axis and a tracking system rotating at that axis.

5.2 Solar Field Energy Balance

In order to find the HTF thermodynamic conditions exiting the solar field, an energy balance needs to be done across the solar field.

The solar field needs to be discretized in elements of length l, where the temperature can be assumed to remain constant. Once the energy balance is completed for a single element, the new temperature may be established and assigned to the next element.

The rate at which the solar radiation hits on the earth surface is called irradiance and is measured in $[\frac{w}{m^2}]$. The irradiation can be separated into three components, direct radiation,
diffuse radiation and reflected radiation. Direct radiation is the one received straight from the sun. Diffuse radiation is reflected by various particles in the atmosphere and is received from all directions in the sky. Reflected radiation is the one reflected by different objects such as the floor or surrounding buildings before reaching the target. Direct radiation is the only component of the irradiance that is usable by parabolic trough collectors because of the fact that direction of incidence is essential for its operation.

We have the value of direct radiation, I_b, as input for the solar field model on the plane normal to the radiation, in hourly basis for a typical year, so we assume that these values remain constant during each hour of the year.

To obtain the amount of energy incident on the receiving element in a particular section of the field, it is necessary to multiply the density of radiation incident on the parabola aperture plane by the cosine of the radiation angle of incidence on that plane and the length of the element.

$$I_{incident} = I_b \cdot \cos(\theta) \quad (5.1)$$

$I_{incident}$ corresponds to radiation per square meter incident on the trough's plane of aperture and θ represents the angle between the vector normal to the plane of aperture and the incident radiation direction.

To find the incidence angle θ, we need to solve the following set of equations:

$$\delta = 23.45 \cdot \left(360 \cdot \frac{284 + n}{365}\right) \quad (5.2)$$

$$w = 15 \cdot (T - 12) \quad (5.3)$$

$$\cos(\theta) = (\cos^2(\theta_z) + \cos^2(\delta) \cdot \sin^2(w))^{\frac{1}{2}} \quad (5.4)$$

Where θ_z corresponds to solar zenith angle, which is the angle between a vertical line and a straight line to the sun. δ corresponds to the solar declination angle, i.e. the sun deviation from respect to the equatorial plane at noon, being positive towards the northern hemisphere. *w* corresponds to the hour angle, it is assumed that the sun moves 15 degrees to the west every hour due to the rotation of the earth, where zero is the solar noon and it is negative in the morning. T corresponds to the solar time, being the solar noon (T=12) when the sun reaches its highest point in the sky. Finally n corresponds to the day of the year with 1 being the first of January.

Then, the energy rate entering the system, for a single element of the solar field, in any given hour of the year, is given by:

$$\dot{E}_{in} = I_{incident} \cdot A \quad (5.5)$$

$$A = l \cdot Ap \quad (5.6)$$

Where A is the aperture area for the element analyzed, and Ap is the parabola aperture length.

The HTF energy losses within the solar field receiver are due to two main reasons: radiation and convection. The HTF running pipe is isolated from the outside by an exterior glass pipe shell and all the air between these pipes is extracted as shown in Figure 5.3, which prevents energy loss by convection.

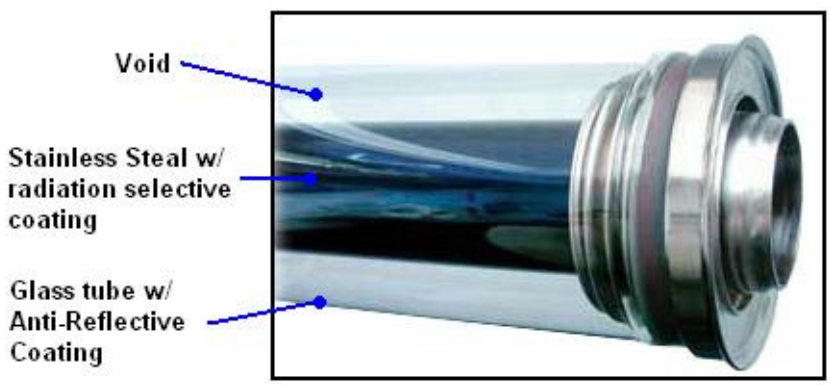

Figure 5.3 Schott Solar Receiver (Schott Solar, 2005)

Radiation losses depend on the temperature difference to the fourth power so that these losses increase rapidly as the temperature of the HFT does. It is difficult to simulate the physics of radiation. In order to accurately describe this phenomenon, information about the characteristics and temperatures not only for the heat emanating surfaces but also for those who receive it is needed, therefore, gathering all that information on a real project application is a difficult task.

To simulate energy losses in the receiver element, a correlation proposed by the National Renewable Energy Laboratory (NREL) from the Department of Energy

(DOE) will be used. The results of a study on the thermal performance of a parabolic trough receiver (NREL, National Renewable Energy Laboratory, 2009) shows that the rate of heat transferred to the environment by the receiver is unique function of its temperature and is possible to relate the heat loss rate of the receiver to the temperature difference between HTF and the ambient.

The NREL study proposes two correlations for two different trough models. These correlations are very similar to each other and in this work the most pessimist one will be used. Equation 6.7 shows the elected correlation.

$$\dot{E}_{out} = 0.41 \cdot \Delta T + 1.21 \cdot 10^{-8} \cdot \Delta T^4 \quad (5.7)$$

Where ΔT represents the temperature difference between the HTF and the surroundings.

Figure 5.4 shows the correlation plotted for a range of temperature difference between the HTF and ambient temperature.

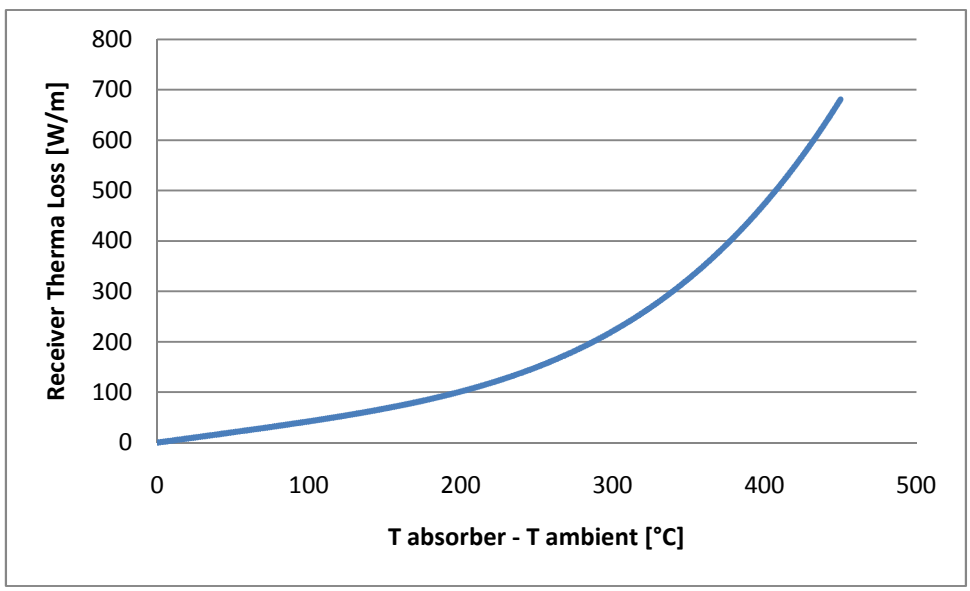

Figure 5.4 Receiver Thermal Loss

5.3 Heat Transfer Fluid

There are many possibilities to choose a heat transfer fluid; mineral oils, synthetic oils, molten salts, pressurized water and antifreeze mixture, water and steam mixture, air, among many others. Therminol VP1 is used in our solar field; it is a synthetic heat transfer oil, which operates in a temperature range of 12 to 400 ° C. This heat transfer fluid is used in the latest solar power plants for electricity generation and shows excellent stability. Despite being flammable, the security requirements and environmental protection requirements are easily satisfied with little effort (Price, Lüpfert, Kearney, Zarza, Cohen, & Gee, 2002).

According to thermal characteristics delivered by the manufacturer, the specific heat for this HTF is given by the following correlation (Therminol, 2009):

$$Cp\ VP1 = 0.002414 \cdot \mathrm{T} + 5.9591 \cdot 10^{-6} \cdot \mathrm{T}^2 - 2.9879 \cdot 10^{-8} \cdot \mathrm{T}^3 + 4.4172 \cdot 10^{-11} \cdot \mathrm{T}^4 + 1.498 \frac{KJ}{Kg°\mathrm{C}} \quad (6.8)$$

The specific heat average value for the working temperature range will be used instead to make calculations faster.

$$Cp\ VP1 = 2.14189 \frac{KJ}{Kg°\mathrm{C}} \quad (6.9)$$

Figure 5.5 shows the correlation delivered by the manufacturer and the average value between 12 and 400 ℃.

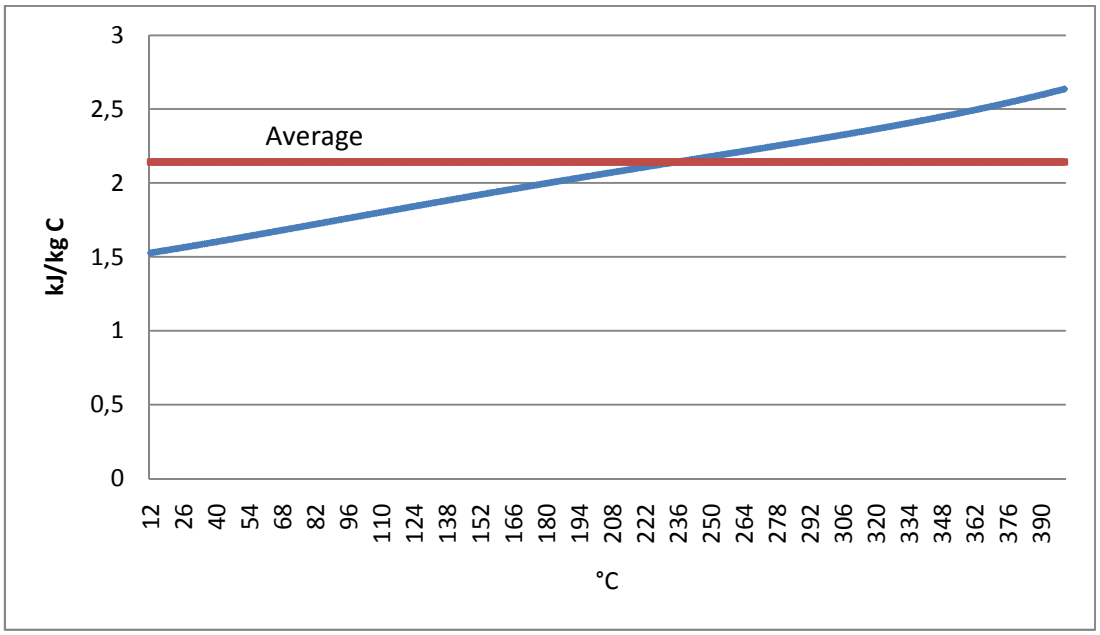

Figure 5.5 Therminol VP1 Specific Heat Correlation and Average

Once the energy balance is calculated for a single element, the HTF outlet temperature can be found using:

$$\dot{E}_{in} - \dot{E}_{out} = (T_{in} - T_{out}) \cdot \dot{m}_{HTF} \cdot Cp\, VP1 \quad (5.10)$$

Both the inlet temperature to the first element and the HTF mass flow will depend on operating conditions and are described further on.

5.4 Heat Exchangers

Once we obtain the HTF outlet temperature at the exit of the solar field, a heat exchanger will be responsible for transferring thermal energy into the appropriate stage in the hybrid power plant.

We will use a counter flow heat transfer model for the heat exchanger with a thermal efficiency of 95%, i.e. 5% of the energy carried by the HTF is lost in the heat exchange process due to inefficiencies.

$$\eta_{HX} = 0.95 \quad (5.11)$$

$$\eta_{HX} \cdot \dot{m}_{HTF} \cdot Cp_{VP1} \cdot (T_d - T_c) = \dot{m}_{AB} \cdot Cp_{AB} \cdot (T_a - T_b) \quad (5.12)$$

Figure 5.6 shows a heat exchanger scheme.

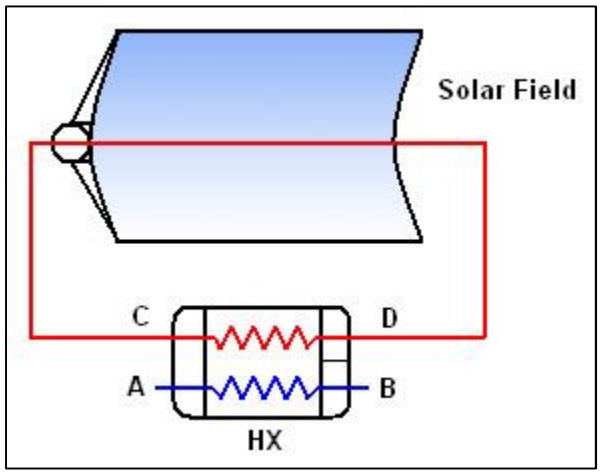

Figure 5.6 Heat Exchanger Scheme

5.5 Solar Field Sizing

So far we have described and analyzed separately all the elements of the geothermal-solar energy system, from the geothermal reservoir to the radiant energy collecting field, including the geothermal power house and solar to steam heat exchangers.

At this point, we need to size the solar field required to couple to the geothermal system in order to fulfill the design criterion. The input is the amount of energy that the solar field must supply to the energy system, which depends on the characteristic of the geothermal thermodynamic cycle that will collect that energy. The amount of energy supplied by the solar field will vary from case to case determined mainly by the maximum temperature that the cycle can achieve. $\dot{E}_{solar}$ will be the thermal power delivered by the solar field in each case analyzed. This implies that the solar field will have to be sized for each case.

Once the size of the solar field is settled, the second step is to define the HTF inlet temperature to the solar filed and its required outlet temperature. The temperature of the HTF leaving the solar field must be the same than the one needed for the steam stream at the exit of the heat exchanger. The inlet HTF temperature to the solar field will be the same temperature of the steam entering the heat exchanger. These temperatures depend on the thermodynamic cycle and will be calculated for each case.

Once we obtain the values of maximum and minimum temperatures for the HTF, the required mass flow rate for the HTF can be calculated using its specific heat.

$$\dot{m}_{HTF} \cdot Cp_{VP1} \cdot \Delta T = \dot{E}_{solar} \quad (5.13)$$

The final parameter to be established before we can size the solar field required in each case is the radiation design value.

Given the daily and seasonal variation of the irradiance, there will be times when the solar field will collect more power than needed and others in that the field will not be able to collect enough power to meet the design criteria.

If a very low design radiation is chosen, we will get a large and expensive solar field that will produce more power than needed most of the time. On the other hand, if a high radiation level is considered as design radiation, we will get a smaller field that would not meet the design criteria.

In this thesis, the following criteria will be used to determine design radiation: radiation will be integrated for each day to obtain daily energy supply for the entire year, then, the closest actual day to the average day will be chosen to represent the average daily solar radiation distribution. The radiation from 11 am to 3 pm will be averaged and this value will be used as the design radiation.

Figure 5.7 plots the day with the maximum energy, the day with the minimum energy and the day that represents the average radiation profile for a typical year in Calama. The design radiation value is also plotted.

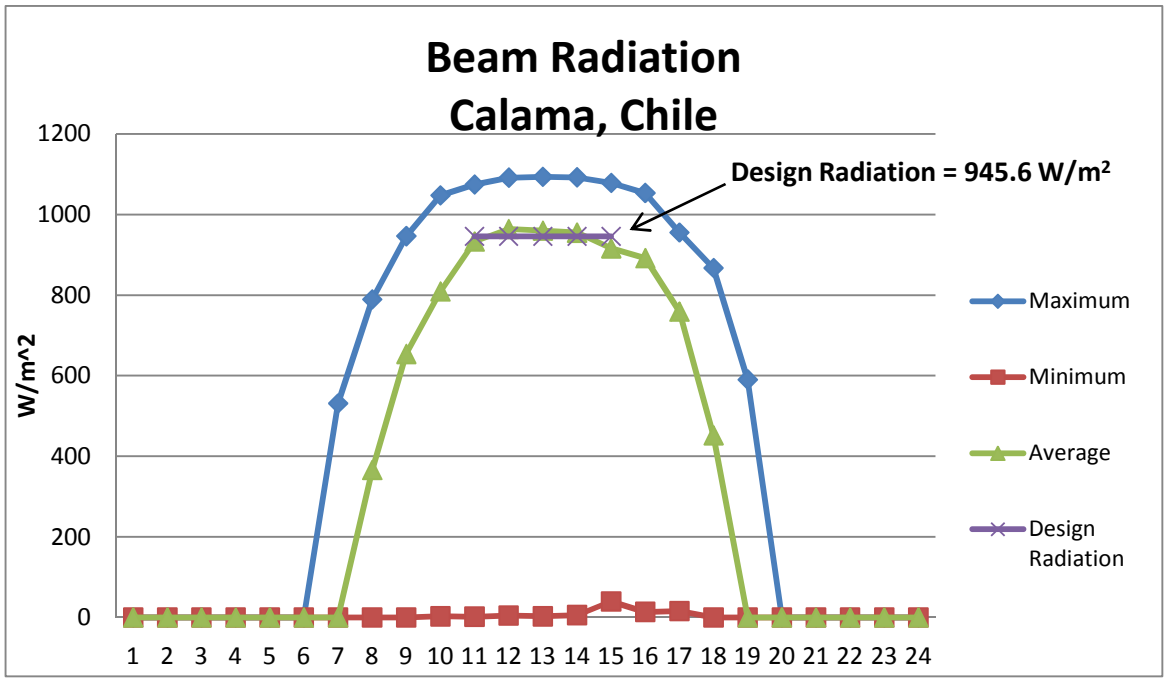

Figure 5.7 Maximum, minimum and average radiation days for typical year in Calama

Finally, with this value we perform an iterative process to determine the length of the solar field, based on the inlet temperature of the HTF and its mass flow rate, we vary the length until we obtain the appropriate outlet temperature, for each case analyzed.

5.6 Simulating the Typical Year

Once the parabolic trough array is dimensioned, we can simulate the operating conditions for each hour of the year. The solar field operates the same for all cases: varying the mass flow rate of the HTF to keep the outlet temperature constant at the design temperature despite the actual radiation value. If the solar radiation in a given hour is higher than the design radiation, then we will have a HTF mass flow rate greater than the nominal value and vice versa.

5.7 Chapter Summary

At this point we have achieved a criterion to size the solar field for each case based on the power required to achieve the design operating conditions and also based on an average value of radiation in accordance with local climatic conditions.

We have also proposed a specific model that describes the energy gains and losses that allow us to forecast the performance of the solar field.

With this information, in addition to the models developed in previous chapters, we are able to simulate the performance of our hybrid power plant, described in the next chapter.

6 Hybrid Power Plant

6.1 Introduction

In this chapter we will integrate all the information discussed in previous chapters to create a single model that describes the processes within the hybrid power plant under certain operational conditions.

We first need to address the fact that the geothermal and the solar fields may have many design arrays, so it is important to define the operation strategies and the different possibilities that we have to attach the solar field to the geothermal power plant, discussed in Appendix A.

6.2 Operational Strategies

There are essentially two strategies that we have proposed for the operation of the hybrid power plant and are the basis of this study.

Strategy N°1 is the one that aims to produce as much energy as possible without altering the basic operation of the geothermal component of the system, i.e. keeping the geothermal optimal mass flow rate from the reservoir fixed.

Strategy N°2 is the one intended to reduce the geothermal resources consumption, lightening the load on the reservoir without compromising energy production. This is achieved by decreasing the geothermal resources outflow and replacing the power output with solar energy whenever it is available.

Strategy N°3 optimizes the operation in order to obtain the maximum possible energy output, allowing the variation of geothermal resources flow rate aiming to the optimization of the energy production efficiency.

Hence, three different operational scenarios aiming different objectives for the hybrid power plants will be reviewed using a single flash geothermal power plant and also a

double flash geothermal power plant making a total of six different cases, plus a base scenario for each single and double flash geothermal power plant for a benchmark.

For all cases we assume that the reservoir is at a constant temperature of 250 ° C.

6.3 Methodology

In each scenario, the operation of the reservoir, the hybrid power plant and the solar filed will be modeled separately and results integrated to obtain final results.

The time horizon for analysis is 30 years of operation after the plant has been built.

The data needed for the simulation are the geothermal well production curve, the solar radiation available and the prevailing climatic conditions at each location.

The mathematical model consists of a single production well connected to the geothermal reservoir. The conditions of pressure and temperature of the reservoir are assumed to be constant for the thermodynamic model.

The production curve of the well will be taken from the literature using a typical production curve (DiPippo, 2008). For the condenser, an ideal pressurized model will be used; assuming that the steam condensates at a temperature of 50 ° C, equivalent to a pressure of 0.01234 MPa, this pressure will be used in all scenarios analyzed.

Solar radiation is obtained using the software Meteonorm (METEONORM, 2009) for the area of Calama, Chile (22° 28‘S, 68° 54’ W) and this information will be assumed to be the same for all years in the time horizon of analysis. This software also provides estimates of the area climatic conditions such as atmospheric temperature, humidity, among others.

Using all these data, a complete year will be modeled for each scenario and the thermodynamic results will then be compared and used as imput for the economic analysis.

The methodology used for economic analysis of all alternatives will be reviewed in Chapter 8.

6.4 Single Flash, Base Scenario

For this scenario, and for all the rest, we will use a single production well with the following productivity curve, shown in figure 6.1.

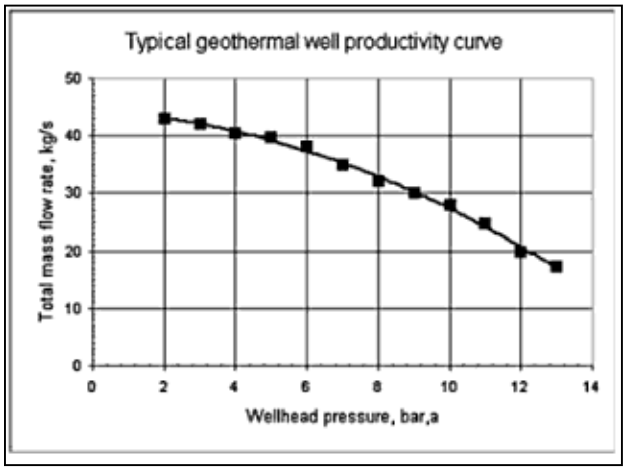

Figure 6.1 Typical geothermal well productivity curve (DiPippo, 2008)

$$\dot{m}_{total} = 44.333 - 0.3363 \cdot P - 0.1357 \cdot P^2 \; [bar] \quad (6.1)$$

Solving equations 4.1 to 4.14 for a geothermal power plant the optimum mass flow rate from the reservoir and the pressure at which the separator operates can be obtained in order to achieve the maximum power output possible. The solution is shown in Table 6.1.

The output power, the total mass flow rate, the separator pressure, the energy produced for a year, assuming a plant factor of 100% (this assumption is made only for operational analysis and will not be considered in the economic evaluation) and the amount of resources extracted during the year are given in table 6.1.

Base Scenario	Single Flash
Optimal mass flow rate	42.22 kg/s
Separator Pressure	0.2897 MPa
Output Power	3974 kW
Produced Energy	**34.81 GWh**
Kg Extracted	**1.331.500 Ton**

Table 6.1 Single Flash Results, Base Case

6.5 Single Flash, Scenario 1.

This scenario aims to increase production of the plant during the daylight hours when electricity demand is higher. To accomplish this, the geothermal well will keep working at its optimum condition. On top of this, solar thermal energy, when available, will be added to increase output power.

The first thing to do is to size the solar field, as discussed in the previous chapter, to obtain the maximum and minimum temperatures from the thermodynamic cycle and the amount of heat that the collector field would contribute.

Figure 6.2 shows a T-s diagram for this case.

$$\dot{E}_{solar} = \frac{\dot{m}_{steam} \cdot (h_{4a} - h_4)}{\eta_{HX}} \quad (6.2)$$

$$T_{4a} = 320.8\,°C \quad (6.3)$$

$$T_4 = 132.4 \quad (6.4)$$

With these data, using the design radiation value and assuming an ambient temperature of 15 °C we get a solar field total aperture area of 4760 m^2. If we assume that the collectors have a 5 meters wide opening, we get a solar field of 952 meters long.

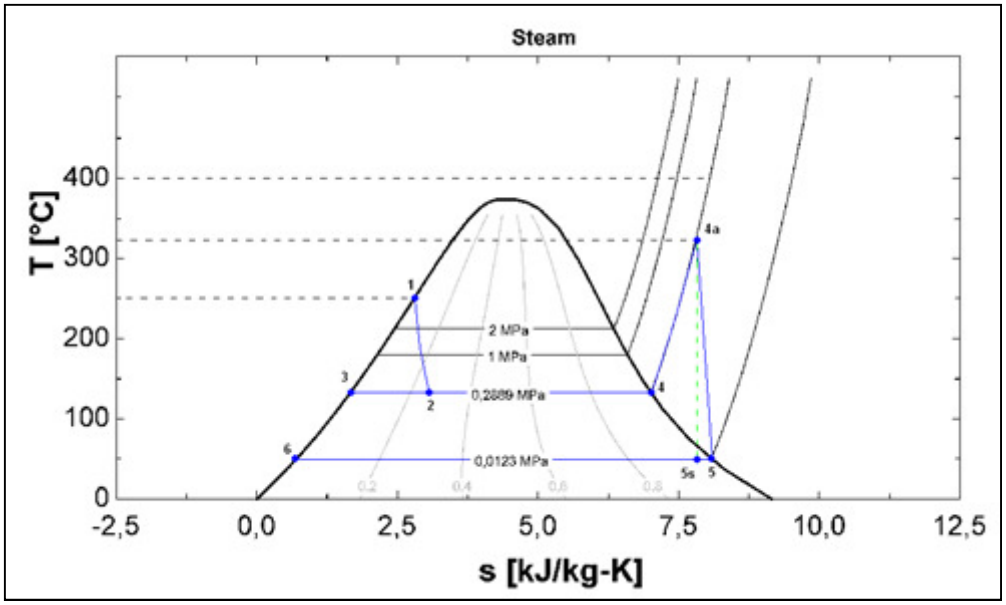

Figure 6.2 Single Flash case 1, T-s Thermodynamic diagram

As we know, certain hours during the year will have more radiation than the design value, some others, less; so certain considerations should be made. If the solar field provides more power than the value it was designed for, and due to the point 4a in the T-s diagram is the highest point to that can be reached regardless of how much solar energy available we have, because it is limited by the turbine's efficiency, the excess will be used to evaporate part of the saturated liquid stream from the main separator and increase the main stream of steam. If the solar energy is not enough, point 4a will fail to achieve its maximum temperature and it will be located somewhere closer to the point 4 to the extreme that when there is no solar power available, point 4 and 4a merge together.

Figure 6.3 shows a hybrid power plant scheme.

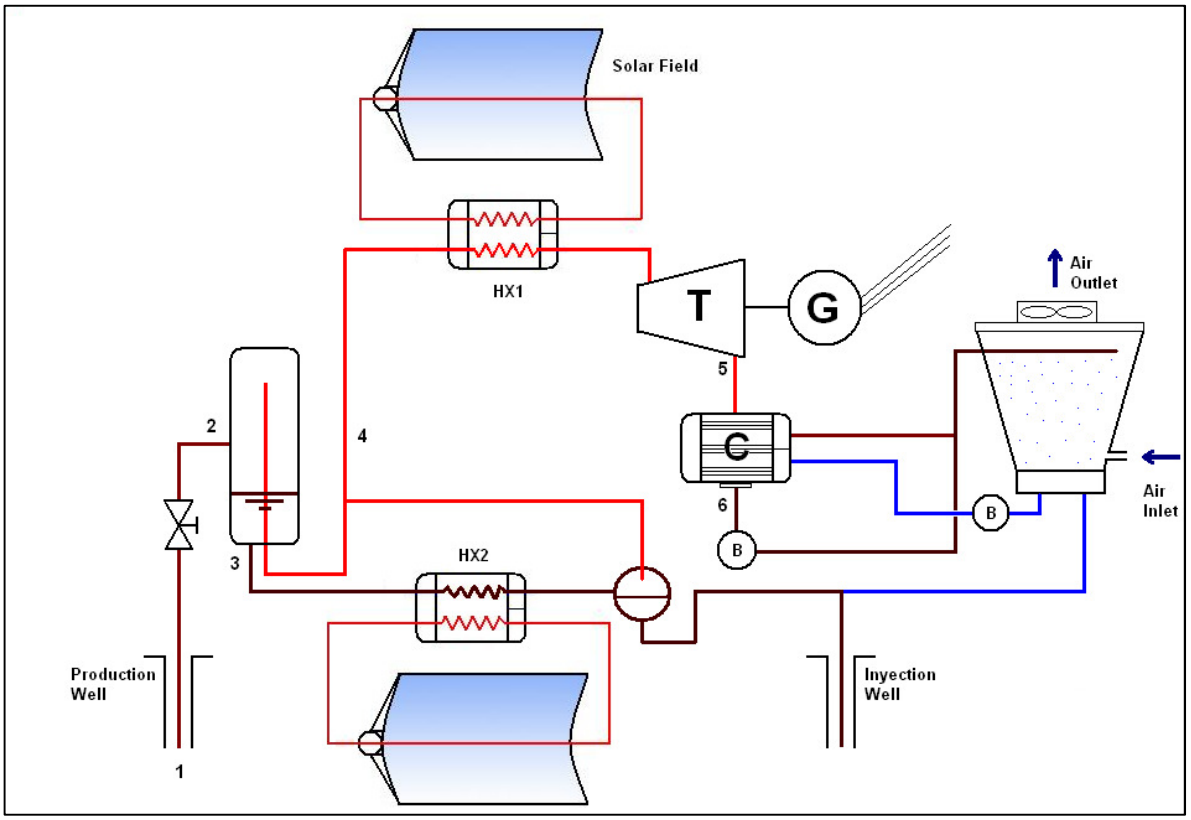

Figure 6.3 Single Flash Plant Diagram, Case 1

When point 4a is below its maximum potential, expansion within the turbine will occur in two stages, the first is an expansion where there is no moisture present, so the turbine efficiency is not affected and remains constant at the value we called η_{td}. And the second stage is where the expansion causes steam condensation affecting the efficiency of the process. To find the specific work done by the turbine we must calculate both stages separately and then add them up.

In order to solve the thermodynamic cycle and to find the hybrid power plant output power, we first calculate the conditions from the reservoir to the main separator.

$$h_1 = enthalpy\big(Water, T = 250, P = P_{sat}(250)\big) \quad (6.5)$$

$$h_2 = h_1 \quad (6.6)$$

$$\dot{m}_{total} = 42.22 \quad (6.7)$$

$$x_2 = \frac{h_2 - h_3}{h_4 - h_3} \quad (6.8)$$

For each heat exchangers, we can calculate the solar power delivered on each of them in any hour of the year following the next rule: if the thermal power available from the solar field is lower than the design value, then

$$HX1 = \dot{E}_{solar} \cdot \eta_{HX} \quad (6.9)$$

$$HX2 = 0 \quad (6.10)$$

Where $\dot{E}_{solar}$ is the thermal power collected trough the solar field in any given hour, η_{HX} is the heat exchange process efficiency, HX1 is the thermal power delivered by HX1 to the main steam between points 4 and 4a and HX2 correspond to the thermal power needed to evaporate the saturated liquid at point 3 in the T-s diagram.

For the opposite case, where the amount of thermal power available from the solar field exceeds design conditions, the thermal power to be delivered to HX1 is equal to the power needed to superheat the main steam flow to move from state 4 to state 4a plus the power needed to take the new steam flow obtained after the HX2, from the state 4 to state 4a. The power required in the HX2 is then determined by solving the following system of equations (eqs.6.11 to 6.13):

$$HX1 + HX2 = \dot{E}_{solar} \cdot \eta_{HX} \quad (6.11)$$

$$HX1 = x_2 \cdot \dot{m}_{total} \cdot (h_{4a} - h_4) + \frac{\dot{E}_{solar} \cdot \eta_{HX} - x_2 \cdot \dot{m}_{total} \cdot (h_{4a} - h_4)}{h_{4a} - h_3} \cdot (h_{4a} - h_4) \quad (6.12)$$

$$HX2 = \frac{\dot{E}_{solar} \cdot \eta_{HX} - x_2 \cdot \dot{m}_{total} \cdot (h_{4a} - h_4)}{h_{4a} - h_3} \cdot (h_4 - h_3) \quad (6.13)$$

The thermodynamic model for the rest of the hybrid power plant is solved using the following equations.

Energy balance in HX2 to find the steam mass flow.

$$(1 - x_2) \cdot \dot{m}_{total} \cdot h_3 + HX2 = (1 - x_2) \cdot \dot{m}_{total} \cdot h_{3a} \quad (6.14)$$

$$x_3 = \frac{h_{3a} - h_3}{h_4 - h_3} \quad (6.15)$$

$$\dot{m}_{steam} = x_2 \cdot \dot{m}_{total} + (1 - x_2) \cdot x_3 \cdot \dot{m}_{total} \quad (6.16)$$

Energy balance for HX1

$$\dot{m}_{steam} \cdot h_4 + HX1 = \dot{m}_{steam} \cdot h_{4a} \quad (6.17)$$

To analyze the turbine expansion, the first thing is to find the pressure at which steam starts condensing when expanded inside the turbine. If the point 4a is the maximum achievable, i.e. the solar power is above the design point, the pressure at which the steam starts to condensate will be equal to the condenser pressure and the efficiency of the expansion process will be maximized.

We will call P_{media} the pressure when condensation starts inside the turbine.

$$h_{4\,media\,S} = enthalpy(Steam, P = P_{media}, s = s_{4a}) \quad (6.18)$$

$$h_{4\,media} = enthalpy(Steam, P = P_{media}, x = 1) \quad (6.19)$$

$$\eta_{td} = \frac{h_{4a} - h_{4\,media}}{h_{4a} - h_{4\,media\,S}} \quad (6.20)$$

Solving simultaneously equations 7.18 to 7.20, where η_{td} and s_{4a} are known, we obtain P_{media} and then we calculate the expansion for the wet stage using Baumann's rule.

$$\eta_t = \frac{h_{4\,media} - h_5}{h_{4\,media} - h_{5s}} \quad (6.21)$$

$$1\eta_t = \eta_{td} \cdot \frac{1 + x_5}{2} \quad (6.22)$$

$$\eta_{td} = 0.85 \quad (6.23)$$

$$x_5 = \frac{h_5 - h_6}{h_7 - h_6} \quad (6.24)$$

$$w = h_{4a} - h_5 \quad (6.25)$$

$$\dot{W}_t = \dot{m}_{steam} \cdot w \quad (6.26)$$

Then, with these relationships we have calculated the power generated by the turbine for any given hour, for any radiation value. This process must be repeated for every single hour of the year using as input the meteorological data of radiation and atmospheric conditions.

6.5.1 Results

Simulating the entire year, in an hourly basis, solving equations 6.1 to 6.26 at each time, the following results are obtained for this scenario.

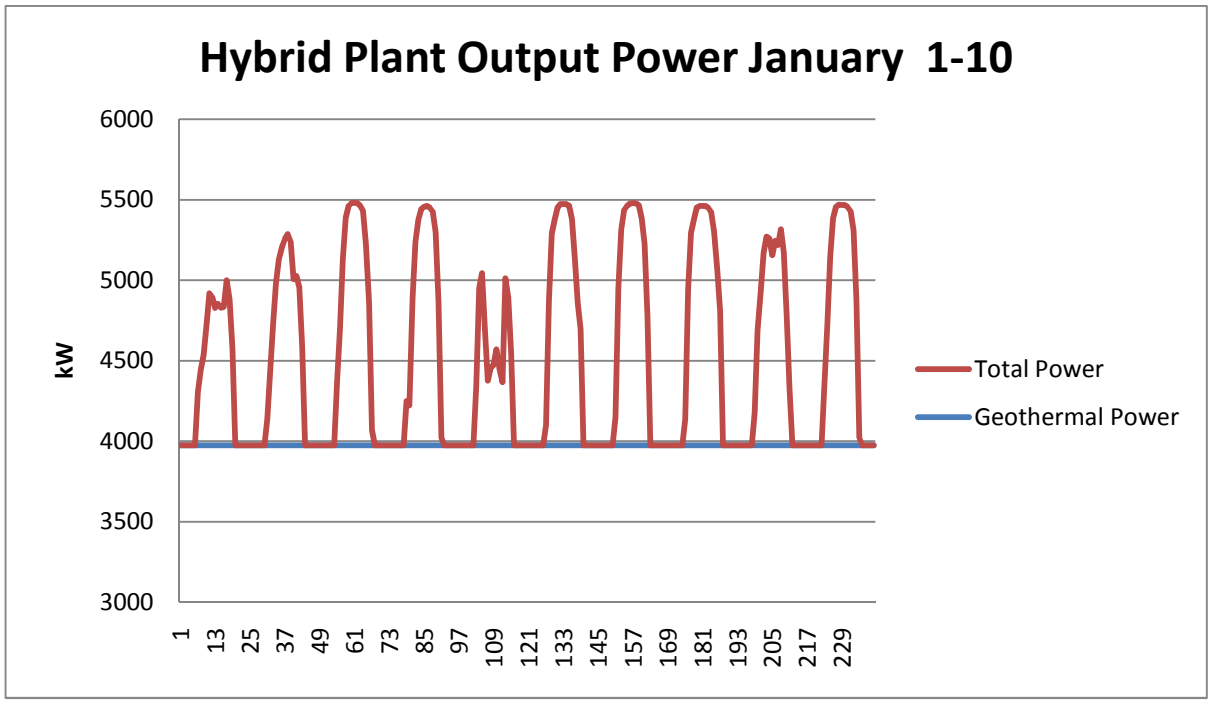

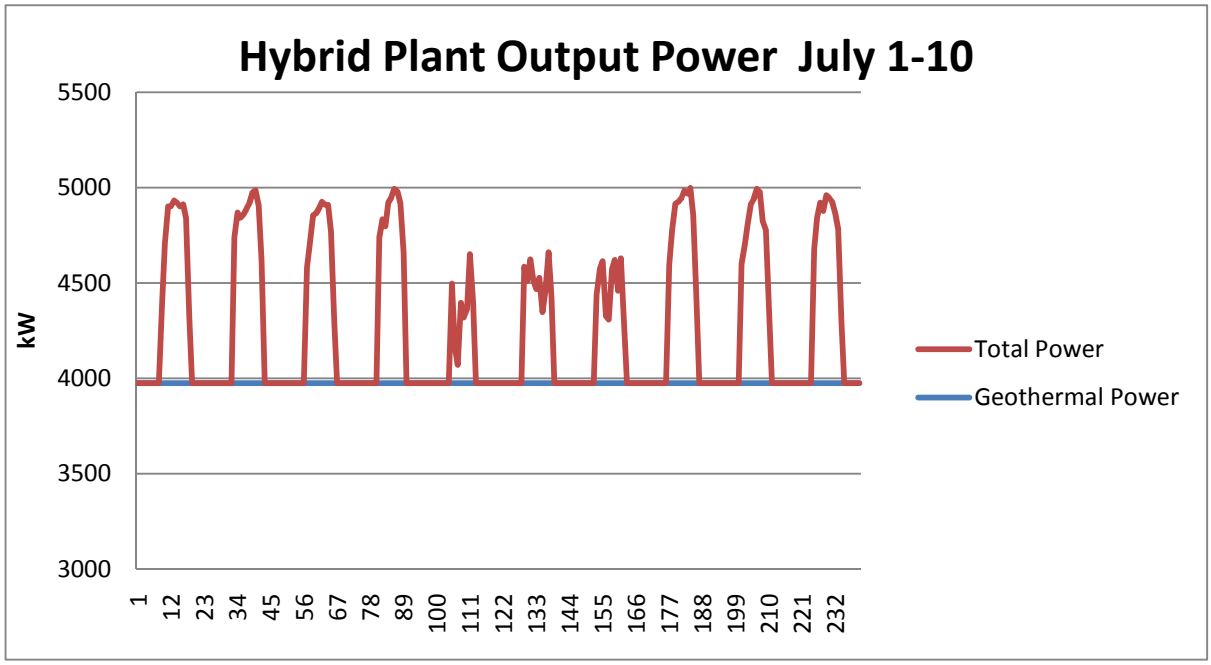

Figure 6.4 Geothermal-Solar Hybrid Power Plant, Single Flash, Case 1 Results

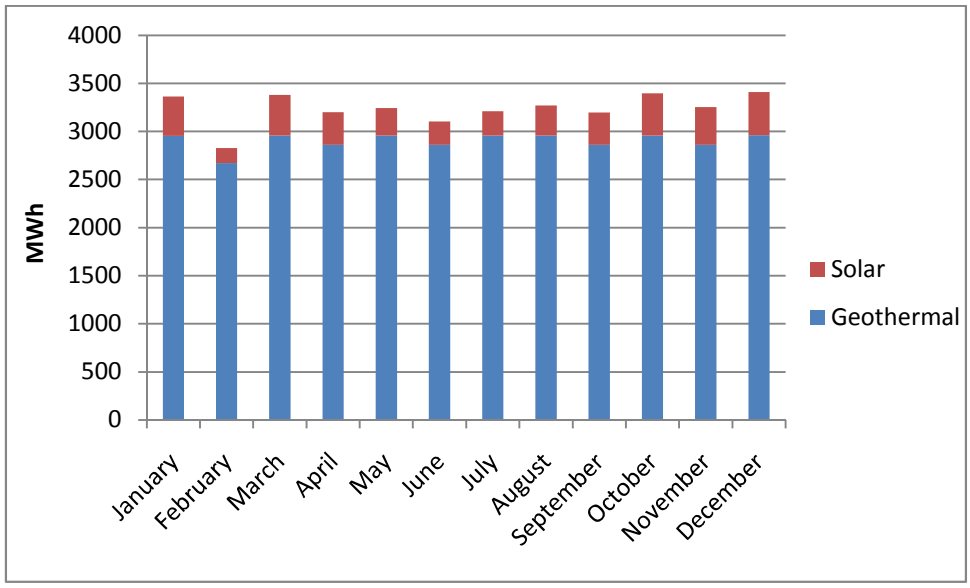

Figure 6.5 Energy Produced Monthly in MWh

The energy generated during the typical year by the geothermal-solar hybrid power plant and the amount of geothermal fluids extracted from the reservoir in this period is detailed in table 6.2.

Energy Produced	**38.85 GWh**
Kg Extracted	**1.331.500 Ton**

Table 6.2 Single Flash, Case 1, Summarized Results

6.6 Single Flash, Scenario 2

The objective of this scenario is to reduce the consumption of the geothermal resource by replacing geothermal energy by solar energy when it is available. The operational basis of this production scheme is to reduce the mass flow of geothermal fluid from the reservoir and use solar energy to compensate for the missing power by keeping the output power equal to the one obtained in the base scenario.

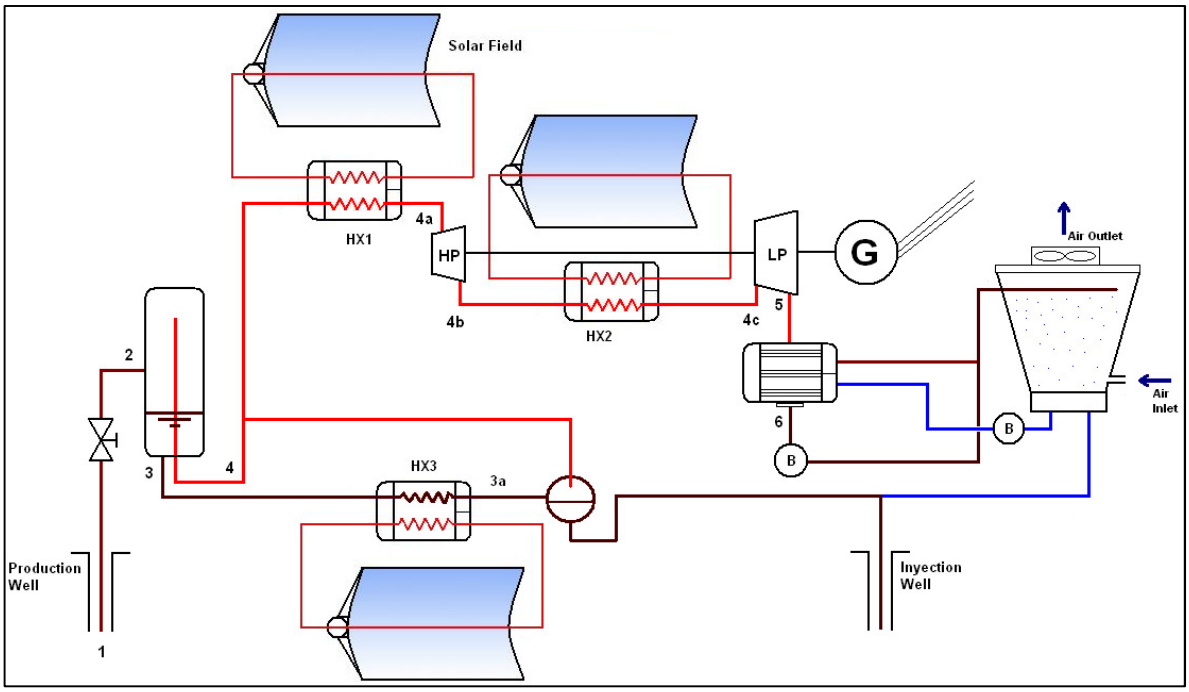

Figure 6.6 Single Flash Plant Scheme, Case 2

In order to find the solar energy needed to size the solar field, we must set the output power of the turbine equal to the base scenario and calculate the geothermal fluid mass flow required, assuming that all the needed solar power is available. For an output power of 3974 kW in the hybrid power plant the minimum flow that we can extract from the geothermal well is 30.25 kg/s at a pressure of 0.9022 MPa according

to the well production curve, yielding 5.1 kg/s of saturated steam in the main steam mass flow. The maximum temperature we may overheat the steam flow is to 400 °C, limited by the HTF working range. This requires a power of 2505 kW in HX1 and then, to reheat the steam again to 400 °C in HX2 533.7 kW are needed according to the nomenclature presented in Figure 6.5. This give as a total solar power needed of 3038 kW.

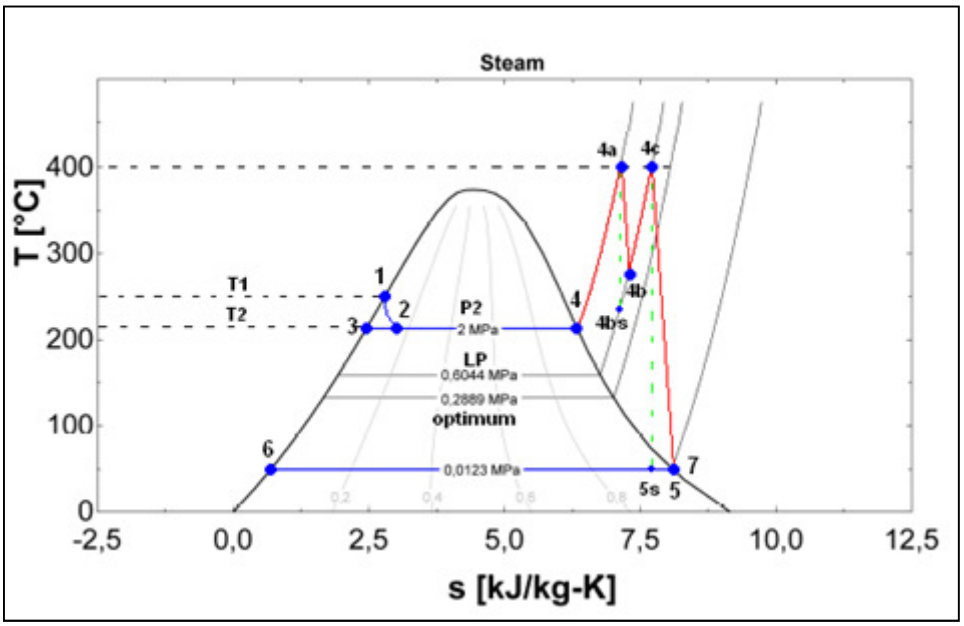

Figure 6.7 Single Flash, Case 2, T-s Thermodynamic Process Diagram

With these data we can easily calculate the size of the solar collector following the methodology outlined in Chapter 5, knowing that the maximum temperature is 400 ° C and the minimum temperature is 175.5 °C.

Note that figure 6.7 shows a well head pressure of 2 MPa, this is only to show the superheating and reheating process and do no match the design conditions.

With these data, we obtain a solar field area of 3685 m^2 of collection area, equivalently to a length of 737 meters assuming an aperture of 5 meters.

To determinate the thermodynamic conditions of the plant for any hour of the typical year, the following procedure were performed.

We perform an iterative process for the geothermal fluid flow rate from the reservoir starting at the optimal point of operation and decreasing its value in each iteration step. Having the geothermal fluid mass flow rate and the available solar thermal power we calculate the power output from the hybrid power plant. The iterative process will stop when the output power approaches the optimum output power found in the base scenario.

For those hours of the year in which there is no solar power available, the process ends in at the first iteration, the heat exchangers do not deliver thermal power and the thermodynamic process is calculated the same way as we did for the base scenario.

As the solar power becomes available, the mass flow rate from the production well is reduced along with an increase in the pressure inside the separator, P2. As long as the pressure of the separator does not exceed 0.6044 MPa, the thermodynamic process, including the distribution of thermal power between the heat exchangers, is solved in the same way described to solve scenario 1, The system only admits one step of overheating due to the turbine isentropic efficiency: if one tries to reheat the steam below this critical pressure, superheated steam will be obtained at the turbine outlet reducing the cycle efficiency.

If solar power collected at the parabolic trough field is enough for the separator pressure to exceed the minimum reheating pressure, then the thermodynamic process is resolved as follows.

It is first necessary to calculate the distribution of power in the heat exchangers.

$$HX1 + HX2 + HX3 = \dot{E}_{solar} \cdot \eta_{HX} \quad (6.27)$$

$$HX1 = x_2 \cdot \dot{m}_{total} \cdot (h_{4a} - h_4) + \frac{\dot{E}_{solar} \cdot \eta_{HX} - x_2 \cdot \dot{m}_{total} \cdot (h_{4a} - h_4 + h_{4c} - h_{4b})}{h_{4a} - h_3 + h_{4c} - h_{4b}} \cdot (h_{4a} - h_4) \quad (6.28)$$

$$HX2 = x_2 \cdot \dot{m}_{total} \cdot (h_{4c} - h_{4b}) + \frac{\dot{E}_{solar} \cdot \eta_{HX} - x_2 \cdot \dot{m}_{total} \cdot (h_{4a} - h_4 + h_{4c} - h_{4b})}{h_{4a} - h_3 + h_{4c} - h_{4b}} \cdot (h_{4c} - h_{4b}) \quad (6.29)$$

$$HX3 = \frac{\dot{E}_{solar} \cdot \eta_{HX} - x_2 \cdot \dot{m}_{total} \cdot (h_{4a} - h_4 + h_{4c} - h_{4b})}{h_{4a} - h_3 + h_{4c} - h_{4b}} \cdot (h_4 - h_3) \quad (6.30)$$

With these values set, we calculate the total power generated by the hybrid power plant and more importantly the mass flow rate flowing from the production well needed to generate this power in combination with the solar thermal power.

There are hours when solar energy is not enough to reheat or even superheat the flow of steam, so it is necessary to analyze the signs of the values of HX1, HX2 and HX3, since they must all be positive. If one value is negative, it means that there is not enough energy to fulfill the design criterions and then, the set of equations represented by Eqs. 6.27 to 6.30 are replaced by the following:

$$HX1 = x_2 \cdot \dot{m}_{total} \cdot (h_{4a} - h_4) \quad (6.31)$$

$$HX2 = \dot{E}_{solar} \cdot \eta_{HX} - x_2 \cdot \dot{m}_{total} \cdot (h_{4a} - h_4) \quad (6.32)$$

$$HX3 = 0 \quad (6.33)$$

If HX2 results negative, then this equation set is replaced by:

$$HX1 = \dot{E}_{solar} \cdot \eta_{HX} \quad (6.34)$$

$$HX2 = 0 \quad (6.35)$$

$$HX3 = 0 \quad (6.36)$$

When these design conditions are met, both at the HP turbine and at the LP turbine, expansion occurs without the presence of moisture and the power at the different stages of the turbine is calculated by solving the required equations for dry expansion. Yet, for many hours, in which actual radiation is lower than the design value, the

power available is not enough to achieve the maximum temperatures and the expansion in both the HP turbine and LP turbine might occur within the saturated zone, decreasing the expansion efficiency. To calculate the power produced in these cases we must follow the procedure using the media pressure and use the Baumann's rule to find the thermodynamic properties.

Solving the equation system, the mass flow rate of geothermal fluid needed to produce the same output power that was achieved in the base scenario is found for every hour of the year.

6.6.1 Results

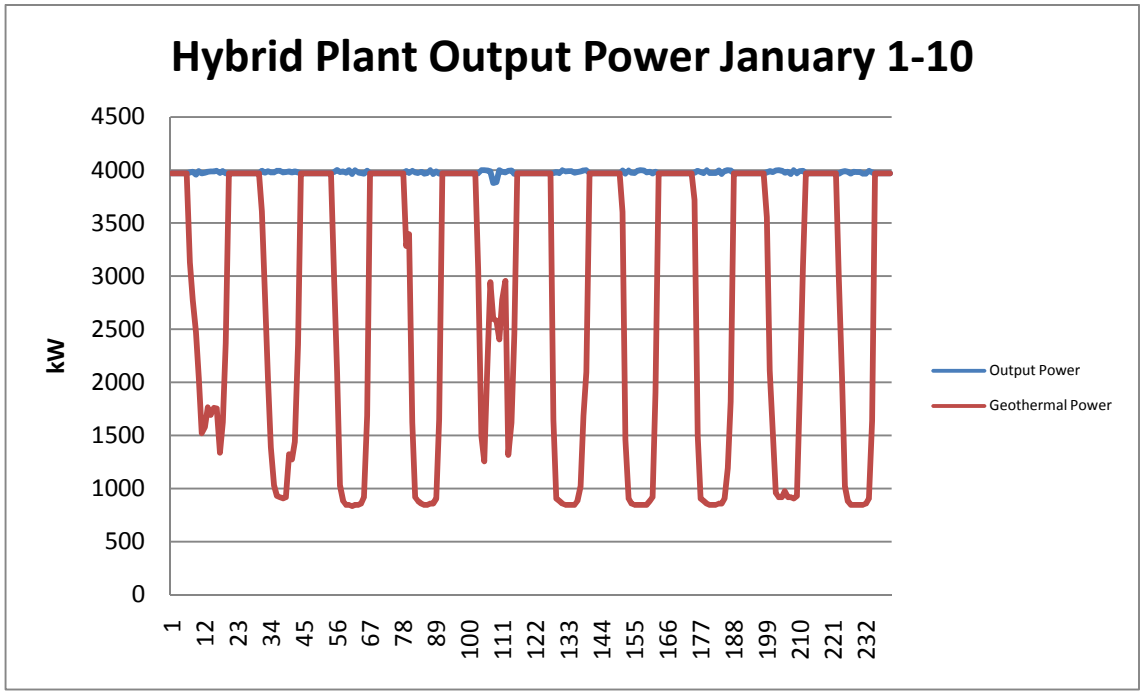

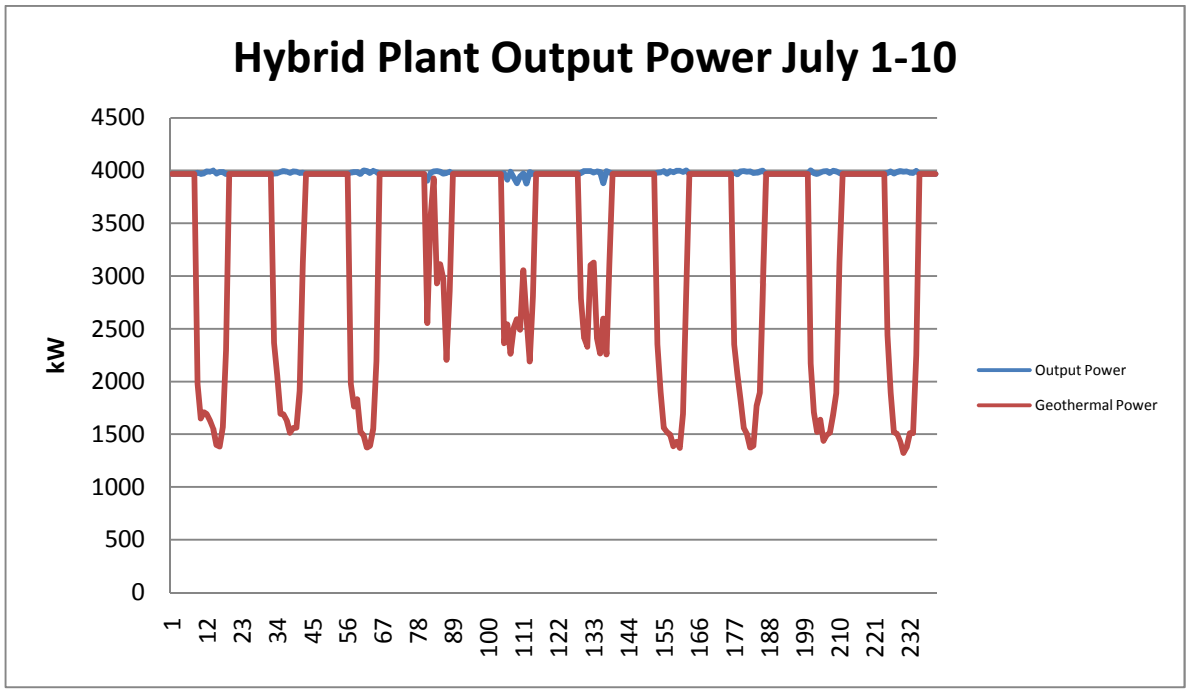

Figure 6.8 Geothermal-Solar Hybrid Power Plant, Single Flash, Scenario 2 Results

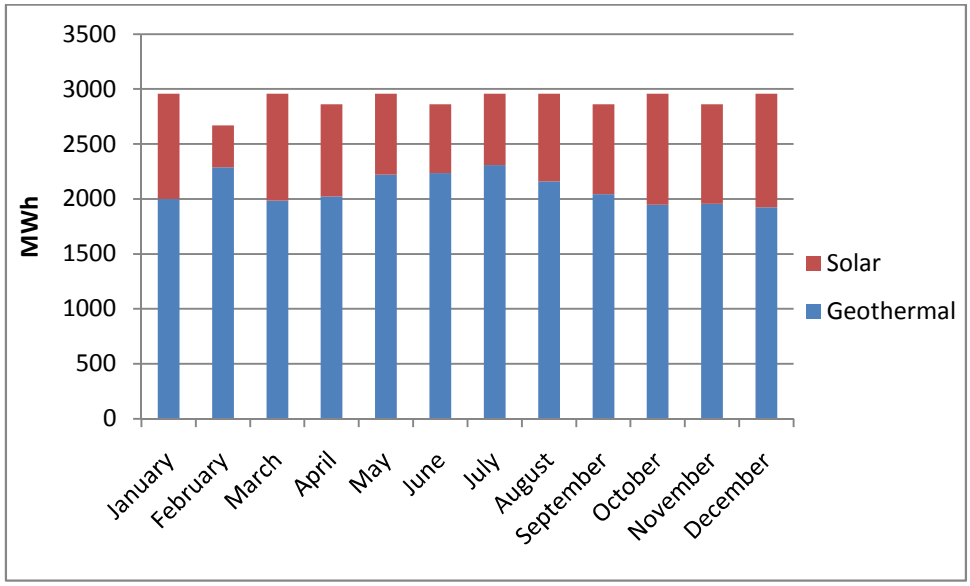

Figure 6.9 Energy Produced Monthly in MW

Energy Produced	34.81 GWh
Kg Extracted	1.193.520 Ton

Table 6.3 Single Flash, Case 2, Summarized Results

6.7 Single Flash, Scenario 3.

Following the same criteria to find the optimum operation point for a geothermal well in, it is possible to perform the exercise for the hybrid power plant assuming that there is enough solar energy available to deliver the maximum power that the power plant needs. Maintaining all the previous restrictions, the HTF temperature in the solar collector field cannot exceed 400 °C and the outlet steam of the turbine must be kept on the edge of the saturated zone at condenser pressure.

Figure 6.10 shows the maximum solar power that can be added to the thermodynamic cycle for different values of total geothermal flow rate and the geothermal power generated in the absence of solar energy. It also plots the total power generated by the hybrid power plant.

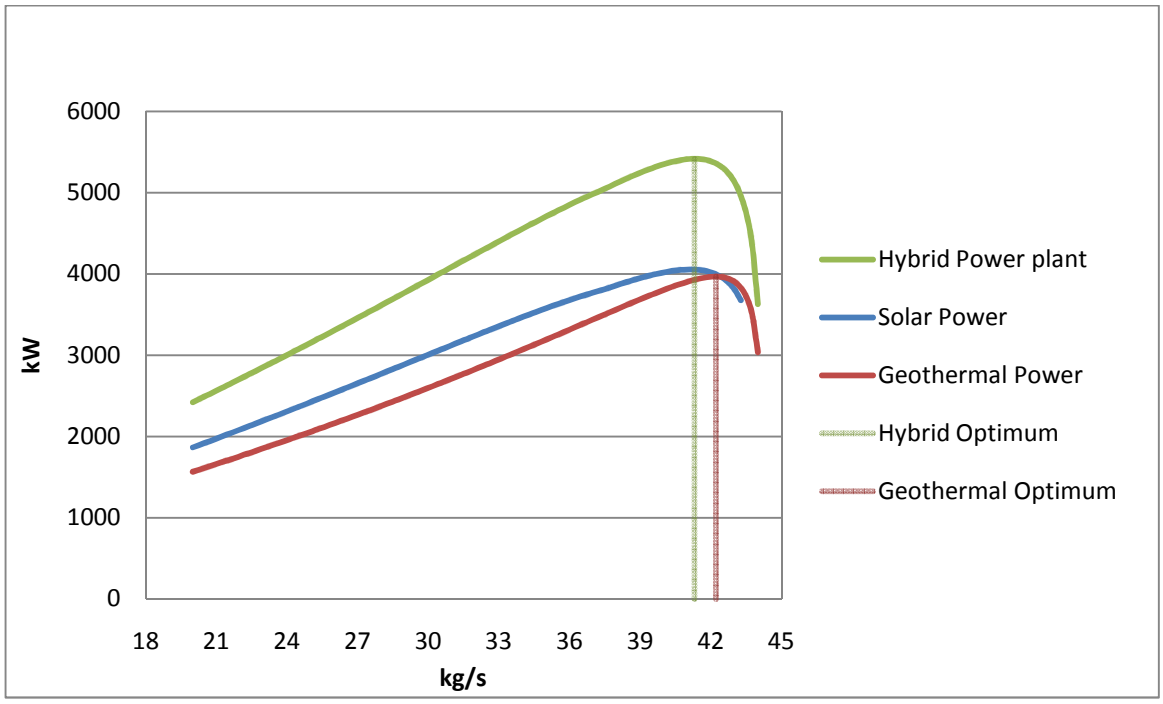

Figure 6.10 Geothermal-Solar Hybrid Power Plant, Single Flash, Case 3 Power Progress

According to Figure 6.10, we see that the optimum operational points differ from geothermal production than for hybrid power plants production. In this scenario, the mode of operation is as follows: when there is no solar energy available, the plant will continue operating at the optimal geothermal point, as used for the base scenario, so the same procedure is done to solve the thermodynamic process. As the available solar energy starts to increase, the total mass flow rate from the production well is maintained at the geothermal optimal production point until the maximum value of solar power that the thermodynamic cycle can absorb is reached. In this situation, there is no difference with the thermodynamic process presented in scenario 1 so it should follow to calculate the power delivered by the cycle. When the available solar energy exceeds the maximum that the geothermal cycle can accept is in the geothermal optimum, then the total mass flow rate from the production well should be reduced, iterating, until the first of the two following situations occur: the thermodynamic cycle absorbs all the available solar power or, the power generated by the hybrid plant decreases (respect to previous iteration).

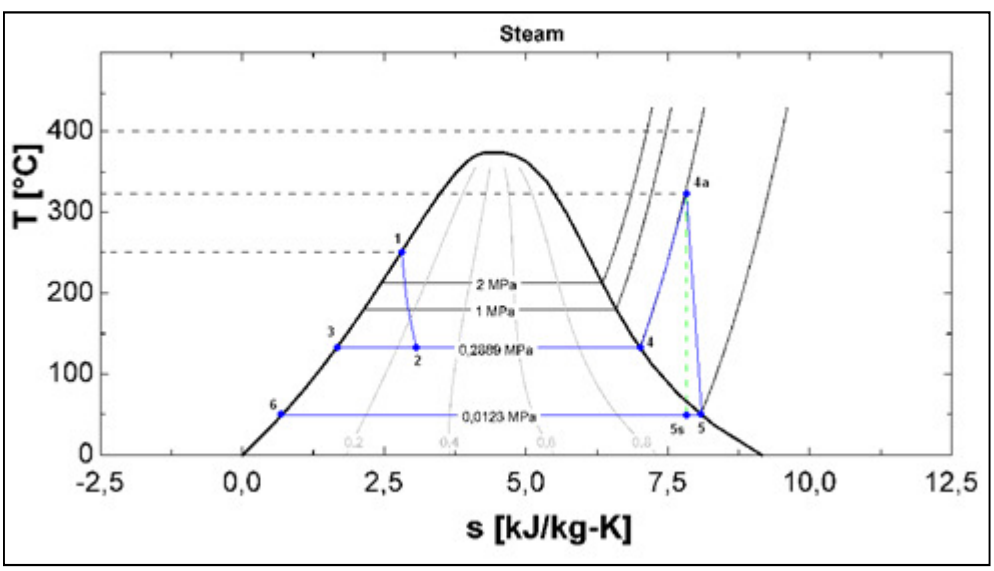

Figure 6.11 Single Flash, Scenario 3, T-s Thermodynamic Process Diagram

Even though reducing the total mass flow rate implies rising the separator pressure, it will not exceed the pressure limit necessary to reheat, so the thermodynamic states

are characterized by the thermodynamic model developed for scenario 1, simply by changing the value of the separator pressure determined by the total mass flow.

If solar energy is enough to stop the iteration process by reaching the optimum point of the hybrid plant, then the excess thermal power from the solar field must be used to evaporate the saturated liquid stream at thermodynamic state 3 and increase the main steam flow.

The optimal operational point for the hybrid power plant is found extracting a rate of 41.3 kg/s of geothermal fluid and providing 4050 kW of solar power in the HX1, reaching a maximum temperature of 345 °C and a separator temperature 140 °C.

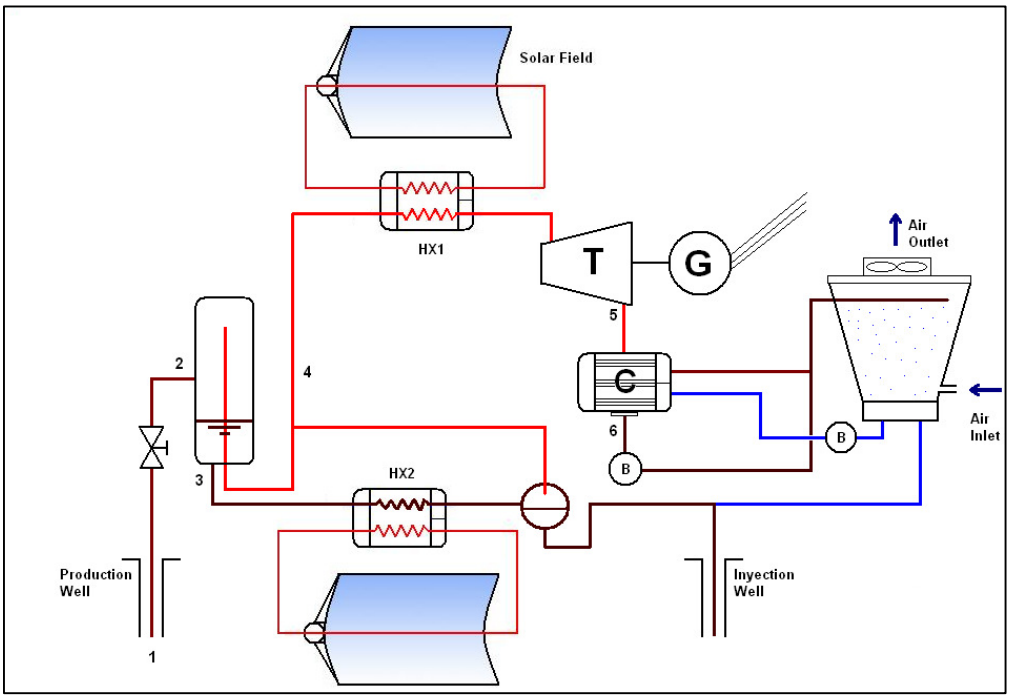

Figure 6.12 Single Flash Plant Scheme, Case 3

Then, following the same procedure as in the previous cases, we get a collector of 4600 m^2 which (920 meters of parabolic collectors arrange in a line, with an aperture of 5 m), to heat 9.3 kg/s between 140 and 345 °C. According to the procedure, we calculate the output power and geothermal fluid flow rate required for each hour of the year.

6.7.1 Results

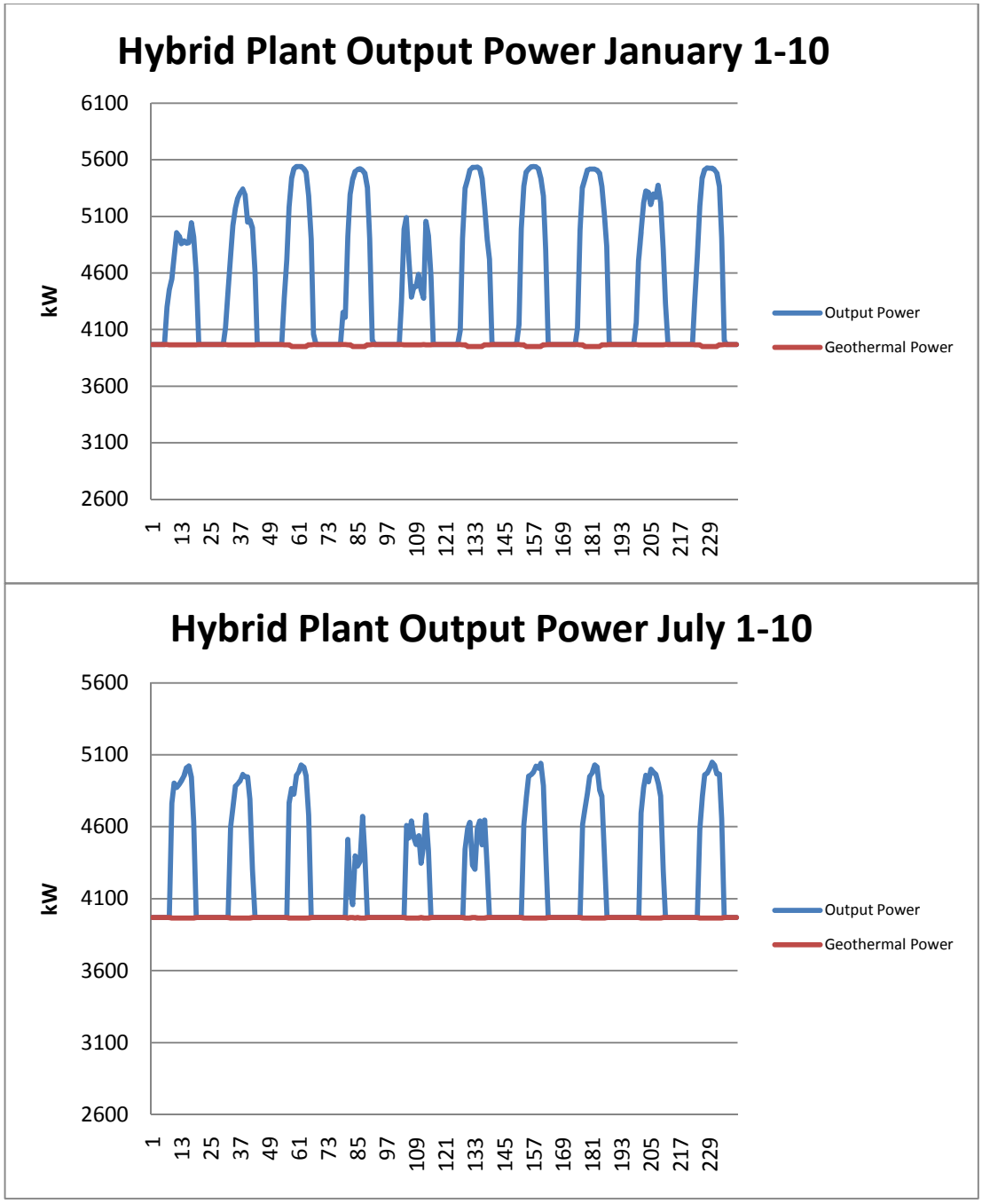

Figure 6.13 Geothermal-Solar Hybrid Power Plant, Single Flash, Case 3 Results

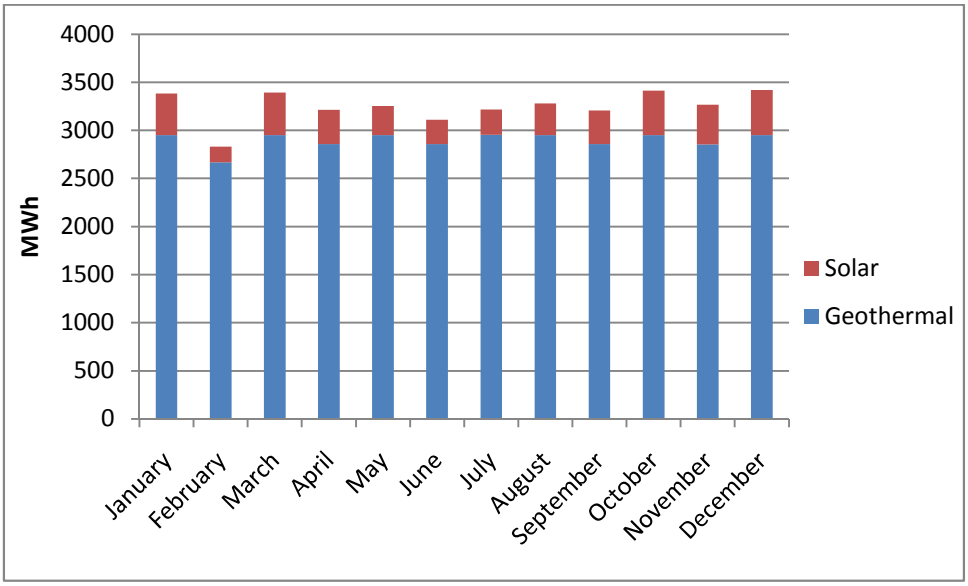

Figure 6.14 Energy Produced Monthly

Energy Produced	**38.98 GWh**
Kg Extracted	**1.327.643 Ton**

Table 6.4 single flash, Scenario 3, summarized results

6.8 Single Flash Hybrid Power Plant Summarized Results

Scenario	Anual Energy Produced		Extracted Flow	Geothermal
Base Scenario	34.81 GWh		1.331.500 Ton	
Scenario 1	38.85 GWh	+11,63 %	1.331.500 Ton	0.0 %
Scenario 2	34.81 GWh	0.0 %	1.193.520 Ton	-10.36 %
Scenario 3	38.98 GWh	+11.98 %	1.327.643 Ton	- 0.29 %

Table 6.5 Single Flash Hybrid Power Plant Summarized Results

6.9 Double Flash, Base Scenario

Using the same production curve for the productive well, and solving equations 4.15 to 4.31 that describe the double flash geothermal power plant thermodynamic process and maximizing the output energy, we obtain the following results.

Base Scenario	Doble Flash
Geothermal Well mass flow rate	40.96 kg/s
Main Separator Temperature	142.7 ℃
Main Separator Presure	0.3896 MPa
Flash Temperature	93.9 ℃
Flash Pressure	0.081 MPa
Output Power	4664 kW
Thermodynamic Eficiency	15.25%

Table 6.6 Double Flash Results, Base Case

These results will be the basis for comparing the performance of the following scenarios that are described in this chapter.

6.10 Double Flash, Scenario 1.

This scenario consists in increasing the output power of a double flash power plant when solar radiation is available, maintaining the same operational conditions for the production well (as the base scenario conditions). This production strategy seeks an increase of the output power during peak hours without affecting the operation of the geothermal power plant, i.e. the geothermal well continues operating at its optimum point, and the energy from the solar field is added to the steam stream.

To size the solar field, we must determine the maximum amount of solar power that the main steam stream can accept, and the maximum and minimum temperatures the solar field will operate. These values are found at a T-s diagram of the thermodynamic process associated with the model of the hybrid power plant.

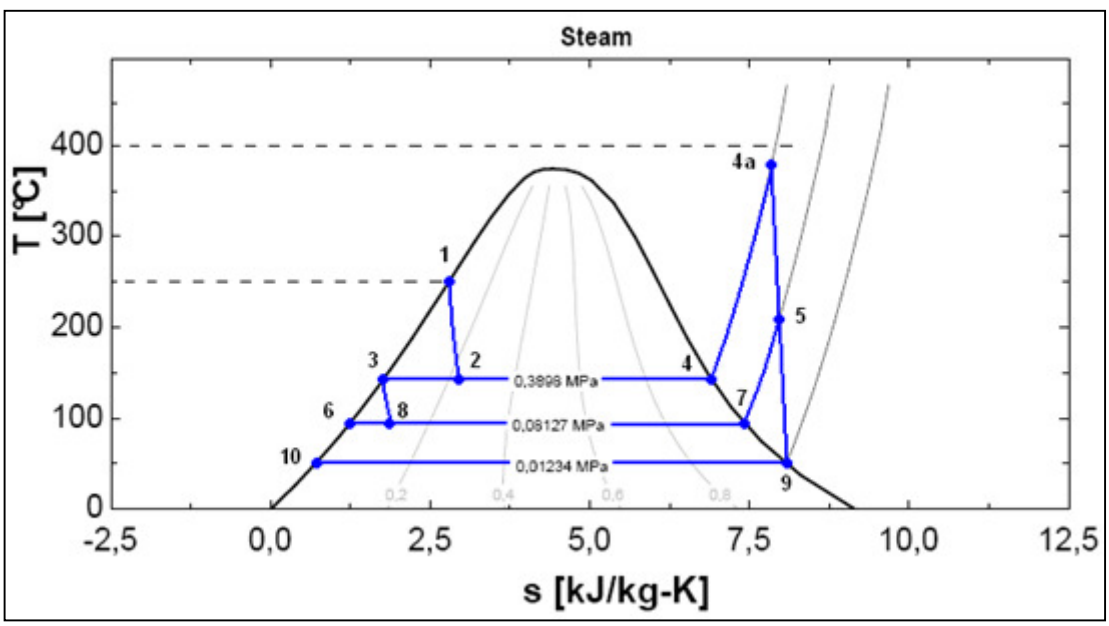

Figure 6.15 Double Flash Scenario 1, T-s Thermodynamic diagram

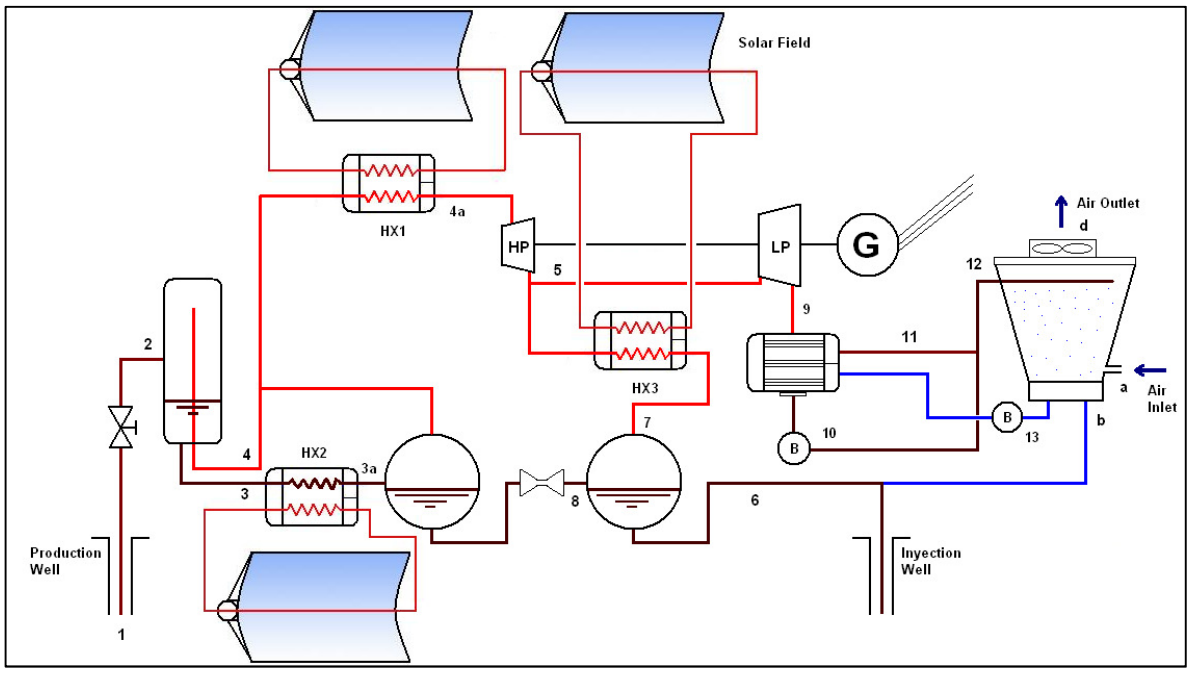

Figure 6.16 Double Flash Power Plant Scheme, Case 1

The maximum and minimum temperatures for the HTF are:

$$T_{4a} = 363.9°C \quad (6.37)$$

$$T_7 = 93.91 \quad (6.38)$$

The design solar power is the following.

$$\dot{E}_{solar} = \frac{\dot{m}_{steam\,4} \cdot (h_{4a} - h_4) + \dot{m}_{steam\,7} \cdot (h_5 - h_7)}{\eta_{HX}} = 5131.89\ kW \quad (6.39)$$

With these results, using design radiation, assuming an ambient temperature of 15 ° C and following the sizing methodology for the solar field described in chapter 5, we obtain a solar field with a collection area of 5820 m^2. If we assume that the collectors have a 5 m aperture, we get a length of 1164 m for the collecting element.

In the same way as in previous cases, when the solar field delivers more energy than it was designed for, the excess will be used to increase the dryness fraction at the main separator, vaporizing part of the saturated liquid at point 3 according to Figure 6.12.

On the contrary, when solar power delivered is less than the design value, different scenarios can occur, depending on the point at which the steam expansion will saturate and enter the wet zone. Different cases define different solar power distributions in the various heat exchangers inside the hybrid power plant.

All possible scenarios are described starting on the smallest solar power available and increasing.

For the case in which there is no solar power, at night or during cloudy periods, there is no heat exchange between the power cycle and the HTF and the power cycle and it behaves as a regular geothermal power plant. Thermodynamic states are found using the same methodology described in chapter 4

The next case is when the power delivered by the solar field is small and the superheating is not enough to keep the high pressure turbine output to remain at the dry steam zone and it saturates before the turbine outlet and therefore in this case, the thermodynamic model solution is found using the following process, outlined in Figure 6.17:

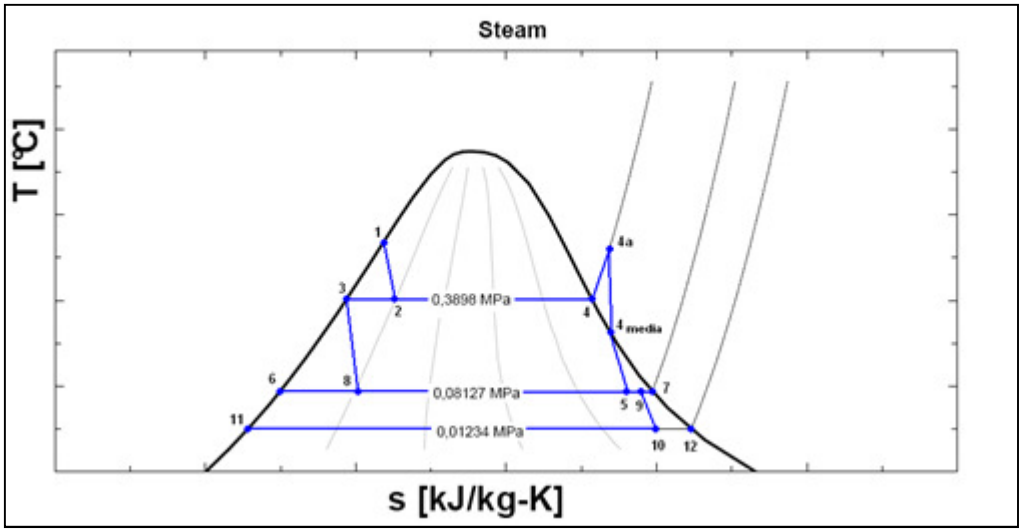

Figure 6.17 Double Flash T-s Diagram, solar energy is not enough to reach the overheat max. temperature at the HP turbine

The scale on Fig 6.17 was modified to better show the process that occurs in the expansion of high-pressure turbine.

$$HX1 = \dot{E}_{solar} \cdot \eta_{HX} \quad (6.40)$$

$$HX2 = 0 \quad (6.41)$$

$$HX3 = 0 \quad (6.42)$$

$$x_2 = \frac{h_2 - h_3}{h_4 - h_3} \quad (6.43)$$

$$\dot{m}_{steam\,2} = x_2 \cdot \dot{m}_{total} \quad (6.44)$$

After the separator, the main steam flow enters the only active heat exchanger, HX1, according to the conditions presented.

$$\dot{m}_{steam\,2} \cdot h_4 + HX1 = \dot{m}_{steam\,2} \cdot h_{4a} \quad (6.45)$$

Then, the expansion in the high-pressure turbine occurs in two stages, the first is a dry expansion and the second stage occurs in the presence of condensation drops, so it should be considered as separate processes due to the isentropic efficiency difference.

$$h_{4\,media\,S} = enthalpy(Steam, P = P_{media}, s = s_{4a}) \quad (6.46)$$

$$h_{4\,media} = enthalpy(Steam, P = P_{media}, x = 1) \quad (7.47)$$

$$\eta_{td} = 0.85 \quad (6.48)$$

$$\eta_{td} = \frac{h_{4a} - h_{4\,media}}{h_{4a} - h_{4\,media\,S}} \quad (6.49)$$

Solving equations 6.46 to 6.49 we found the value of P_{media}, then we can calculate the efficiency of the high pressure turbine expansion stage and the specific work of the turbine along with determining the thermodynamic conditions at the outlet.

$$\eta_{t\,wet} = \frac{h_{4\,media} - h_5}{h_{4\,media} - h_{5s}} \quad (6.50)$$

$$\eta_{t\,wet} = \eta_{td} \cdot \frac{1 + x_5}{2} \quad (6.51)$$

$$x_5 = \frac{h_5 - h_6}{h_7 - h_6} \quad (6.52)$$

$$w_{HP} = h_{4a} - h_5 \quad (6.53)$$

At the exit of the high pressure turbine, the main steam flow meets the steam flow from the second flashing stage. These streams are at the same pressure but their thermodynamic conditions are different, an energy and mass balance is necessary to obtain the thermodynamic conditions of the mixture.

$$h_8 = h_3 \quad (6.54)$$

$$x_8 = \frac{h_8 - h_6}{h_7 - h_6} \quad (6.55)$$

$$\dot{m}_{steam\,8} = (1 - x_2) \cdot x_8 \cdot \dot{m}_{total} \quad (6.56)$$

$$\dot{m}_{steam\,9} = \dot{m}_{steam\,8} + \dot{m}_{steam\,2} \quad (6.57)$$

$$\dot{m}_{steam\,9} \cdot h_9 = \dot{m}_{steam\,8} \cdot h_8 + \dot{m}_{steam\,2} \cdot h_5 \quad (6.58)$$

$$x_9 = \frac{h_9 - h_6}{h_6 - h_6} \quad (6.59)$$

Then with the thermodynamic conditions at point 9,

$$\eta_{t,LP} = \frac{h_9 - h_{10}}{h_9 - h_{10s}} \quad (6.60)$$

$$x_{10} = \frac{h_{10} - h_{11}}{h_{12} - h_{11}} \quad (6.61)$$

$$\eta_{t,LP} = \eta_{td,LP} \cdot \frac{x_9 + x_{10}}{2} \quad (6.62)$$

$$\eta_{td,LP} = 0.85 \quad (6.63)$$

$$w_{LP} = h_9 - h_{10} \quad (6.64)$$

We can calculate the power generated by the low pressure turbine.

$$\dot{W}_t = \dot{m}_{steam\,2} \cdot w_{HP} + \dot{m}_{steam\,9} \cdot w_{LP} \quad (6.65)$$

$$\dot{Q}_{cond} = \dot{m}_{steam\,9} \cdot (h_{10} - h_{12}) \quad (6.66)$$

This way we get the total power, $\dot{W}_t$, generated by the hybrid plant in the case that solar power delivered by the solar field is not enough for the output of the high pressure turbine to remain superheated.

Another particular operating condition occurs when the power of the collector is enough to keep the output of the high pressure turbine on a superheated steam condition, however, is not sufficient to keep the expansion at the low pressure turbine working on the dry steam zone.

This case includes the range of operating conditions from when the power delivered by the solar field is only enough to keep the steam dryness fraction equal to one at the

exit of the high pressure turbine, to when the solar power is enough to superheat up to the design temperature the primary steam flow and also superheating the flow from the second flashing stage to reach the thermodynamic conditions at the output of the high pressure turbine, i.e. when point 5_{media} meets point 9.

Figure 6.18 shows a T-s diagram with an intermediate sample case for the situation described above.

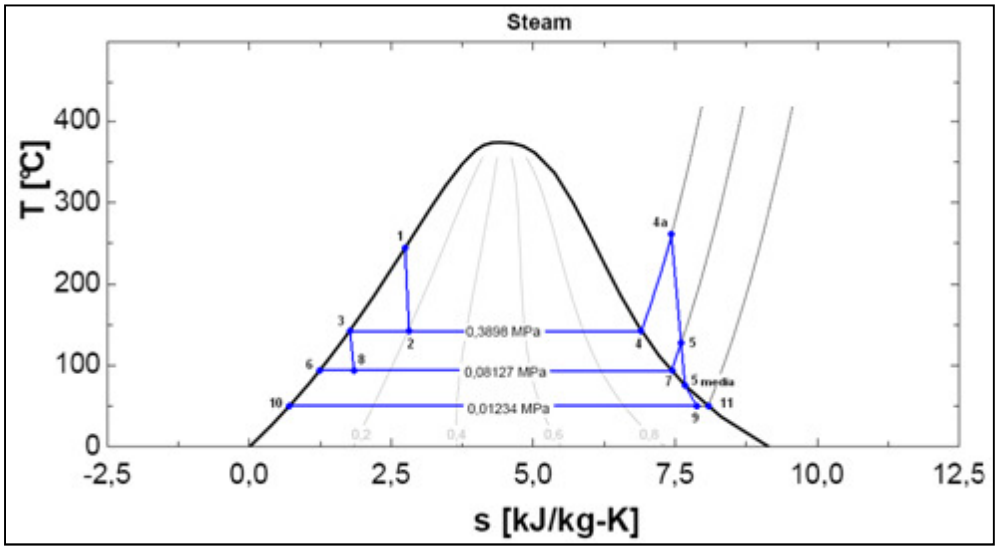

Figure 6.18 Double Flash T-s Diagram, solar energy is not enough to reach the overheat max. temperature at the LP turbine

In this case, the procedure used to solve the thermodynamic states and find the power generated by the hybrid power plant is the same done before but adjusted to this specific situation, solving simultaneously the following set of equations that represents the process within the power cycle.

$$HX1 + HX2 = \dot{E}_{solar} \cdot \eta_{HX} \quad (6.67)$$

$$HX3 = 0 \quad (6.68)$$

$$x_2 = \frac{h_2 - h_3}{h_4 - h_3} \quad (6.69)$$

$$\dot{m}_{steam\,2} = x_2 \cdot \dot{m}_{total} \quad (6.70)$$

$$\dot{m}_{steam\,2} \cdot h_4 + HX1 = \dot{m}_{steam\,2} \cdot h_{4a} \quad (6.71)$$

$$\eta_{td} = 0.85 \quad (6.72)$$

$$\eta_{td} = \frac{h_{4a} - h_5}{h_{4a} - h_{5\,s}} \quad (6.73)$$

$$w_{HP} = h_{4a} - h_5 \quad (6.74)$$

$$h_8 = h_3 \quad (6.75)$$

$$x_8 = \frac{h_8 - h_6}{h_7 - h_6} \quad (6.76)$$

$$\dot{m}_{steam\,8} = (1 - x_2) \cdot x_8 \cdot \dot{m}_{total} \quad (6.77)$$

$$\dot{m}_{steam\,8} \cdot h_7 + HX2 = \dot{m}_{steam\,8} \cdot h_5 \quad (6.78)$$

$$h_{5\,media\,S} = enthalpy(Steam, P = P_{media}, s = s_{4a}) \quad (6.79)$$

$$h_{5\,media} = enthalpy(Steam, P = P_{media}, x = 1) \quad (6.80)$$

$$\eta_{td} = \frac{h_5 - h_{5\,media}}{h_5 - h_{5\,media\,S}} \quad (6.81)$$

$$\eta_{t\,wet} = \frac{h_{5\,media} - h_9}{h_{5\,media} - h_{9s}} \quad (6.82)$$

$$\eta_{t\,wet} = \eta_{td} \cdot \frac{1 + x_9}{2} \quad (6.83)$$

$$x_9 = \frac{h_9 - h_{10}}{h_{11} - h_{10}} \quad (6.84)$$

$$w_{LP} = h_5 - h_9 \quad (6.85)$$

$$\dot{W}_t = \dot{m}_{steam\,2} \cdot w_{HP} + (\dot{m}_{steam\,2} + \dot{m}_{steam\,8}) \cdot w_{LP} \quad (6.86)$$

$$\dot{Q}_{cond} = (\dot{m}_{steam\,2} + \dot{m}_{steam\,8}) \cdot (h_{11} - h_{10}) \quad (6.87)$$

Finally, if the solar power available is enough to meet the design conditions, represented in the T-s diagram in Figure 6.15, the process to solve the thermodynamic system to find the hybrid power plant output power is simple since all values are defined by the design conditions according to the assumptions made and any excess energy should be used to increase the amount of steam available in the high pressure stage the same way as was done in the previous scenarios.

With all possible scenarios and the procedures described, we can simulate a full year according to the behavior of the solar field described in Chapter 5 and obtain the hourly output power plus the total energy produced and total amount of geothermal resources extracted for the entire year.

6.10.1 Results

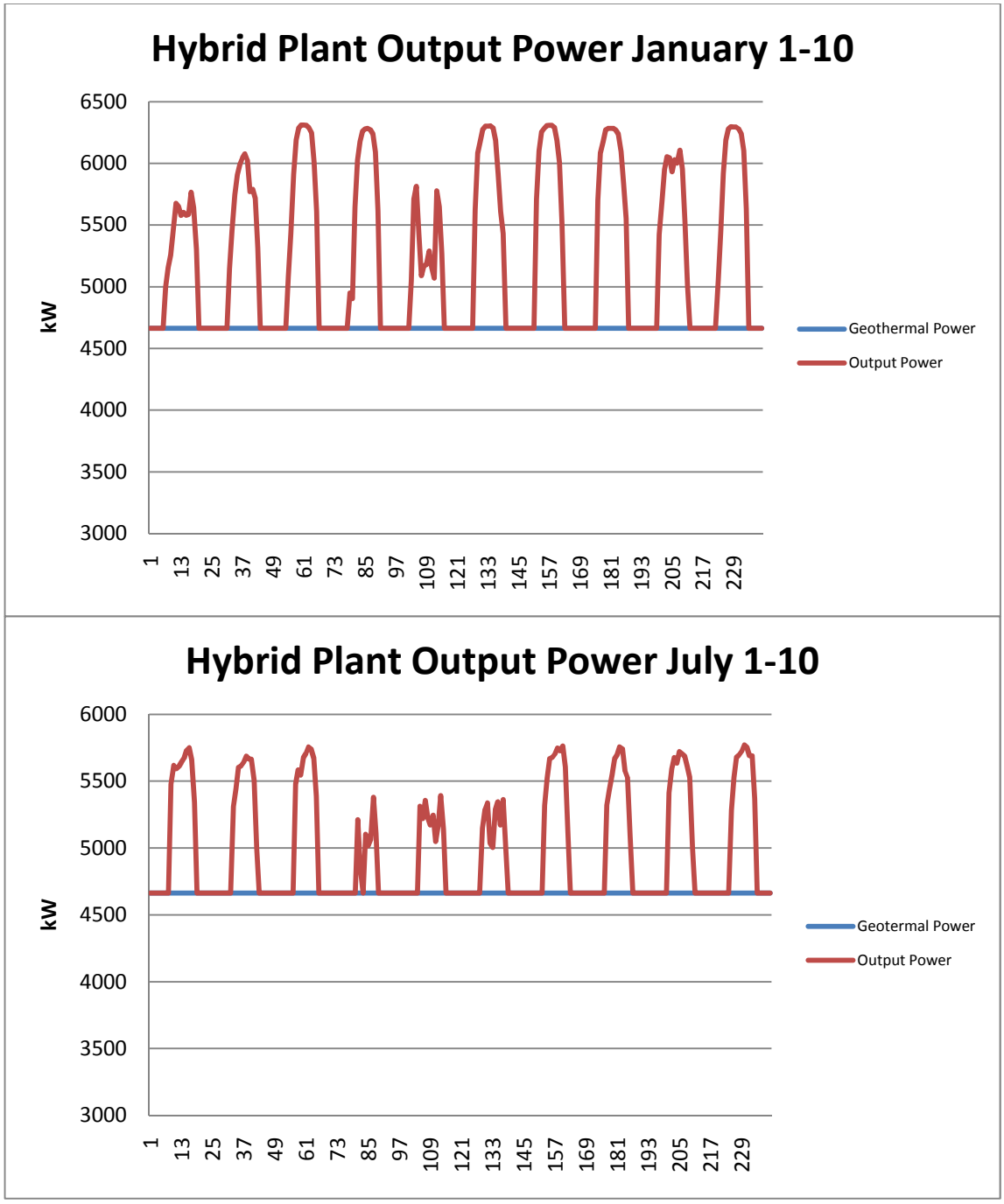

Figure 6.19 Geothermal-Solar Hybrid Power PlantDouble Flash, Case 1 Results

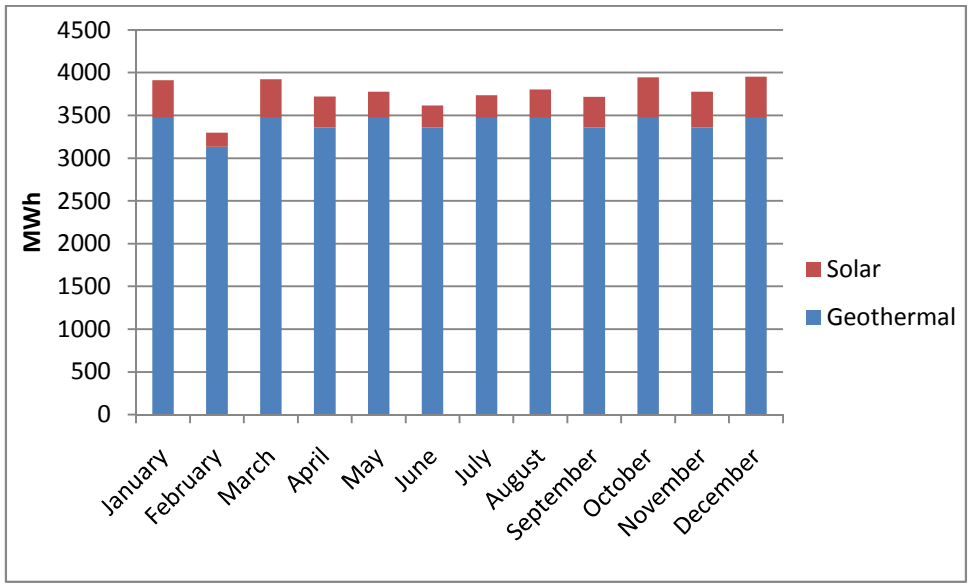

Figure 6.20 Energy Produced Monthly MWh

Energy Produced	**45.18 GWh**
Kg Extracted	**1.291.715 Ton**

Table 6.7 Double flash, Scenario 1, summarized results for a year of operation

6.11 Double Flash, Scenario 2

The objective of this scenario is to maintain the output power of the hybrid power plant fixed replacing geothermal power by solar power as it becomes available to decrease the consumption of geothermal resources.

In this case we will fix the output power at the level obtained for the double flash base scenario; 4664 kW.

The hybrid power plant idealized scheme for this scenario, shown in Figure 7.17 is similar to that used in the previous scenarios except that here an extra heat exchanger is added because the in some cases is possible to reheat the primary flow of team. The scheme is shown together with its corresponding T-s diagram for the design conditions in Figure 6.21

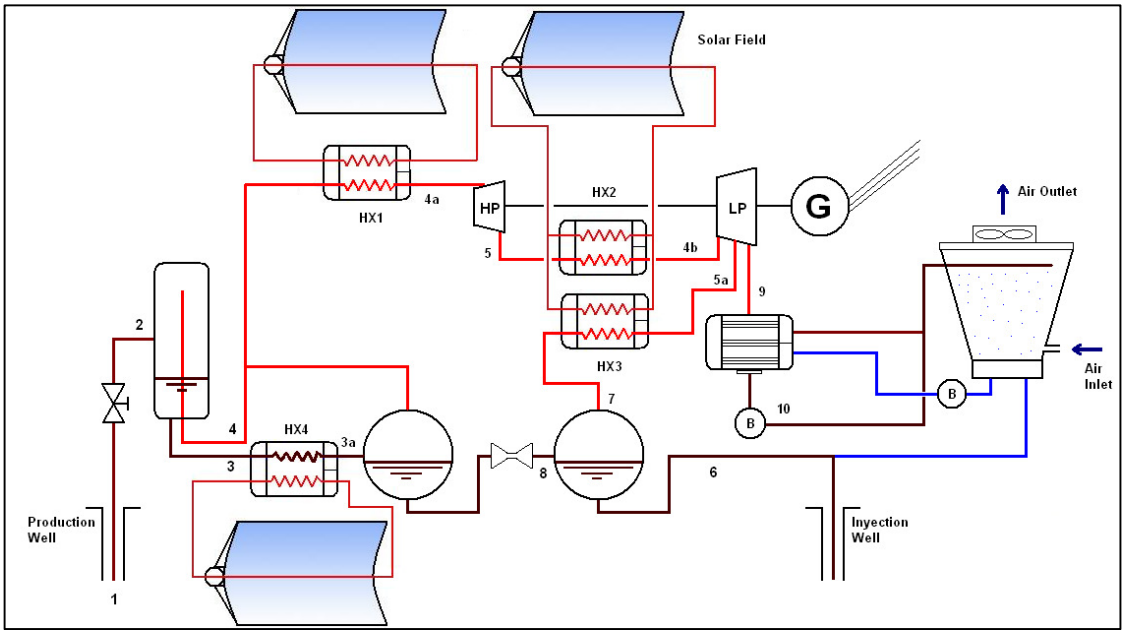

Figure 6.21 Double Flash Plant Scheme, Case 2

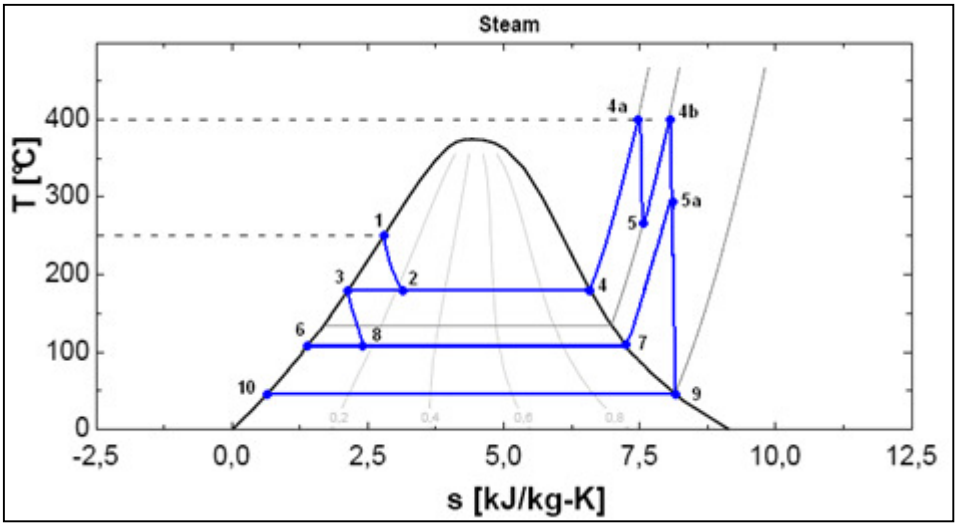

Figure 6.22 Double Flash, Case 2, T-s Thermodynamic Process Diagram

To achieve the required output power, the lowest values the geothermal well can operate is at a rate of 27.56 kg/s, and adding a total of 3528 kW of thermal power from the solar field to produce the 4664 kW output power at the axis of the electric generator. These values are represented in Figure 7.19 which shows a progression of the maximum power output of the hybrid power plant along with the power supplied by the geothermal well and the maximum energy input provided by the solar field.

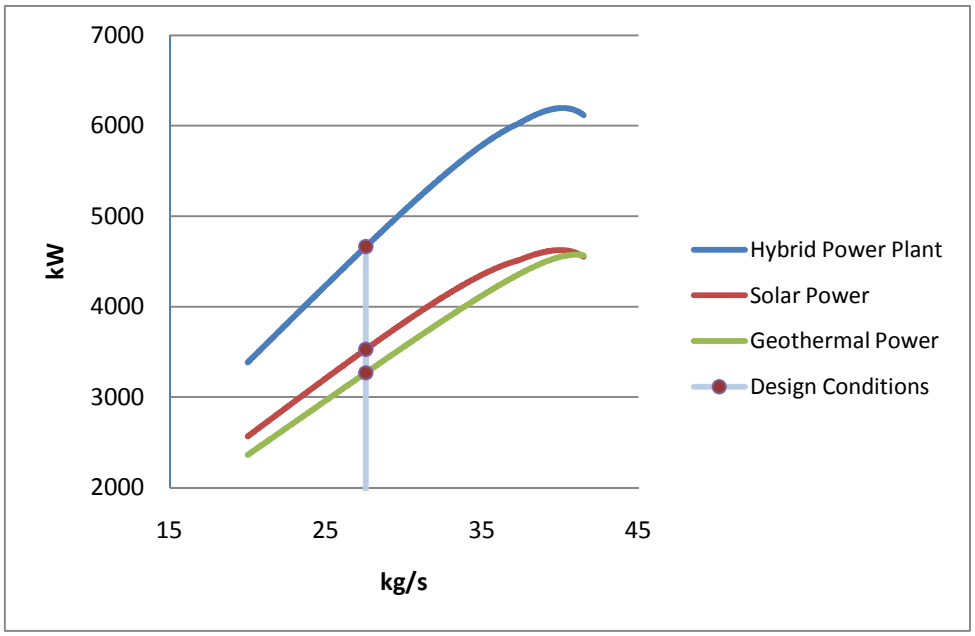

Figure 6.23 Double Flash, Case 2, Power Progress

The maximum temperature reached by the main steam line after the first heat exchanger is 400 °C at point 4a and the same at point 4b according to Figure 6.21 and the minimum working temperature for HTF is 110.7 °C at point 7. With these data and design conditions, we can calculate the size of the solar field needed to meet the requirements.

$$\dot{E}_{solar} = \frac{\dot{m}_{steam\,2} \cdot [(h_{4a} - h_4) + (h_{4b} - h_5)] + \dot{m}_{steem\,8} \cdot (h_{5a} - h_7)}{\eta_{HX}}$$

$$= 3713.7\ kW$$

$$\dot{m}_{solar} \cdot \overline{C_p} \cdot \Delta T = 3713.7\ kW$$

$$\dot{m}_{solar} \cdot 2.12 \cdot (400 - 110.7) = 3713.7\ kW$$

$$\dot{m}_{solar} = 6.06\ kg/s$$

With this numbers, a 4250 m^2 of solar collectors are needed, assuming an aperture of 5 meters, we obtain a total length of 850 meters for the heat collecting element.

The methodology used to address the various thermodynamic states is analogous to the one used in scenario N°2 for the single flash power plant except that in this case we have an extra heat exchanger that must considered. For each hour of the year, there will be an iterative process starting from the optimal geothermal production point used in the base scenario and the mass flow rate from the geothermal well will decrease until the power output of the hybrid power plant meets the value of the output power of the base case.

In cases where the power from the solar field is zero, as it is at night or cloudy days, the hybrid power plant operates as a conventional geothermal power plant. As the available solar power increases, different thermodynamic states can be achieved, using similar parameters as in scenario N°2 for the single flash power plant. If the solar radiation is greater than the design value, the energy coming from the solar field will reduce the mass flow rate of the geothermal well below design levels saving geothermal resources by evaporating water from the stream represented by number 3 in Fig. 6.21.

6.11.1 Results

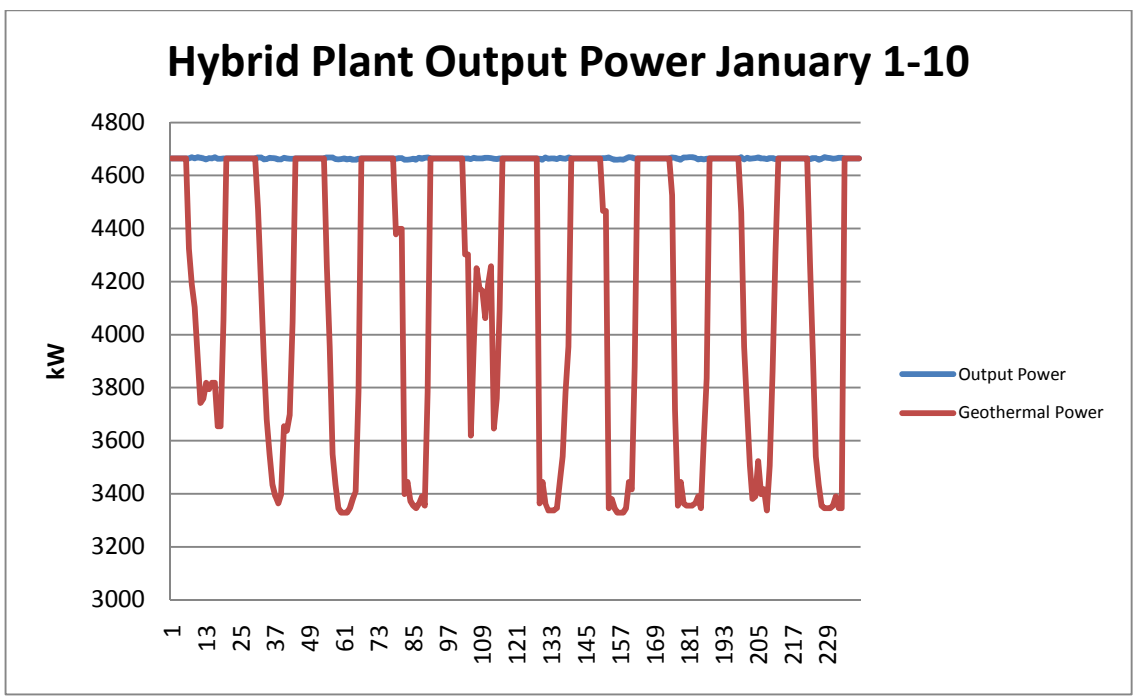

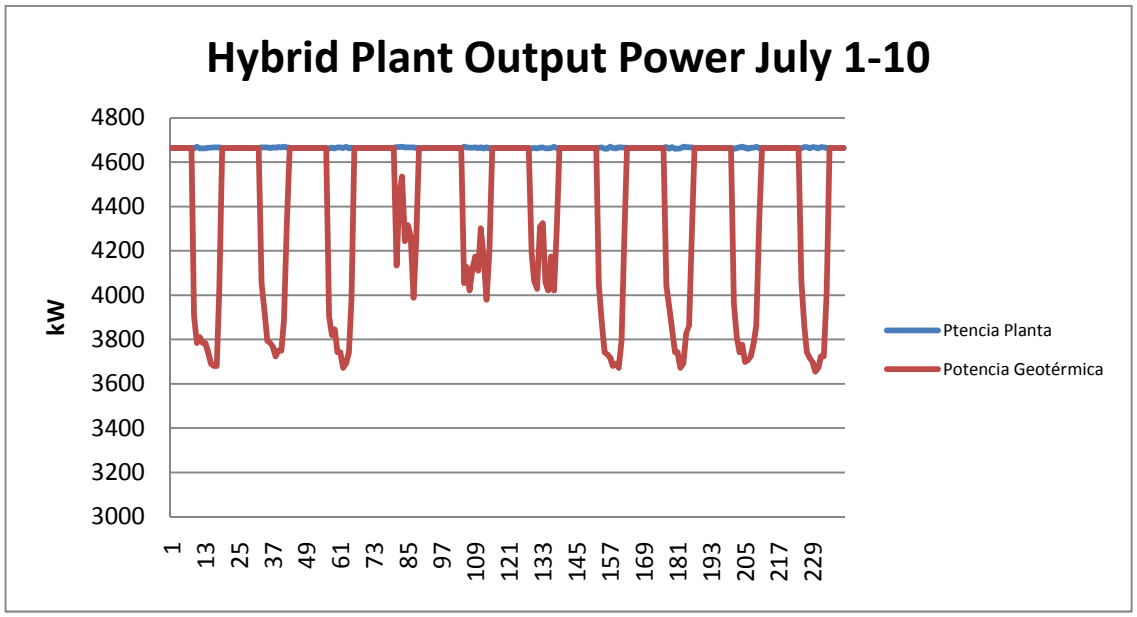

Figure 6.24 Geothermal-Solar Hybrid Power Plant, Double Flash, Scenario 2 Results

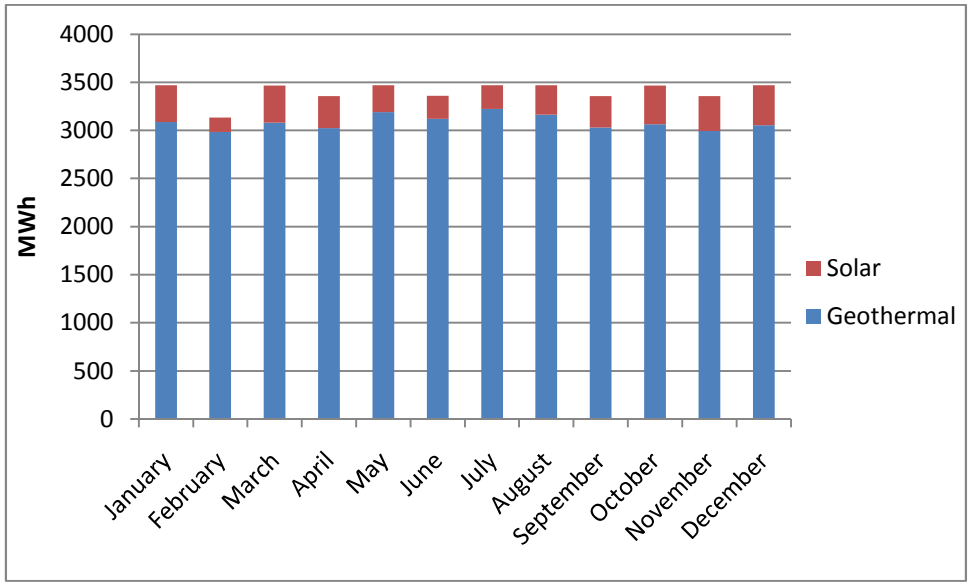

Figure 6.25 Energy Produced Monthly

Energy Produced	**40.83 GWh**
Kg Extracted	**1.152.424 Ton**

Table 6.8 Double flash, Scenario 2, summarized results for a year of operation

6.12 Double Flash, Scenario 3

As before, the central idea is to produce as much energy as posible using all resourses available, getting the most out of them. Thus, jointly optimizing the geothermal well and the solar field, we obtain the following optimum point of operation: 40.15 kg/s flowing from the wellhead, for a maximum output power of 6196 kW. The optimal point is shown in Figure 6.26.

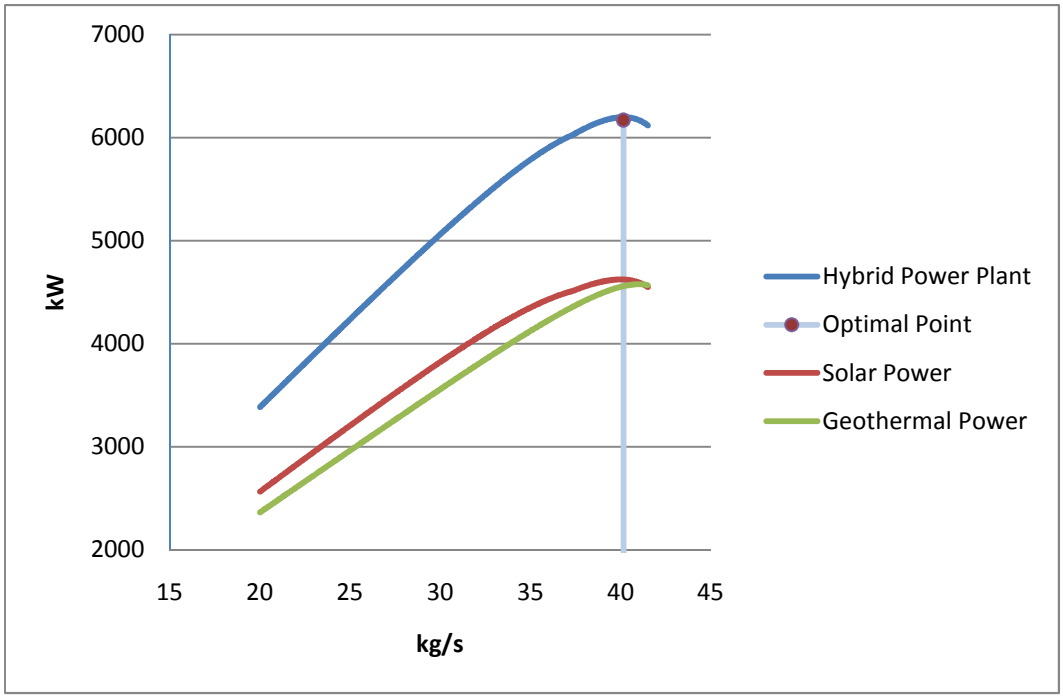

Figure 6.26 Double Flash, Case 3, Power Progress

In this case, the pressure at the wellhead does not exceed the value needed for reheating after the first stage of expansion, so the thermodynamic diagram has the same configuration as the one used in scenario 1 for double flash power plant shown in Figure 7.15 and hence the scheme of the physical configuration of the plant also corresponds to the arrangement shown in Figure 6.16

The sizing of the solar field for the design conditions gives the following results.

$$\dot{E}_{solar} = \frac{\dot{m}_{steam\,2} \cdot [(h_{4a} - h_4) + (h_{4b} - h_5)] + \dot{m}_{steem\,8} \cdot (h_{5a} - h_7)}{\eta_{HX}}$$

$$= 4796.8\ kW$$

$$\dot{m}_{solar} \cdot \overline{C_p} \cdot \Delta T = 4796.8\ kW$$

$$\dot{m}_{solar} \cdot 2.12 \cdot (366.3 - 96.2) = 4796.8\ kW$$

$$\dot{m}_{solar} = 8.377\ kg/s$$

To meet these parameters, a 5445 square meters solar field is needed, equivalent to a line 1089 meters long of solar collectors with an aperture of 5 meters.

The operational strategy is the same as the one presented in scenario 3 for the single flash power plant, seeking to obtain the largest energy output using solar and geothermal resources optimally.

6.12.1 Results

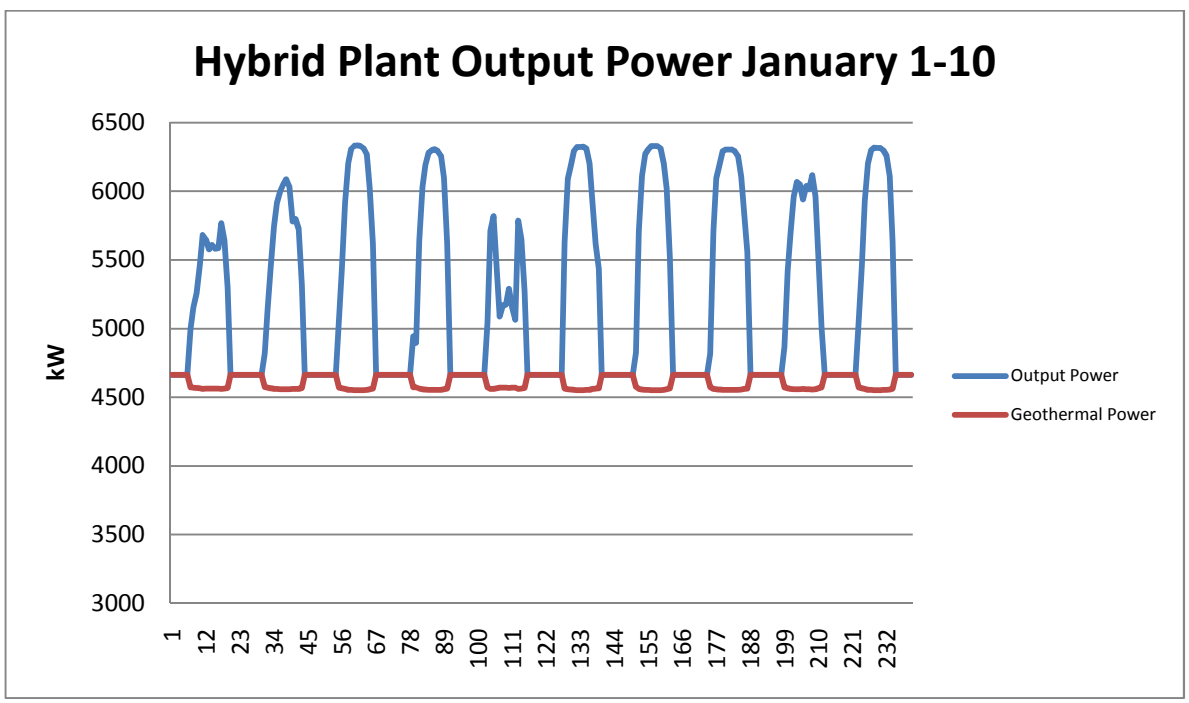

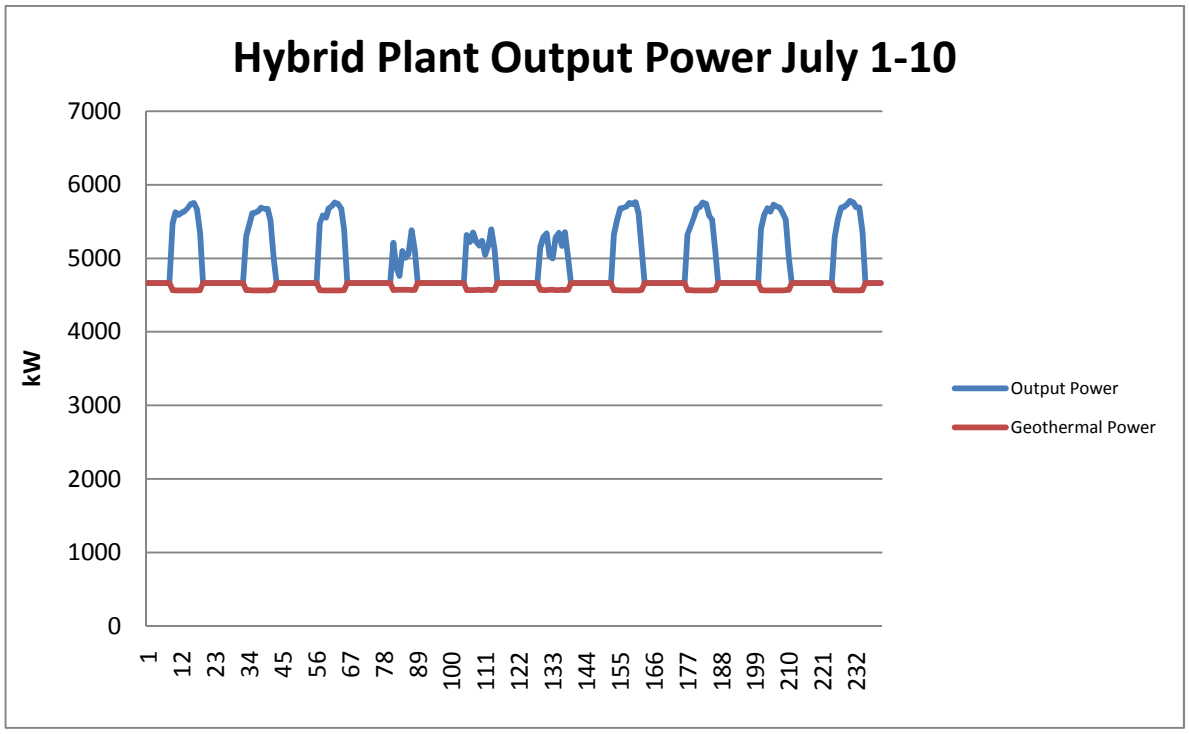

Figure 6.27 Geothermal-Solar Hybrid Power Plant, Double Flash, Scenario 3 Results

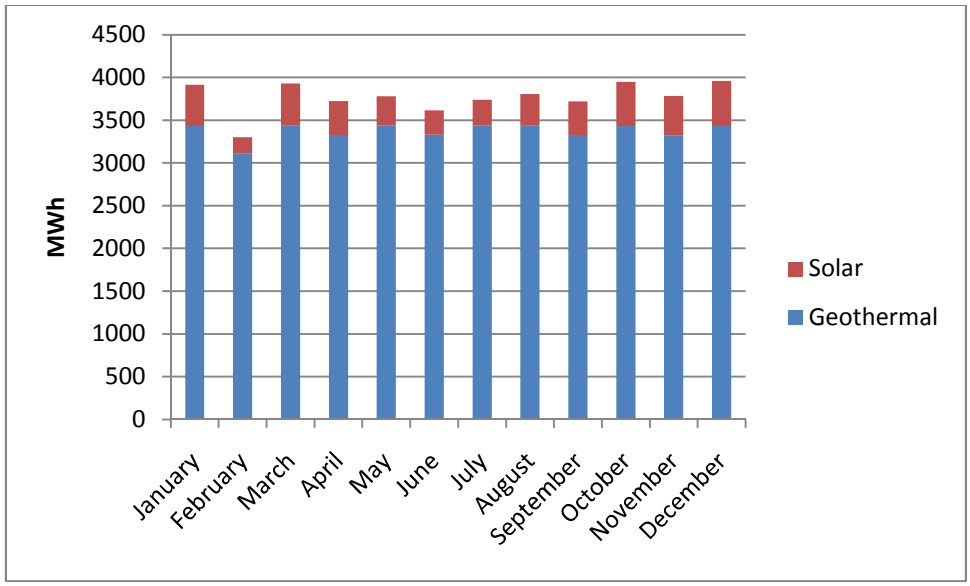

Figure 6.28 Energy Produced Monthly MWh

Energy Produced	45.22 GWh
Kg Extracted	1.282.406 Ton

Table 6.9 Double flash, Scenario 3, summarized results for a year of operation

6.13 Double Flash Hybrid Power Plant Summarized Results

Scenario	Anual Energy Produced		Extracted Geothermal Kg	
Base Scenario	40.81 GWh		1.291.715 Ton	
Scenario 1	45.18 GWh	+10.70 %	1.291.715 Ton	0.0 %
Scenario 2	40.83 GWh	+0.04 %	1.152.424 Ton	-10.78 %
Scenario 3	45.22 GWh	+10.80 %	1.282.406 Ton	- 0.72 %

Table 6.10 Double Flash Hybrid Power Plant Summarized Results

6.14 Hybrid Power Plant Summarized Results, All Scenarios.

Type	Scenario	Energy GWh	ΔSingle	ΔDouble	Kg Extracted Ton	ΔSingle	ΔDouble
Single	Base	**34.81**	--	--	**1.331.500**	--	--
	Scenario1	**38.85**	**+11.63 %**	--	**1.331.500**	**0.0 %**	--
	Scenario2	**34.81**	**0.0 %**	--	**1.193.520**	**-10.36 %**	--
	Scenario3	**38.98**	**+11.98 %**	--	**1.327.643**	**-0.29 %**	--
Double	Base	**40.81**	**+17.24 %**	--	**1.291.715**	**-2.99 %**	--
	Scenario1	**45.18**	**+29.79 %**	**+10.70 %**	**1.291.715**	**-2.99 %**	**0.00 %**
	Scenario2	**40.83**	**+17.29 %**	**+0.040 %**	**1.152.424**	**-13.44 %**	**-10.78 %**
	Scenario3	**45.22**	**+29.91 %**	**+10.80 %**	**1.282.406**	**-3.69 %**	**-0.72 %**

Table 6.11 Hybrid Power Plant Summarized Results, All Scenarios.

6.15 Thermodynamic Results Summary and Analysis

The main variables resulting from modeling the thermodynamics of the hybrid power plant operation in different scenarios are: energy produced, output power profile, geothermal resources consumption, solar field size and complexity of operation.

6.15.1 Energy Produced

The energy produced by each scenario depends on factors such as the efficiency of the thermodynamic cycle, the amount of geothermal resources used and the solar field size.

Figure 6.29 shows the amount of energy produced by one geothermal well over a year of operation for each scenario.

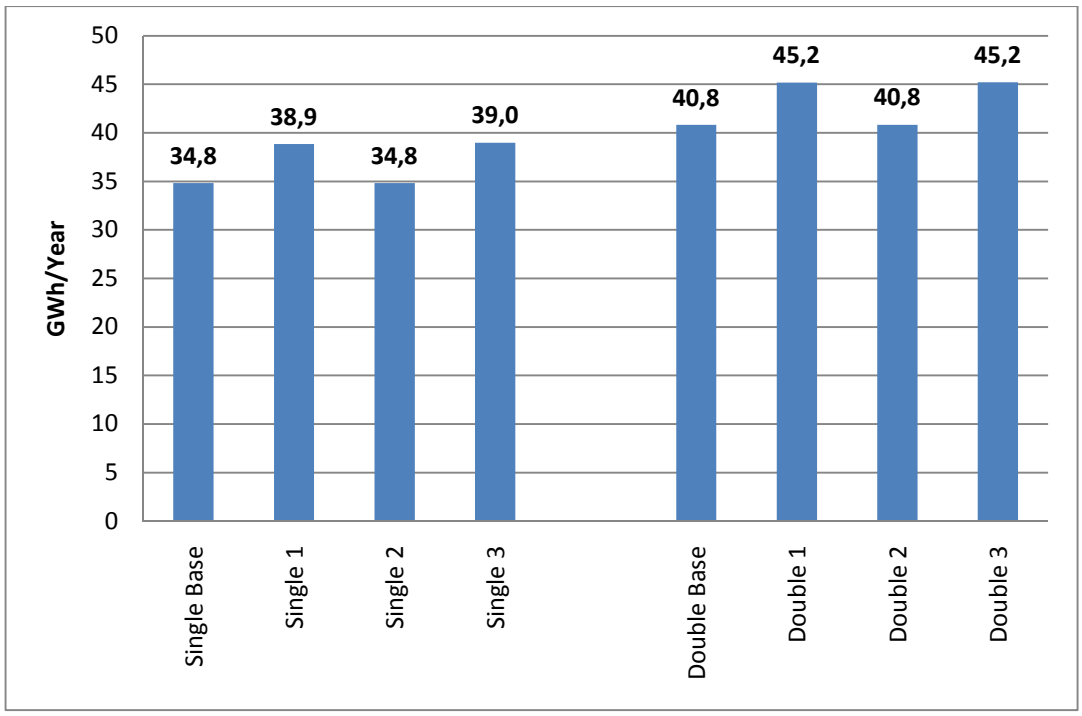

Figure 6.29 Energy Produced

6.15.2 Geothermal Resourse Consumption

The geothermal resource consumption depends on the scenario because of the specific objectives of each scenario directly affect the amount of resources consumed. Figure 7.24 summarizes geothermal resource consumption for each of the scenarios proposed.

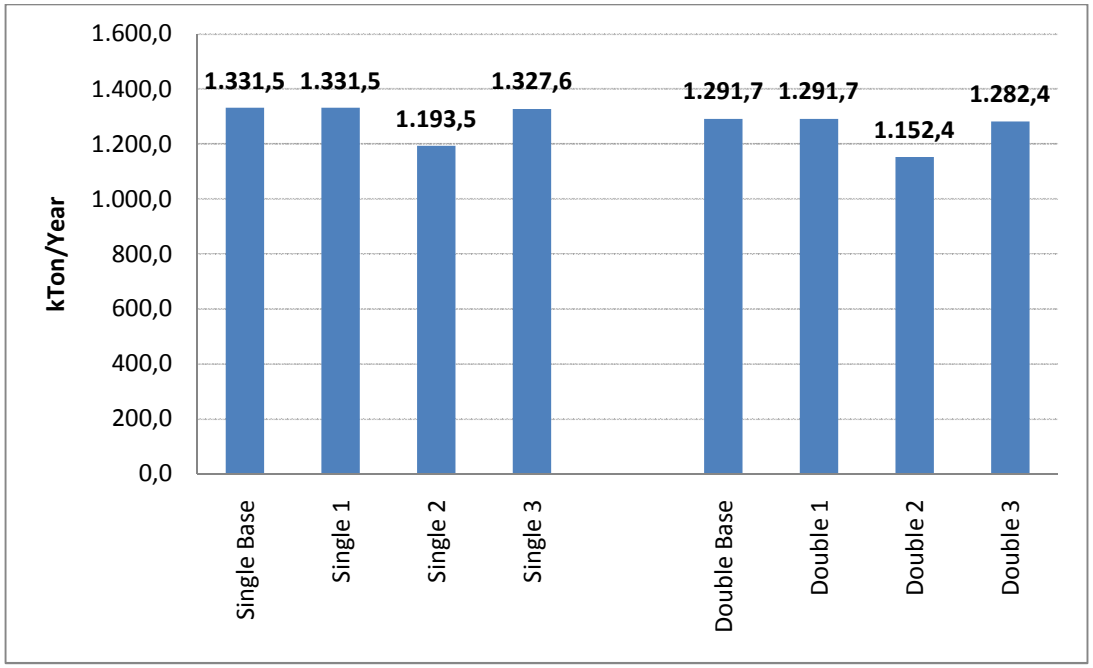

Figure 6.30 Geothermal Fluids Consumption

With these data we can obtain a measure of the utilization of the geothermal resources in each scenario calculating the specific energy delivered by the power plant per kilogram of extracted geothermal brine. These data are shown in Figure 7.31.

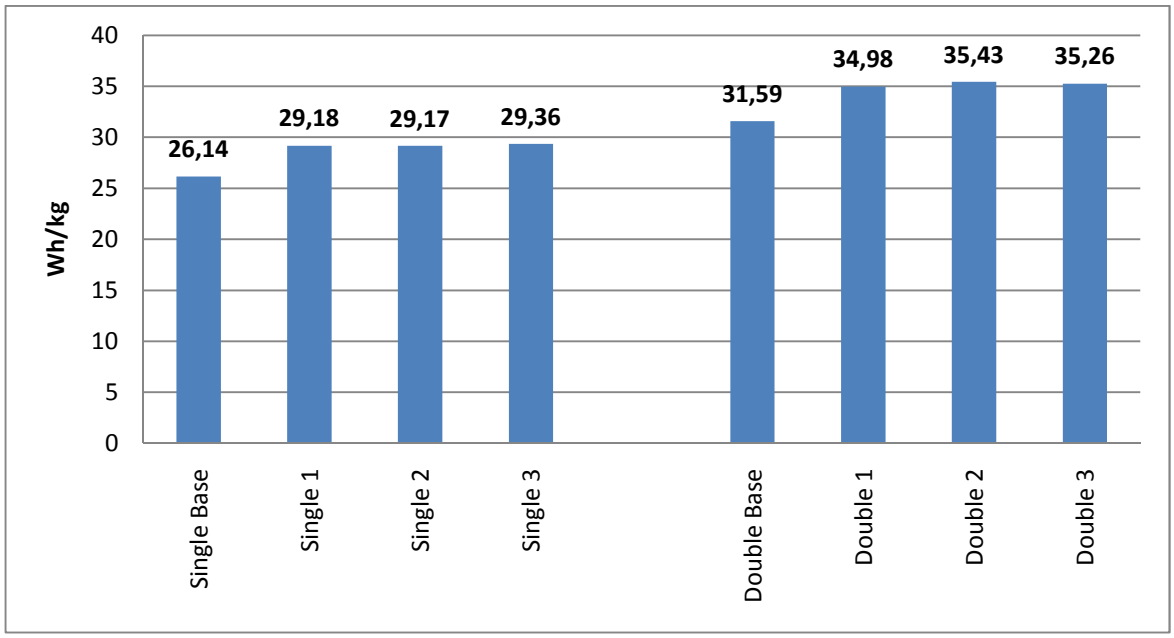

Figure 6.31 Specific Energy Output

6.15.3 Solar Field

The solar field size depends on the specific operating conditions in each scenario, Figure 6.32 shows the sizes needed per well for each of the proposed scenarios.

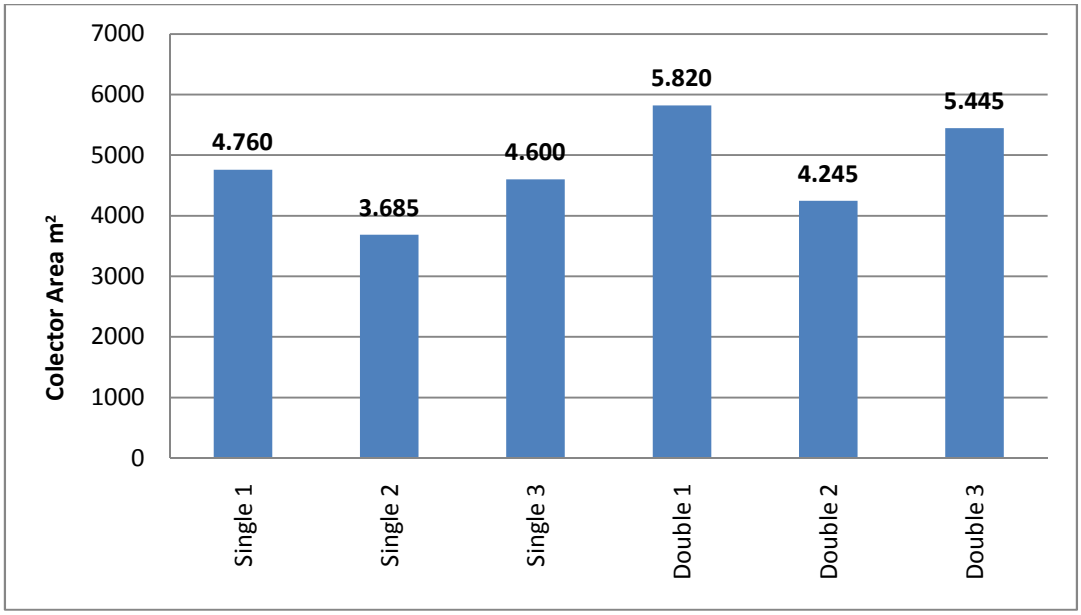

Figure 6.32 Solar Field Size

The solar field size is proportional to the energy added in each scenario, so one can have a measure of the annual average efficiency on the energy collected by the solar field by normalizing the size of the collector by the average power per well.

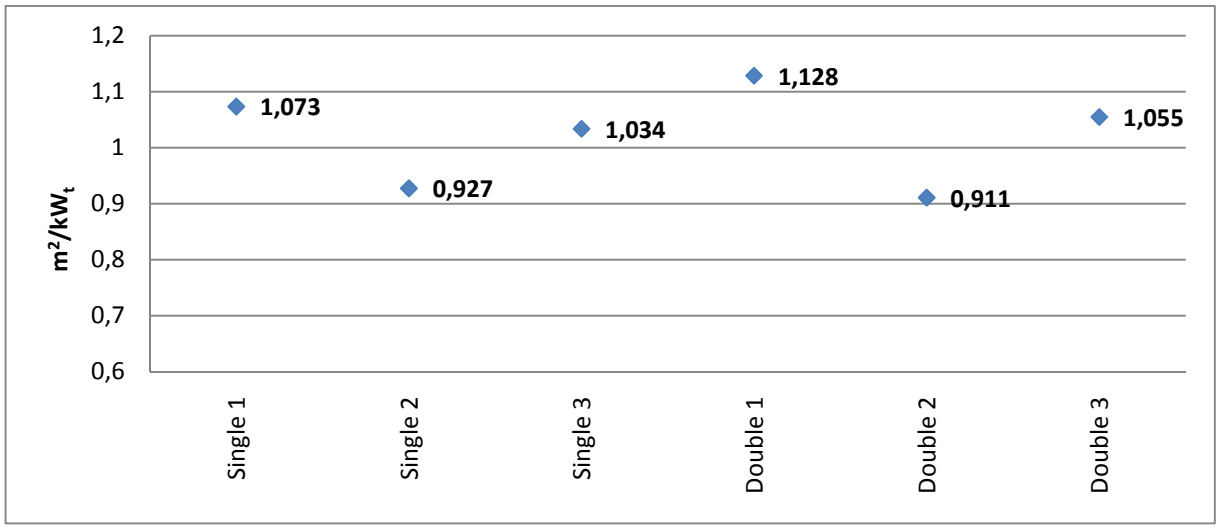

Figure 6.33 Specific Solar Field Size

6.15.4 Analysis

According to our objectives, all cases are successful in achieving their goals with interesting results in each of the proposed scenarios.

In cases where the aim was to reduce geothermal consumption, i.e., scenario N° 2, both single and double flash technologies, substantial reductions are achieved to the load on the reservoir. The single flash technology achieves a 10.36% reduction on the geofluids consumption to generate the same energy generated in the base case, the double-flash technology achieves reductions of 10.78% compared to its respective base cases. It is important to note that the double flash technology achieves a 13.44% reduction in the use of geothermal resources when compared with the base case of the single flash technology, generating 17.3% more energy thanks to energy input supplied by the solar collector field and the use of the double flash evaporation technology.

The scenario N° 2, for both single and double flash technologies, shows the smallest solar field sizes in their respective technologies, due to two factors: first, the solar energy needed in this scenario is lower than in the other cases, and more importantly, the better thermodynamic efficiency obtained in this scenario, due to the reduction of mass flow rate from the producing well, implies a higher working pressure together with the increased steam temperature achieved by adding solar energy, greatly increases the efficiency of the thermodynamic cycle.

This effect is reflected in the specific size of the collector required to operate the plant, with the lowest value among all scenarios, being 0.927 m^2/kW and 0.911 m^2/kW for single flash and double flash technologies, respectively.

With regard to the scenarios where the objective was to maximize energy output, the scenario N° 3 in single flash as well as in the double flash, produces the most electricity. This energy is generated using geothermal resources very efficiently, obtaining very high values for the specific consumption of geothermal fluids.

Although scenario N° 3 is for both technologies the scenario with the highest energy output, the scenario N° 1 has an advantage over the N° 3; that there is no need to regulate the mass flow rate from the reservoir resulting in a much simpler operation of the geothermal field, yielding results only slightly higher regarding the geothermal resource consumption and virtually the same results in the production of energy when compared to Scenario 3 in their respective technologies.

An important point in the analysis of different scenarios is the daily output power profile, where the scenarios 1 and 3 for both technologies have a profile with a daily peak around noon, variable and highly dependent on solar radiation. Even though the difference between daily maximum and minimum varies only around 20%, the power curve is not as attractive as a flat curve. A positive point for these curves is that in general, the output power peak occurs in the hours when the system undergoes electrical peak demand, resulting in the highest spot prices and therefore, selling the

energy produced in a regime that relies on solar radiation may achieve very desirable sale prices.

The power curve in scenarios N°2 is flat, making it very attractive in generating sales contracts, particularly with large energy consuming industries such as mining projects prevailing in the Chilean northern interconnected power grid.

6.16 Chapter summary

We have computed the models proposed and we have obtained thermodynamic results for each hour of the year in each of the cases analyzed, and we have a criterion for comparison different operating alternatives based on their operational performance.

These results show that in each case meets the stated objective, what remains is to perform an economic analysis of the cases proposed to obtain a broad view of the various trading strategies.

7 Economic Analysis

7.1 Introduction

The objective of the economic evaluation is to analyze from a financial perspective the performance of all the alternatives proposed in order to select the best configuration.

To perform an economic evaluation it is first necessary to understand the Chilean electricity market and the geothermal project development. With this information, we can develop a model that represents more accurately the characteristics of the market in which the proposed scenarios would develop.

7.2 Chilean Electricity Market

The electricity market in Chile is composed of major players: the electricity generating companies, the transmission companies, distribution companies, the clients regulated and unregulated and a coordinating agent. All actors involved are independent and take their decisions only to maximize their own benefit. The government controls and regulates the proper functioning of the electricity market.

Geographically, the Chilean electricity system is separated into four areas, from north to south, a) the Northern Interconnected System, b) Central Interconnected System, c) Electrical System of Aysen and d) Magallanes Electrical System. The first two systems account for 99% of the installed capacity in Chile (CNE, Capacidad Instalada de Generación, 2009) and each operates independently.

To ensure the proper functioning of each system, a criterion to meet instantaneous demand must be applied, since not all the generating units can operate all the time. This is why both interconnected systems have their own coordinating unit named Economic Load Dispatch Center responsible for coordinating the operation of the generating units with instantaneous demand of each system. The criterion used by the

coordinating centers is regulated by law. The goal is to minimize the generation marginal cost, i.e., the plants are allowed to dispatch power in ascending order according to their variable operating costs, ensuring the most efficient operation of the system.

With regard to Aysen and Magallanes electricity systems, there is only one electricity company in each, so the coordination is made by these companies privately.

The variable costs of generation include the costs of fuel used by each plant and operating and maintenance costs. These costs must be informed by each generating unit on regular basis.

For a geothermal power plant, fuel costs are zero and the operation and maintenance costs are fairly low, so the variable operating costs for a geothermal power plant are among the lowest within the electricity generation technologies, which ensures its operation into the system whenever the power plant is available, achieving high capacity factors. In general a geothermal plant will stop producing electricity only for scheduled maintenance. The variable costs of operating a geothermal plant are comparable with those of hydro and wind power plants technologies.

7.3 Geothermal Project Parameters

A geothermal energy project is divided into two major stages: the exploration phase and operation phase. Both must be taken into account when evaluating a geothermal project.

The objective of the exploration phase are: to locate high geothermal potential zones, estimate the volume of the geothermal fluid reservoir and its temperature, to characterize the rock formations that formed the reservoir, determinate the chemical properties of the geothermal fluid, estimate the potential of the reservoir, among many other technical characteristics.

To achieve these objectives there are a number of exploration techniques and strategies such as geological, hydrological, geochemical, geophysical and aerial surveys, bibliographic compilations, seismic studies and many others. The exploration phase ends with the drilling of one or more test wells that increase the confidence level on the characteristics of the geothermal resource under consideration; however it is not possible to obtain absolute certainty about the reservoir characteristics with current technologies.

Risk is an intrinsic factor for geothermal energy projects throughout the entire process of project development. The possibility of not finding the resources previously predicted is always present and one can only know with certainty the actual characteristics of the geothermal reservoir after many productive wells have been drilled and technical data is gathered during several years of regular operation.

One way to internalize the risk in the economic evaluation model is through a decision tree by assigning different probabilities to different events and weighing the various financial indicators by the respective probabilities of occurrence. Figure 8.1 shows an illustrative example of a highly simplified decision tree for the development of a geothermal energy project with an estimated net present value (NPV) of the project considering the risk of failure in the estimates.

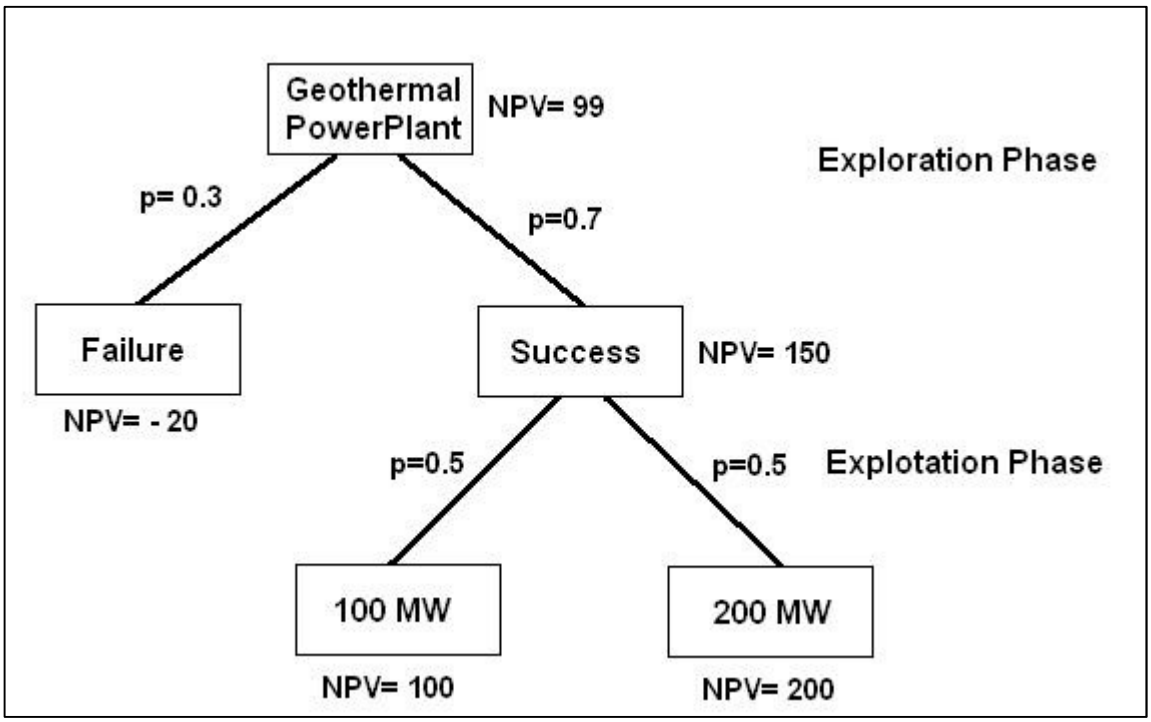

Figure 7.1 Geothermal Decision Tree

Due to the risk present in geothermal development, the economic evaluation of geothermal projects is uncertain. If the initial phases demonstrate low progress other generation technologies will prevail; however geothermal projects have positive externalities such as energy resources independence, clean development and diversification of the energy sources. Many countries have chosen to encourage the development of such technologies using market tools that reduce the private risk of the investment, for instance, U.S. geothermal companies benefit from reduced taxes, New Zealand opted by drilling and testing geothermal wells under state coverage which is then transfered to private companies (Bloomquist, 2004) (WHITE, 2006).

In this analysis, we assume that the geothermal project is at exploitation phase of the resource and all the power extracted is sold at the same price. We also assume that every well drilled behaves the same way as the typical geothermal well used for the thermodynamic analysis.

7.4 Methodology

A series of economic assumptions will be made to model the behavior of all the cases proposed earlier for the lifetime of the project. Then the results of the economical performance are analyzed and compared to draw conclusions.

7.5 Economic Model

7.5.1 Costs

The costs associated with the construction of the powerhouse and the exploitation of the geothermal and solar resources can be separated into capital costs and operation costs.

Capital costs include all the investment required for the power plant. These correspond to the costs of manufacturing of plant components, building the hybrid power plant, the costs of initial drilling and make-up drilling and steam gathering system, construction costs of the solar field and the cost of land.

The operation costs are the costs needed to keep operating the plant during its lifetime, including the cost of operation and maintenance, administrative costs, insurance taken and others.

7.5.1.1 Capital Costs

7.5.1.1.1 Prospection Phase

The discovery and exploration phase of a geothermal reservoir has a cost that represents an investment for the company developing the project. This cost varies considerably from field to field. In this study we use a prospection period of three years prior to the operational stage of the power plant. The total cost will be assumed equal to USD 20 million based on data supplied by the US Department of Energy (DOE, 1997). This cost is distributed equally to each year of the prospection phase.

7.5.1.1.2 Power House

The construction of the plant is considered to last a period of one year at a cost of 1194 US$/kW installed for a single flash power plant (DOE, 1997). For double flash power plants we assume a surcharge of 30% due to the greater complexity of this technology, so we use 1552 US$/kW. These costs include exclusively the construction of the power house.

7.5.1.1.3 Well Costs

For production wells will be considered a cost of 1272.59 US$/m (Vaca, 2008) for wells drilled to a depth greater than 2500 m. This value includes the cost of drilling and the gathering system. In this analysis we assume that all productive wells have a depth of 2500 meters with a cost of 3.18 MM USD/Well.

Since this value corresponds to a mature industry with many years of experience in geothermal wells drilling and considering that this is not the case in Chile, we assume an initial cost per well of USD 5 million. As companies engaged in drilling become more experienced, their costs will decrease to reach those mentioned above. A cost-reduction rate of 5% per year will be considered, achieving a reduction in drilling costs from 5 million to 3.18 million in 9 years.

Regarding the injection wells, we will assume that this kind of well has the same characteristics of a productive well, and therefore the drilling costs will be the same.

7.5.1.1.4 Land Cost

Land cost depends on the location of the project. In Chile, the geothermal areas where conditions are ideal for developing a geothermal solar hybrid power plant are those found in flat terrain and with high levels of solar radiation during the year. These characteristics are given in the general area of Calama (22° 28' S, 68° 54' W), placed in the Atacama Desert, the driest in the world, with vast plains suitable for the installation of solar fields. In Chile, the value of the land for geothermal concessions near Calama such as El Tatio, Apacheta, La Torta and Tuyajto is approximately 500 US$/Ha.

For the development of the geothermal power plant and its respective wells, we considered a land size of 5 hectares. For the solar field we will assume that it occupies an area equal to twice the solar field total aperture size in each scenario.

7.5.1.1.5 Solar Field

The solar field size to be installed on each proposed scenario varies and depends on the operating conditions of each case. The solar field consists mainly of concentrating mirrors, supporting structures, heat collecting elements and related connectors. The unitary cost of all these elements used here is 234 US$/m^2 (NREL, 2003) and includes all the infrastructure except for solar field terrain cost.

7.5.1.1.6 Others

Some costs common to all alternatives have not been included in this analysis, like the costs of connection to the electrical system. Parasitic loads in a geothermal power plant are small and in this analysis will not be included.

7.5.1.2 Generation Costs

Generation costs include several expenditures that depend on the amount of energy produced such as operation and maintenance of the geothermal field, operation and maintenance of the powerhouse and transmission costs as well as some fixed costs of generation, such as staff salaries, the solar field maintenance, administrative costs such as patents and licenses, etc.

7.5.1.2.1 Geothermal O&M

According to the Chilean National Energy Commission, the generation costs for a geothermal power plant operating in northern Chile corresponds approximately to 2 US$/MWh (CNE, 2009), however, other international studies differ from this number, giving values closes to 7 US$/MWh. In this study we use the projected O&M cost for 2010 of 7.57 US$/MWh (DOE, 1997).

7.5.1.2.2 Solar Field O&M

The costs of operating and maintaining the solar field depend on the size of the solar field, but there are significant economies of scale in operating larger solar fields, since the equipment used to clean the mirrors is very specific and must be purchased regardless of field size. The U.S. SunLab laboratory indicates that the annual cost of operation and maintenance of a small solar field is 10.9 US$/m^2 (NREL, 2003).

7.5.2 Income

The only income accounted in this study is the one received from the sale of the electricity produced. Others revenues may come from the treatment of the geofluid chemical features depending on the local mineral characteristics, some non condensable gases emanating from the reservoir might be commercialized. None of these incomes are considered.

All scenarios assume that the selling price of energy is equal to the average price of private contracts in the Northern Interconnected Power Grid. The electricity selling price for the November, 2008 to February, 2009 period equals 137.59 USD / MWh. (CNE, 2009). It will be assumed that all the energy produced is sold at this price.

7.5.3 Taxes

In Chile, every company must tribute 17% of their net operating profit. If there are periods where the net operating profit is negative, the company is authorized to subtract their losses from the next period profit.

7.5.4 Power Plant Size

For the economic analysis, for each different scenario will be considered a power plant with a minimum capacity equal to ten identical productive wells, each of them characterized by the typical production curve used as reference in the previous chapter. The power of each producing well in each scenario will be considered as the average of the instantaneous power for each hour of the year, obtaining an annual power average for the producing well. This value will be used to calculate the plant output power each year.

Accordingly, for the base case single flash technology, the power rating is 39.74 MW, which sums ten producing wells at the optimum point. Similarly, in the base case double flash, the power rating of the plant is 46.64 MW.

These sizes are consistent with the typical 40 MW modular plants used in the geothermal industry.

Based on these sizes, the solar field size calculated before, for each, case will be used as a reference to calculate the actual solar field size based on the nominal power rate for each scenario.

7.5.5 Decline in Wells Productivity

The prediction of the geothermal reservoir depletion over time is extremely complex and requires information that is unavailable in the early stages of geothermal projects. To gather the information needed to understand the thermodynamic and mass transfer processes occurring within the reservoir, numerous tests must be performed, includes monitoring of various wells for an extended period of time in different geographical locations of the reservoir, chemical tracer tests in the injection wells, studies of natural recharge processes within the reservoir, study the production management plan for geothermal reservoir among many others.

Because of this, prior to the exploitation phase, only some predictions about the expected results of the operation can be made. It is not before several years of production and monitoring that a reliable model of the physical processes and thermodynamics can be defined.

With this in mind, it is unlikely to determine with any degree of accuracy the behavior in time of a particularly productive well (Lovekin, 2000).

In most real cases, the productive wells decrease their production over time so it is necessary to drill make-up wells to maintain the output power over a certain limit. This phenomenon is attributed to local depletion of the reservoir and depends on the particular geological conditions of each well. In general, statistical studies conducted

in various geothermal fields have found a reduction in mass flow rate over time for each productive wells, and also this decline rate itself decays over time due to matching between local exploitation and local recharge rates (Sanyal, Butler, Brown, Goyal, & Box, 2000).

In this analysis, we will use an initial decline rate for the reservoir equal to 8% per annum and this rate will decay 10% every year.

A single reservoir pressure will be modeled for all wells, due to the fact that the production of a single well affects the production of other wells, the mass flow of new production wells drilled will be the same as current production from old wells, including the declining productivity of the reservoir. This represents the worst case scenario, because in real reservoirs, not every well is affected in the same way by the production of other wells and this depends strongly on local hydrological and geological characteristics.

For those scenarios in which the amount of geothermal fluids extracted is lower than in the single flash technology base case, the assumed decline rate is reduced by the same percentage as does the consumption of the respective scenario. The amount the decay rate drops over time will remain at 10%.

Due to declination and make-up drilling, the output power of the project will vary over time, so the nominal output power for the hybrid power plant, accounted for the initial investment, must be the maximum value of output power achieved over time.

7.5.6 Make-Up Drilling Plan

If we assume that we have the capacity to drill four production wells per year, the power plant will take three years to reach its full potential and once that happens, make-up wells must be drilled to offset the decline in productivity experienced by the reservoir.

With respect to injection wells, it is assumed that one well is drilled for reinjection for every five productive wells. The drilling of these wells will be made prior to the five production wells are drilled.

7.5.7 Annual Discount Rate, Project Lifetime and Depreciation

The annual discount rate used is 15%. The time horizon considered is 30 years. Both the powerhouse and the wells investments will be depreciated over 10 years starting the accounting year right after the investment is made.

7.5.8 Economic Indicators

To compare and evaluate the scenarios proposed, two approaches will be used to analyze the economic benefit of each case. The first one is the variation of the net present value (NPV) of the project among the different scenarios raised and the second one is to analyze the performance of the extra investment made to transform the geothermal power plant in to an hybrid power plant, we will use as indicator of the efficiency of the investment the variation of net present value of the project over the variation of the investment made with respect to their respective base cases. We will also analyze the levelized energy cost (LEC, minimum energy selling price that allows the project to be profitable) as the benchmark with other electricity production technologies to compare the competiveness on the generation market.

7.6 Economic Analysis Results

7.6.1 Single Flash, Base Scenario

In the base scenario for the single flash geothermal power plant, the results of project performance over the 30 years lifetime can be seen in the chart below, Fig 7.2

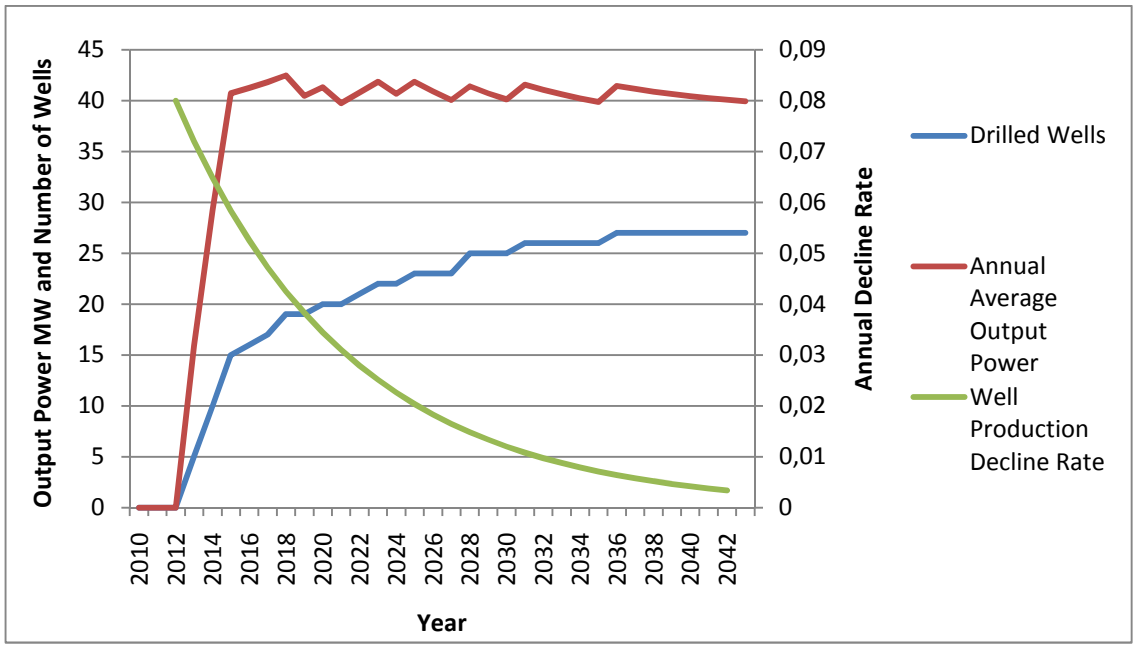

Figure 7.2 Single Flash, Base Case, Lifetime Performance

As expected, as time passes is necessary to drill make-up wells, during the third year of production, the goal of maintaining a power output equivalent to 10 productive wells is achieved by drilled a total of 12 productive wells at a rate of 4 wells per year. From this stage forward it is necessary to drill new wells to maintain the output power plant over this target. This is done drilling one well per year in the early stages and gradually decreasing to drill one well every four years after 30 years of operation finishing the lifetime period with 27 wells drilled, where 22 of them are productive and 5 are injection wells.

The rate of decline of the reservoir in this case begins at 8% and decreases at a rate of 10% per year ending the lifetime at 0.3%. The main economic indicators of this project are shown in Table 7.1.

NPV [MM US$]	**61.13**
Discounted CAPEX [MM US$]	**101.56**
Simple Payback Time [Years]	**10**
IRR	**0.26**
LEC [US$/MWh]	**86**

Table 7.1 Single Flash, Base Case, Main Economic Indicators

These economic indicators are used as a basis for comparing the performance of the scenarios number 1 to 3 for the single flash technology.

7.6.2 Single Flash, Scenario 1

The results for the 30 year operation for this scenario are shown in Fig 7.3

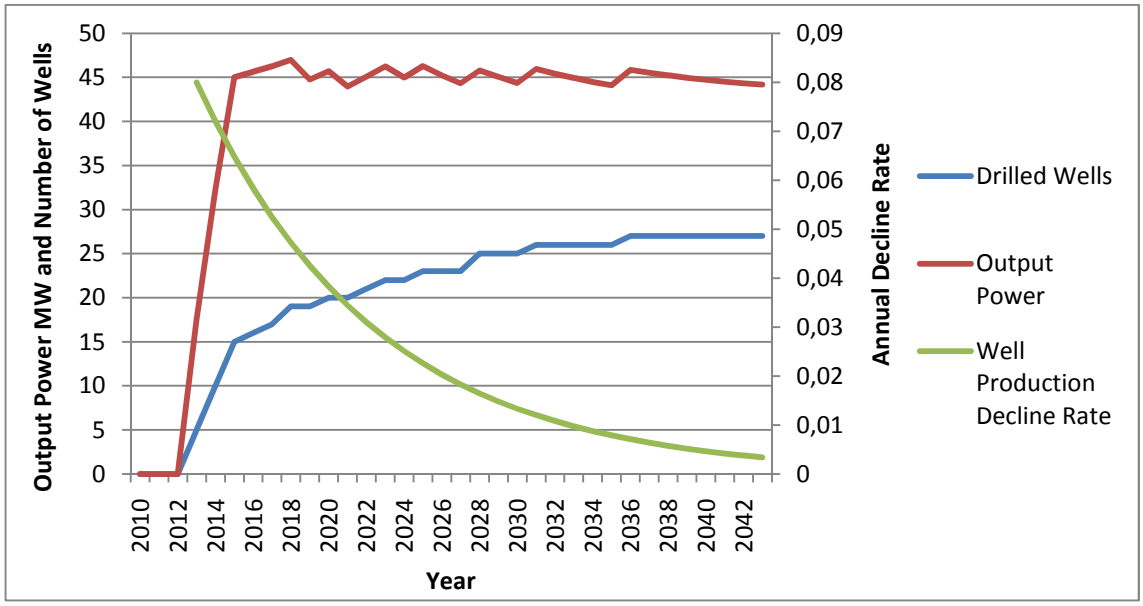

Figure 7.3 Single Flash, Scenario 1, Lifetime Performance

This scenario maintains the same decline rate as the base scenario since both scenarios have the same geothermal resource consumption, because of this, the number of wells required to maintain the output power on the target is also the same, ending the 30 year period with a total of 27 wells drilled, 22 of them corresponding to productive wells.

The energy generated in this scenario is enhanced by the energy supplied by the solar field, but, both the initial investment and O&M cost increase due to the inclusion of this new technology. The economic performance of developing this scenario under the operating conditions imposed is shown in Table 8.2.

NPV [MM US$]	65.09
Discounted CAPEX [MM US$]	112,57
Simple Payback Time [Years]	10
IRR	0,25
LEC [US$/MWh]	87,92

Table 7.2 Single Flash, Scenario 1, Main Economic Indicators

The most important results of this scenario correspond to a net present value increased by 6% over the base case and an 11% increase in the discounted investment value.

There is also a small decrease in the internal rate of return of one percentage point.

The simple payback time remains at 10 years, because the increase in investment is compensated by an increase in energy sales.

7.6.3 Single Flash, Scenario 2

Results for the operation of this scenario are shown in Fig 7.4

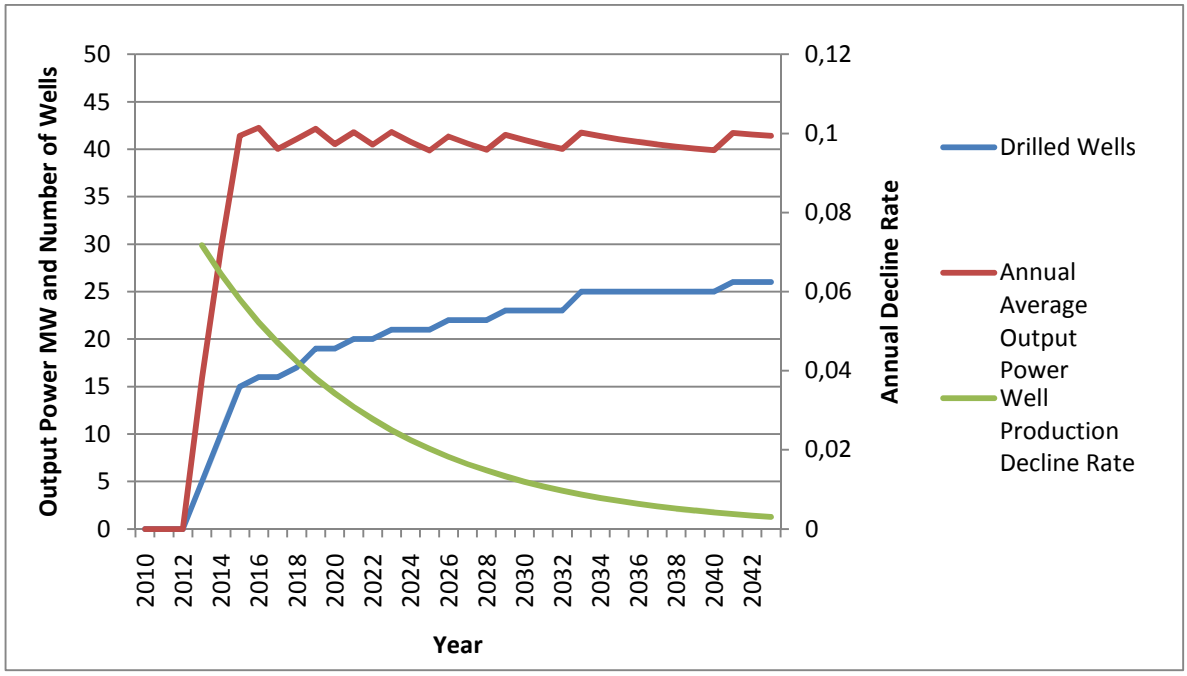

Figure 7.4 Single Flash, Scenario 2, Lifetime Performance

In this scenario, the rate of decline of the wells decreases respect the base scenario, starting at 7.17% due to decreased extraction load on the reservoir. This translates into a decrease in the number of wells drilled finalizing the 30 year period with a total of 26 wells where 21 of them are production wells.

The total energy produced is similar to the base case and the economic development of this scenario is summarized in Table 8.3.

NPV [MM US$]	55,58
Discounted CAPEX [MM US$]	105,97
Simple Payback Time [Years]	10
IRR	0,24
LEC [US$/MWh]	90,78

Table 7.3 Single Flash, Scenario 2, Main Economic Indicators

According to these data, it is not economically convenient to invest in this type of technology with the objective of reducing the rate of extraction of geothermal resources because the investment made is not recovered under the provision of drilling fewer wells. This is manifested in loss of value of the project by 9% and a lower internal rate of return of 2 percentage points.

7.6.4 Single Flash, Scenario 3

Expected performance for this scenario over its lifetime is summarized in Fig. 8.5.

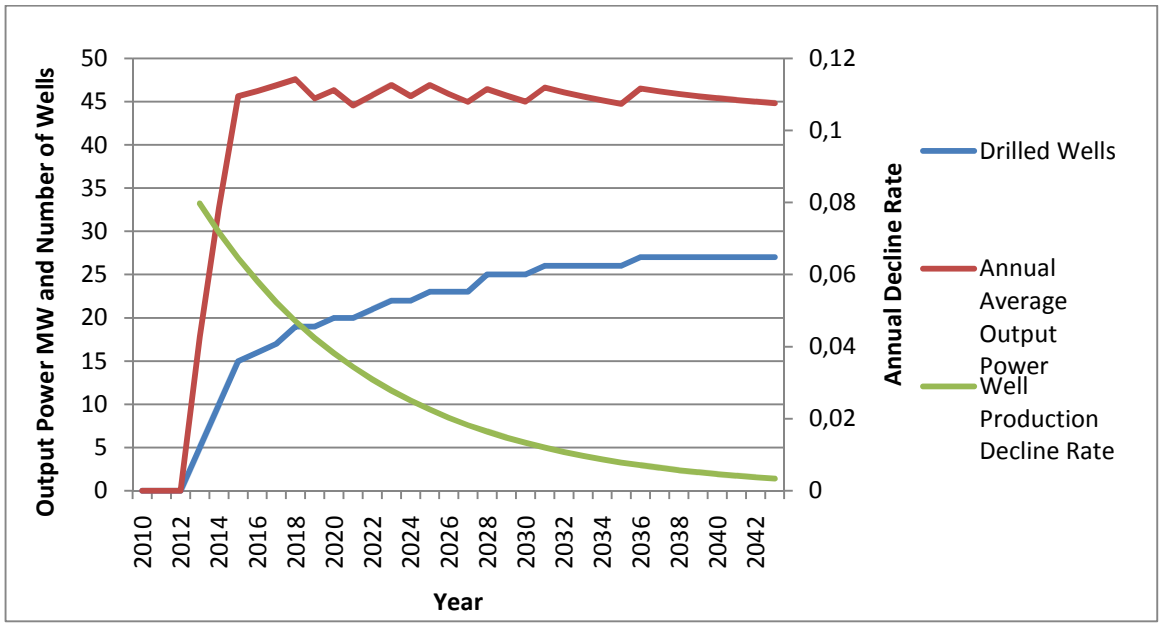

Figure 7.5 Single Flash, Scenario 3, Lifetime Performance

This scenario is essentially the same as Scenario 1. In this case, the energy produced is slightly higher and the rate of decline is a little smaller, but the reduction in geofluids extraction is not enough to reduce the amount of wells drilled over the lifetime, matching the base scenario with 27 wells drilled after 30 years of operation.

The economic parameters that characterize this scenario are presented in Table 7.4.

NPV [MM US$]	**66,93**
Discounted CAPEX [MM US$]	113,15
Simple Payback Time [Years]	10
IRR	0,25
LEC [US$/MWh]	**87,21**

Table 7.4 Single Flash, Scenario 3, Main Economic Indicators

According to these data, there is a 9% rise on the net present value of the project when compared the base case, explained by the greater amount of energy sold. The Discounted CAPEX in this case increases by 11%.

7.6.5 Double Flash, Base Scenario

Fig. 7.6 shows the expected performance for the double flash base scenario over the 30 year lifetime period.

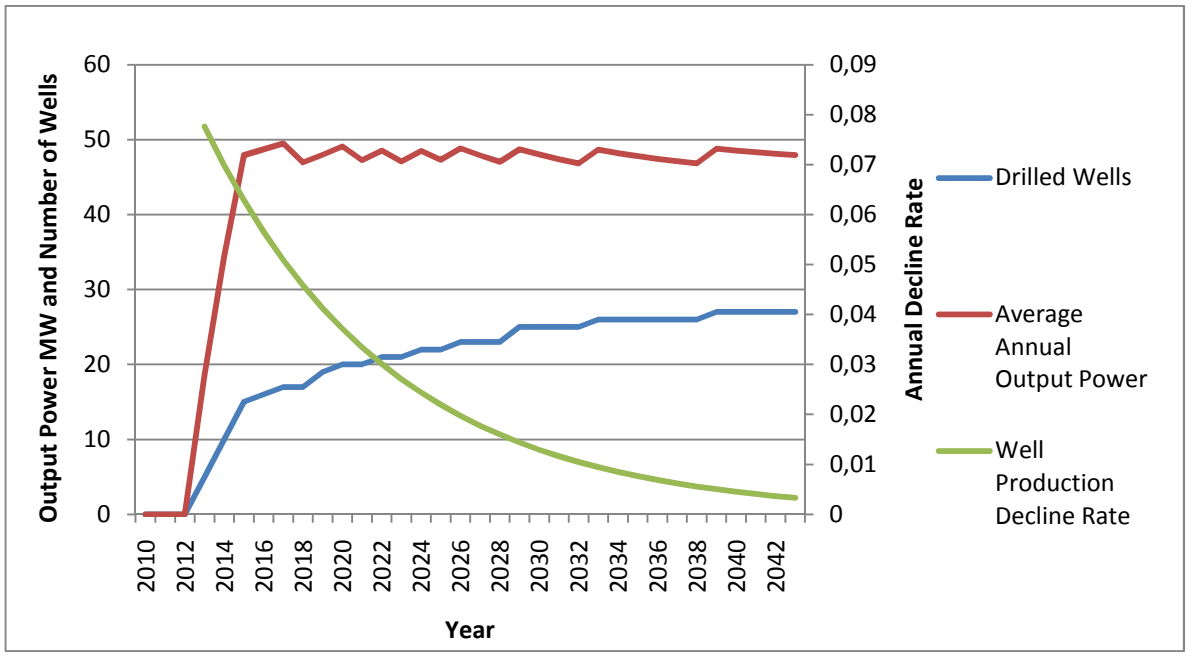

Figure 7.6 Double Flash, Base Case, Lifetime Performance

In this case, the geothermal resource consumption is lower than single flash technology, so the decline rate is smaller, starting at 7.7%, but this reduction is not enough to reduce the amount of wells drilled finishing the lifetime period with 27 wells drilled, same as the single flash base scenario. The power supplied by the thermodynamic cycle in this scenario is higher so the amount of energy sold in this scenario is also higher.

The characteristic economic indicators of the development of this geothermal alternative are given in Table 7.5

NPV [MM US$]	72,44
Discounted CAPEX [MM US$]	118.13
Simple Payback Time [Years]	10
IRR	0,26
LEC [US$/MWh]	85,42

Table 7.5 Double Flash, Base Case, Main Economic Indicators

In this case we observe an 18.5% increase in net present value of the project due to the change to double flash technology, representing an increase of 16% on the total investment valued at present time.

In this scenario, the internal rate of return remains at 26% and the simple payback time also remains in 10 years as in all previous cases.

In the following three scenarios, for the double flash technology, the benchmark parameters will be the ones obtained for this base scenario.

7.6.6 Double Flash, Scenario 1

Fig. 7.7 shows the behavior of the hybrid geothermal-solar project under the assumptions of the double flash scenario 1.

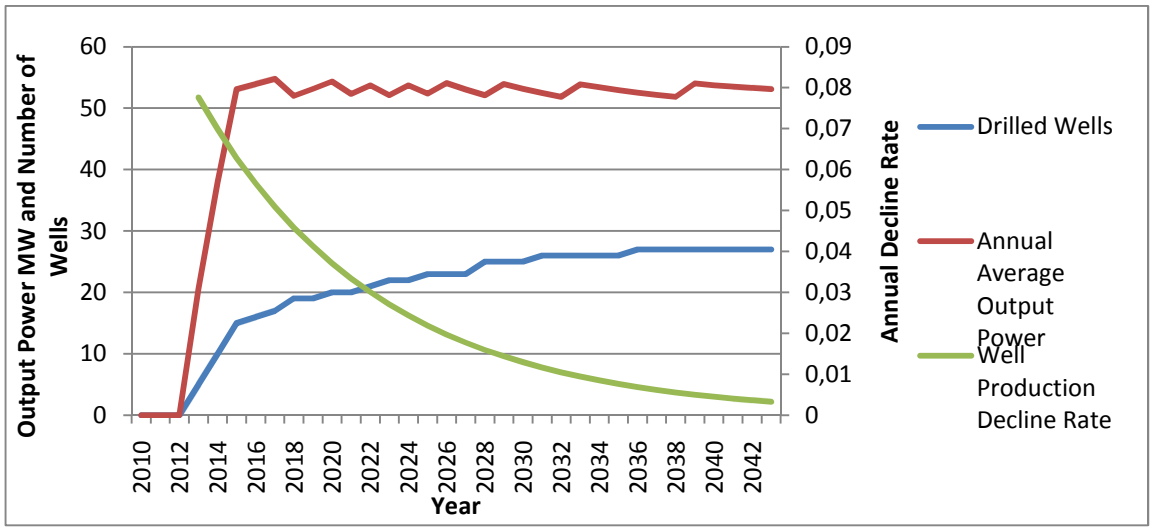

Figure 7.7 Double Flash, Scenario 1, Lifetime Performance

In this case, the geothermal resource consumption does not change with respect to the double flash base scenario remaining constant the number of wells drilled and also the wells decline rate.

The amount of energy produced in this case increases considerably thanks to the contribution of solar energy improving the performance of the geothermal field.

The parameters that characterize the development of this scenario are summarized in Table 7.6.

NPV [MM US$]	**74,92**
Discounted CAPEX [MM US$]	133,52
Simple Payback Time [Years]	10
IRR	0,25
LEC [US$/MWh]	88,86

Table 7.6 Double Flash, Scenario 1, Main Economic Indicators

The most important results of this scenario correspond to an increase in net present value of 3% over the double-flash base case, accumulating a 23% increase when compared with the base case of the single flash technology.

To accomplish the raise in present value of the project it is necessary a 13% rise in the investment, discounted to present value, over the double-flash base case.

The simple payback time remains at 10 years because the increase in investment is offset by an increase in annual energy sales. With respect to the internal rate of return, it decreases one percentage point over the base case.

7.6.7 Double Flash, Scenario 2

Expected performance for this scenario over its lifetime is shown in Fig. 7.8.

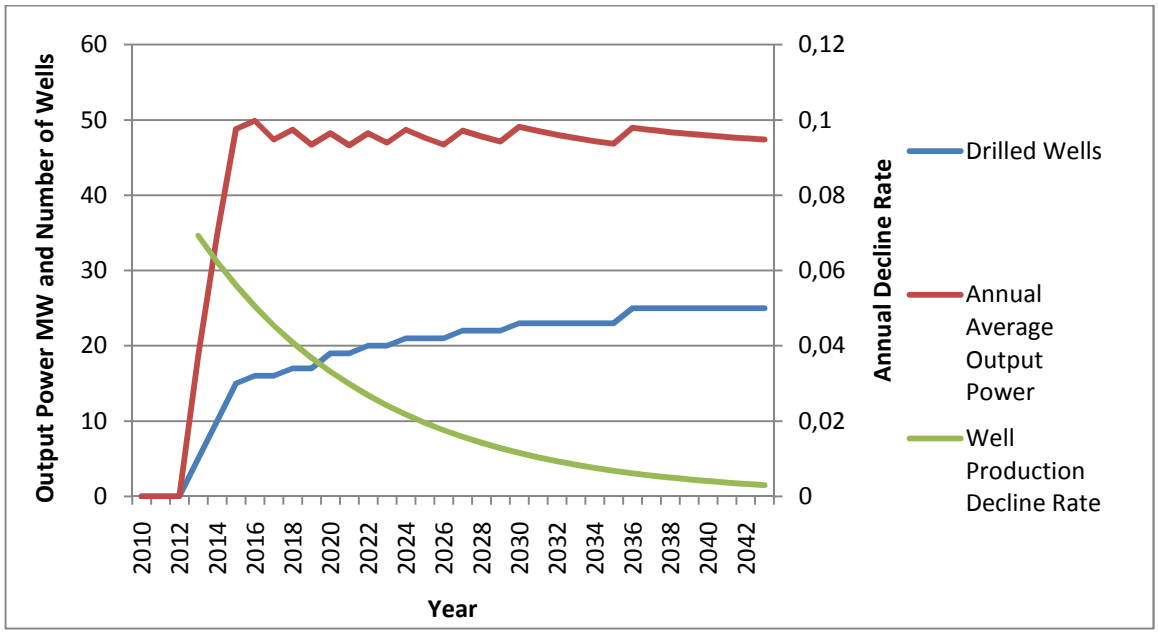

Figure 7.8 Double Flash, Scenario 2, Lifetime Performance

In this case, the output power over time is very similar to the double flash base scenario, but the geothermal resource consumption is lower due to the contribution of solar energy, reducing the reservoir decline rate, and thus decreasing the number of

productive wells needed to operate. The decline rate begins at 6.92% and after 30 years of operation, 25 wells where 20 of them are productive wells are needed to be drilled.

The economic parameters that reflect the performance of the hybrid power plant in this scenario are summarized in Table 7.7.

NPV [MM US$]	65,74
Discounted CAPEX [MM US$]	123,36
Simple Payback Time [Years]	10
IRR	0,24
LEC [US$/MWh]	90,28

Table 7.7 Double Flash, Scenario 2, Main Economic Indicators

Based on economic data of this alternative, it is not attractive to use the hybrid power plant in order to save geothermal resources, because there is a decrease in the value of the project, in this case, a 9% over the base case double flash. This is produced because the increase in investment occurs in early stages of the project and the savings, i.e. the reduced amount of wells needed, manifests late in the lifetime of the project accounting for low present value cash flows.

The internal rate of return shows a decrease of 2 percentage points and the investment done has increased by 4%.

7.6.8 Double Flash, Scenario 3

The third scenario for the double flash technology behaves according to the chart shown in Fig 8.9.

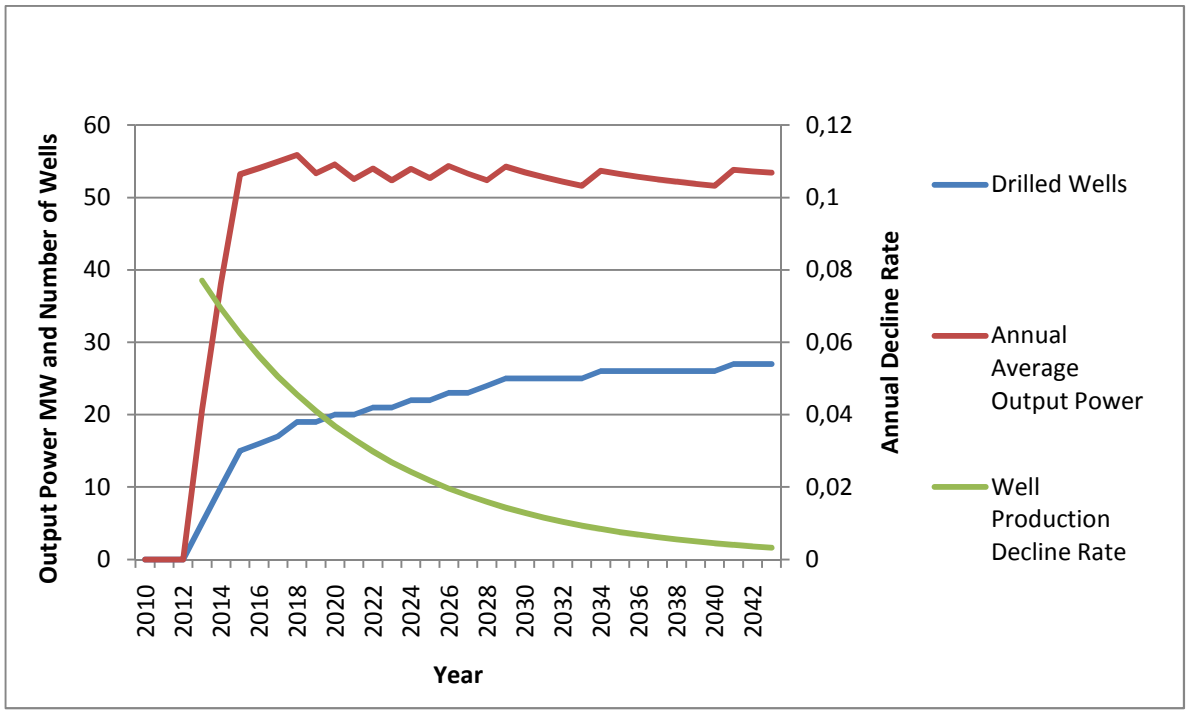

Figure 7.9 Double Flash, Scenario 3, Lifetime Performance

In this case, some savings are achieved with the use of geothermal resources but it is not enough to decrease the amount of productive wells drilled, finishing the lifetime period with 22 productive wells, same situation as the corresponding base scenario.

There is a significant increase in the output power allowing the generation of more electricity than in the previous cases.

The economic indicators that characterize this scenario are shown in Table 7.8.

NPV [MM US$]	76,35
Discounted CAPEX [MM US$]	133,82
Simple Payback Time [Years]	10
IRR	0,25
LEC [US$/MWh]	88,32

Table 7.8 Double Flash, Scenario 3, Main Economic Indicators

In this case, we have a 5% increase on the net present value of the project compared to the double flash base case, and a cumulative project value rise of 25% over the single flash base case.

The internal rate of return shows a small decrease of one percentage point while the simple payback period of investment remains constant.

The investment related to this scenario shows an increase of 13% over the double flash base case.

7.7 Analysis and Discussion

One of the most relevant parameter when evaluating a project is the net present value of the estimated cash flows. This value shows a comparative performance of a project taking into account the opportunity cost represented by the discount rate used for calculation.

In this analysis we are interested in the variation of the net present values for the different scenarios analyzed. These values are shown in Figure 7.10.

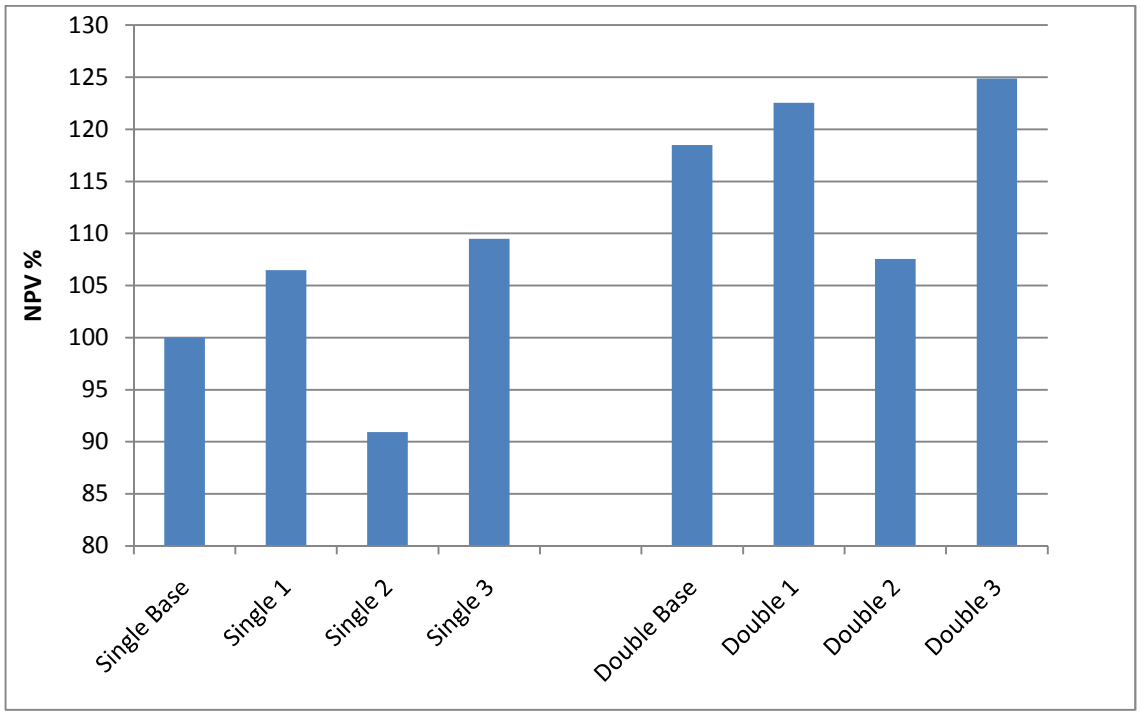

Figure 7.10 Net Present Value variation

The first thing shown in Fig 7.10 is the fact that all scenarios have positives values for their NPV's meaning that all the projects are profitable. The important thing to notice is the variation NPV compared to the respective base case.

For both single and double flash technologies, there is an increase in NPV when scenario number 1 or 3 are applied, compared to their respective base scenario. Scenario number 3, for both technologies, is the one with the greatest increase in

NPV. This means that under the assumptions made, the extra energy produced over the lifetime of the project compensates the extra investment made for the solar field.

Due to the loss of NPV evidenced in the scenario number 2, in which the proposed goal was to decrease the consumption of geothermal resources. From an economic standpoint and based on the assumptions made, it is not recommended to adopt it given that the increase in initial investment to install the solar fields is not compensated by reduction of the number of wells needed for energy production. Although a decrease in the number of productive wells necessary due to the decrease in the rate of extraction of geothermal resources does save future investments, such savings happens so spaced in time and distributed throughout the project lifetime that the present value of those savings is smaller than the investment needed to achieve those savings, decreasing the total project NPV. We will analyze this effect deeply in the next chapter, because this might be strongly dependent on the reservoir deployment assumptions.

To analyze the economic efficiency of different scenarios, the following indicator is proposed.

$$\frac{\Delta NPV}{\Delta I}$$

Where ΔI represents the variation in the amount of investment required respect to the corresponding base case, quantifying the extra cost of implementing each scenario. For the double flash base case, ΔI represent the investment gap between single flash and double flash technologies.

ΔNPV represents the change in net present value of the corresponding scenario with respect to the base scenario, quantifying the gains related to implementing the hybrid power plant. For the double flash base case, the difference between the NPV of both base scenarios will be used.

The values for the different efficiency of the solar investment are shown in Figure 7.11.

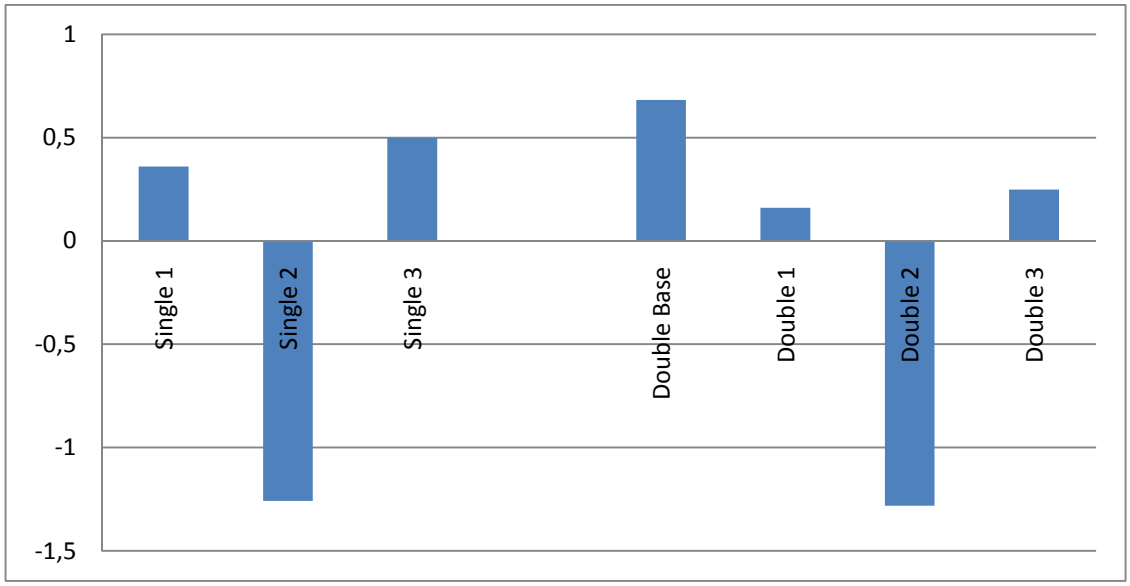

Figure 7.11 Efficiency of the solar investment

According to the figure, the efficiency of the solar investment shows how many dollars the NPV will change if you invest one extra dollar on the solar field. It is clear that in scenarios number 2 it represents a destruction of value under the assumptions made. We note also that the base case for the double flash is the technology that has the highest investment efficiency, it means that switching from a single flash geothermal power plant to a double flash represents the best investment so it must be the first choice to consider when looking for alternatives to generate more value for the energy generation project prior to the construction of the power plant.

With respect the scenarios where solar energy is used, both for single flash and double flash technology, the scenario number 3 is the one that is more efficient in creating value followed closely by the scenario number 1.

Finally, based on the assumptions made for this model, it is conceptually better from the economic point of view to invest in solar technology in order to help produce

more energy from the geothermal reservoir because it produces more energy, rather to use solar energy aiming to reduce consumption of geothermal resources.

To analyze the competitiveness of these technologies with respect to other forms of generation will use the methodology of levelized energy cost (LEC). The LEC corresponds to the minimum selling price of electricity that make a generation project still profitable. To calculate the LEC it is necessary to account for all the incomes and expenses and then equal the NPV to zero to find the electricity price that will pay for the investment and the operation of the energy project. This value is a characteristic parameter to compare different forms of generation economically.

The LEC of various conventional generation technologies are shown in Figure 7.14 according to the California Energy Comision, (CEC, 2007). This figure also shows the LEC obtained for each generation scenario proposed for our geothermal solar hybrid power plant.

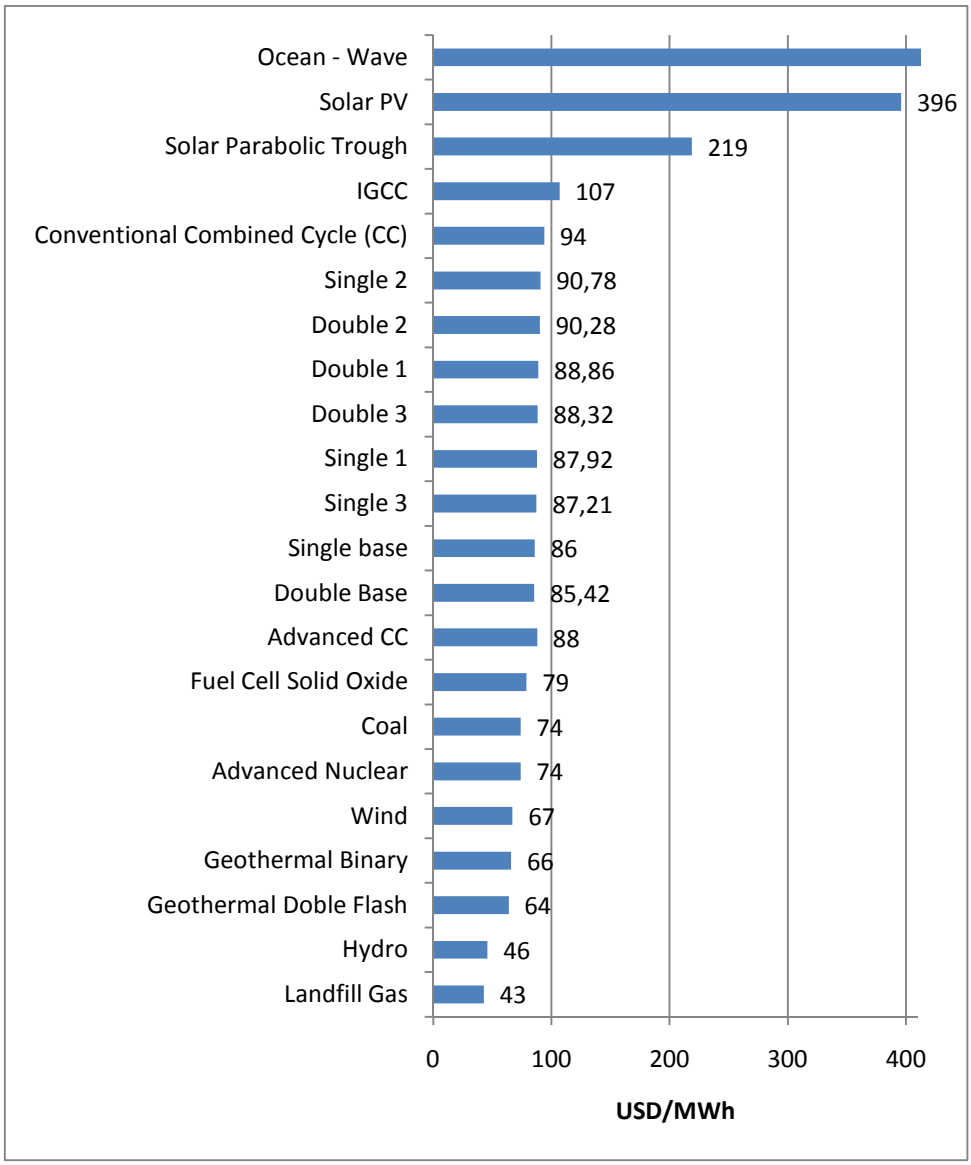

Figure 7.12 Levelized Cost of Energy Comparison (CEC, 2007)

Clearly, the level of costs obtained through this hybrid technology is competitive with other generation technologies even on the market of conventional electricity generation.

It is important to note that the LEC associated with solar thermal technology is by far larger than the one obtained by the geothermal solar hybrid plant, which is mainly

due to the fact that solar energy in our case is used with a much higher efficiency than ordinary solar thermal power plant, which means lower costs and represents an important opportunity for the industry related to solar thermal generation to develop and expand to other markets.

Another important point is that the hybrid generation principle can be applied to geothermal plants already built, improving the efficiency of the exploitation of the geothermal resources and increasing the amount of energy produced by these plants, contributing to a clean, sustainable and economical way to produce electricity.

The basic conditions for the implementation of geothermal solar hybrid power plants are a minimum level of solar radiation, land flat enough to install the solar field and hydrological and geological conditions favorable for the exploitation of geothermal resources, all happening in the same place.

The general area of Calama in northern Chile is particularly favorable for the installation of this technology due to the arid plains provided by the Atacama Desert and high solar radiation levels present in this area coupled with a high geothermal potential evidenced by more than a dozen geothermal exploration concessions given to various companies in the area.

8 Sensitivity Analysis

8.1 Introduction

Many of the assumptions made in the economic analysis are subject to variations over time or depend on market conditions. In this chapter, we present some scenarios where some of the most changed influential parameters for the development of the hybrid power plant have been changed.

For the sensitivity analysis, the NPV of the project will be used as the benchmark. The parameters analyzed are: energy selling price, solar field components cost and the decline rate of the geothermal reservoir.

We will analyze three scenarios, one optimistic, which increase the selling price of energy and reduce costs of the solar field, a pessimist, which reduce the selling price of energy and increases the cost of the solar field and finally a scenario that changes the decline rate of the geothermal reservoir in those cases where the consumption of the geothermal resources is reduced.

8.2 Optimistic Scenario

This scenario will increase the selling price of electricity by 25% and decrease the cost of the solar field by 25%, the results are shown in Figure 8.1

In this scenario is clear that in all the cases better economic results are obtained, increasing the project's value by 10% for those alternatives which favored the production of energy, i.e. cases numbered 1 and 3. In cases number 2, there is a big reduction of the loss of value presented before, decreasing by half the gap between the present value of each case number 2 and the present value of its respective base case.

With respect to the solar investment efficiency in Figure 8.2, we obtain an increase up to 0.5 in the solar investment efficiency, which is a reflection of decreased levels of investment and increased profits given the assumptions made in this scenario.

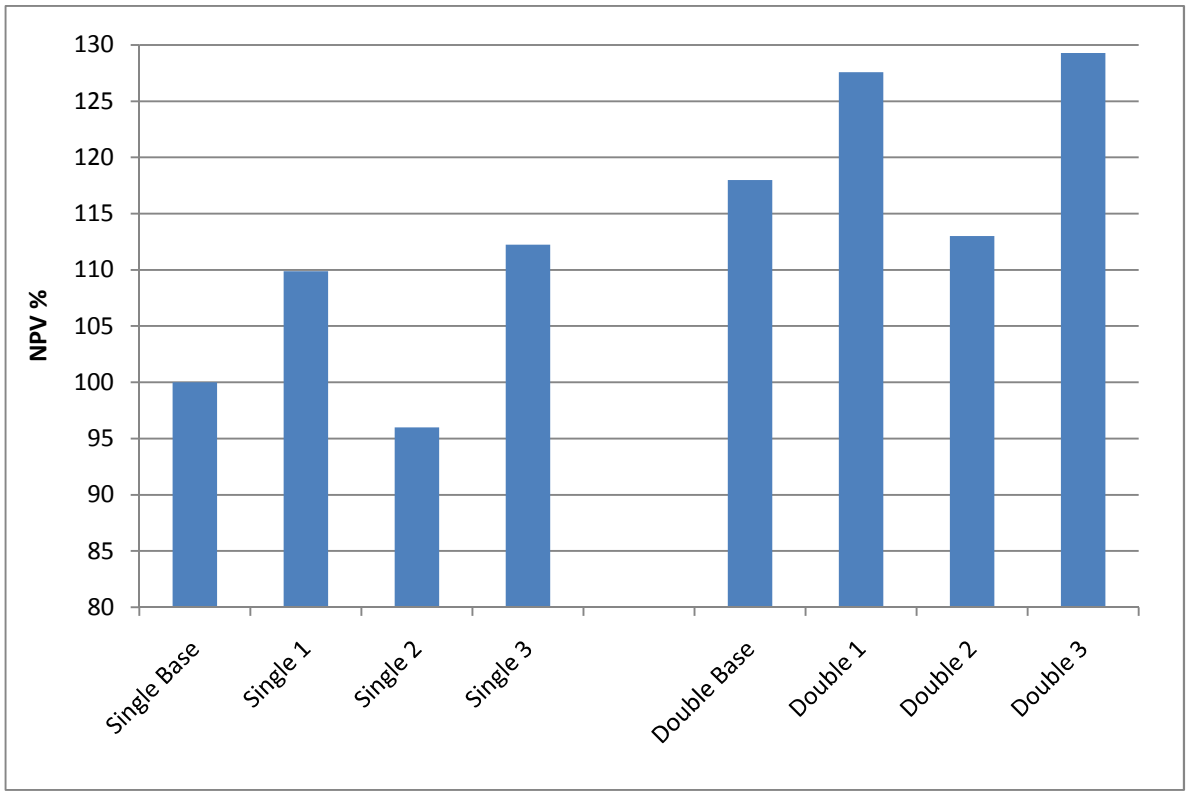

Figure 8.1 NPV Variation, optimistic scenario.

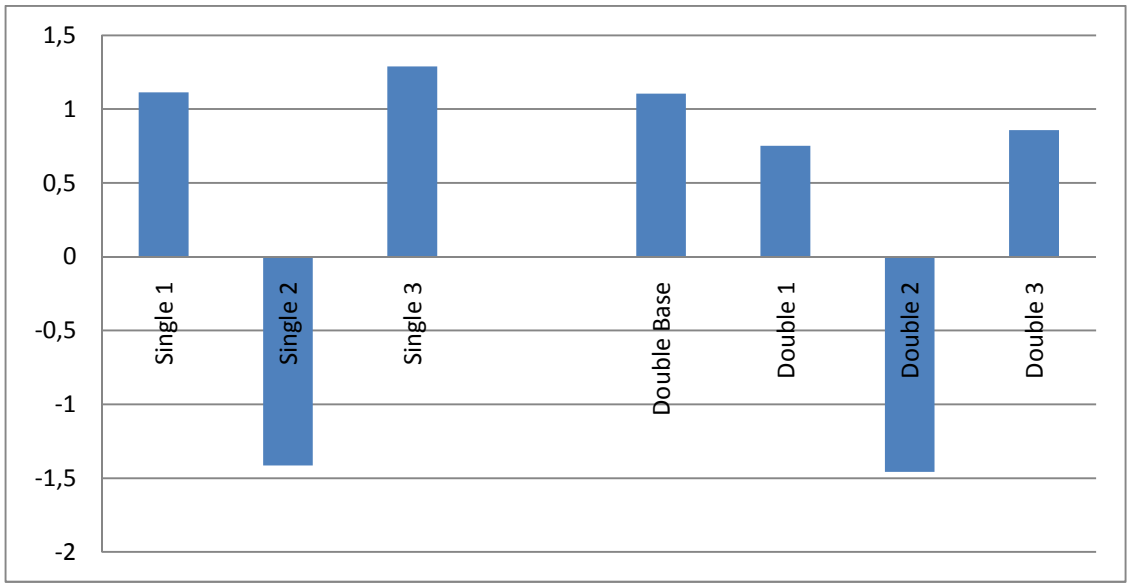

Figure 8.2 Solar Investment Efficiency, optimistic scenario

8.3 Pessimistic Scenario

This scenario will decrease the selling price of electricity by 25% and increase the cost of the solar field by 25%, the results are shown in Figure 8.3 and figure 8.4

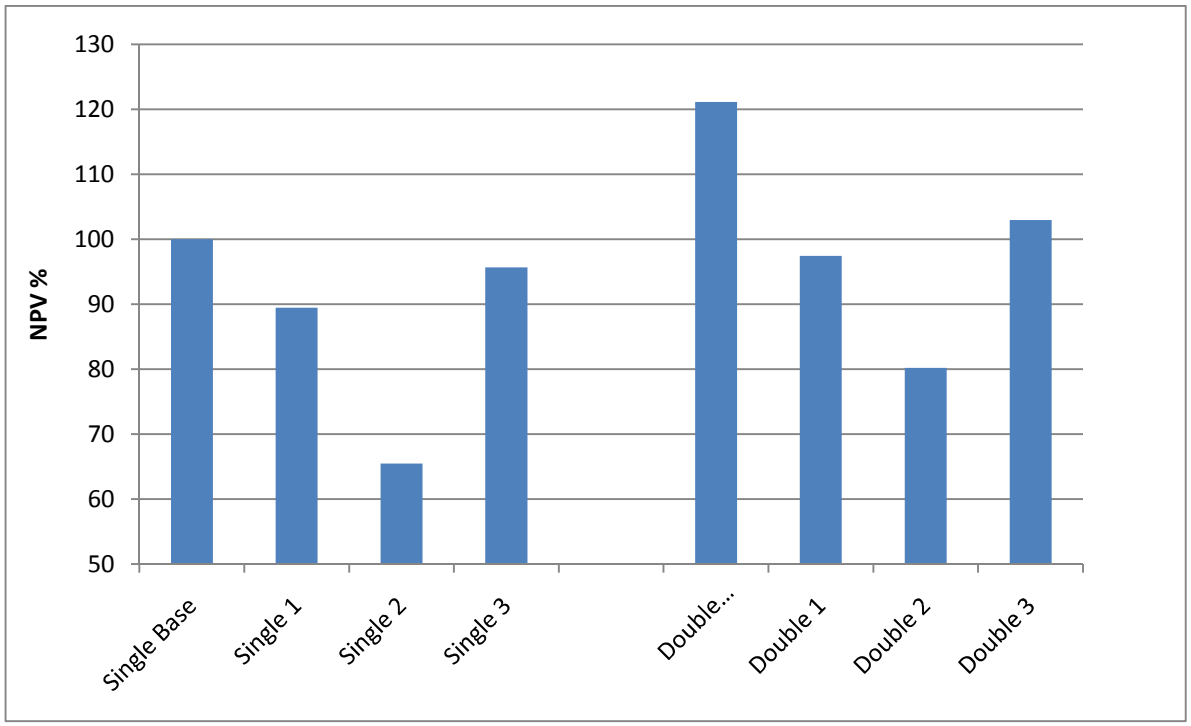

Figure 8.3 NPV Variation, pessimistic scenario

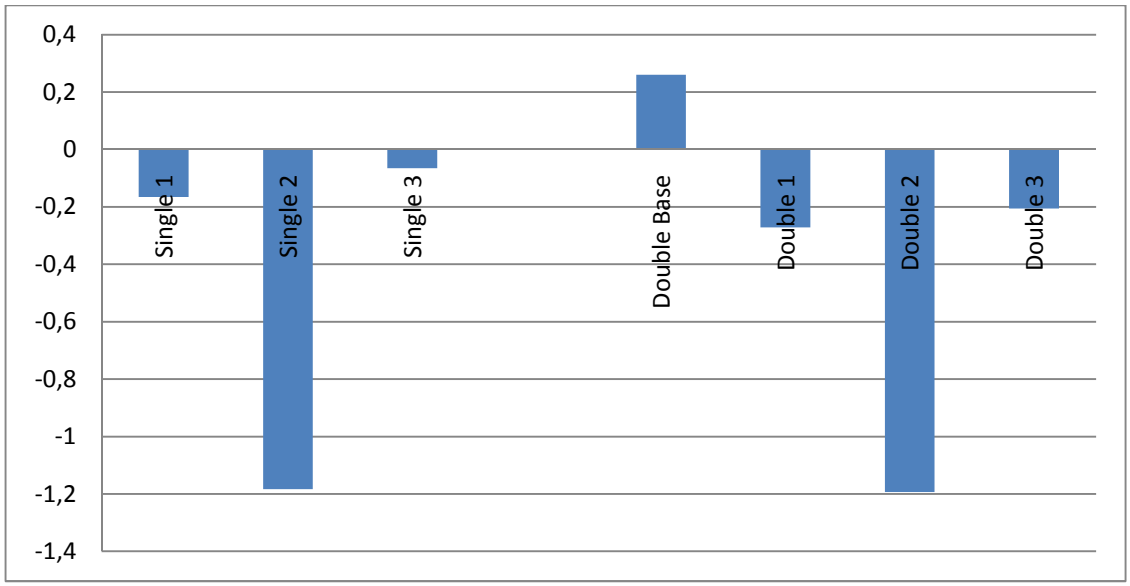

Figure 8.4 Solar Investment Efficiency, pessimistic scenario

This scenario shows the dependence of hybrid technology, as is expected, to the markets of the comprising components and its related output products, the energy produced. By increasing costs of the solar field and decreasing the selling price of

energy, all cases show a decrease in the NPV of the project. There is a certain threshold level for a certain pair of the selling price of energy and cost of the solar field that enable this technology to be economically convenient.

With respect to Figure 8.4, all the cases that include solar energy show a negative value of the solar investment reflecting the loss of value generated by it.

8.4 Decline Rate Scenario

In this scenario we will change the decline rate rule of the geothermal reservoir. In our economical analysis we assumed that changing repeatedly the mass flow rate from the reservoir did not have an impact on the behavior of the reservoir. There are no practical or theoretical studies on the matter so it was assumed that a certain decrease in the geothermal resources consumption will equal a proportional decrease in the depletion rate. In this part of the analysis we will consider the hypothesis that states that continuous changes in the mass flow rate from the reservoir will produce pressure waves within the reservoir that will fracture the rock and will improve the reservoir's internal irrigation system. If this hypothesis is correct, we will assume that in scenarios number 2, where the mass flow rate from the reservoir experiments big changes on a daily basis, the depletion rate will drop to half. In this Scenario we will keep all the rest of the parameters the same way they were for the economical analysis.

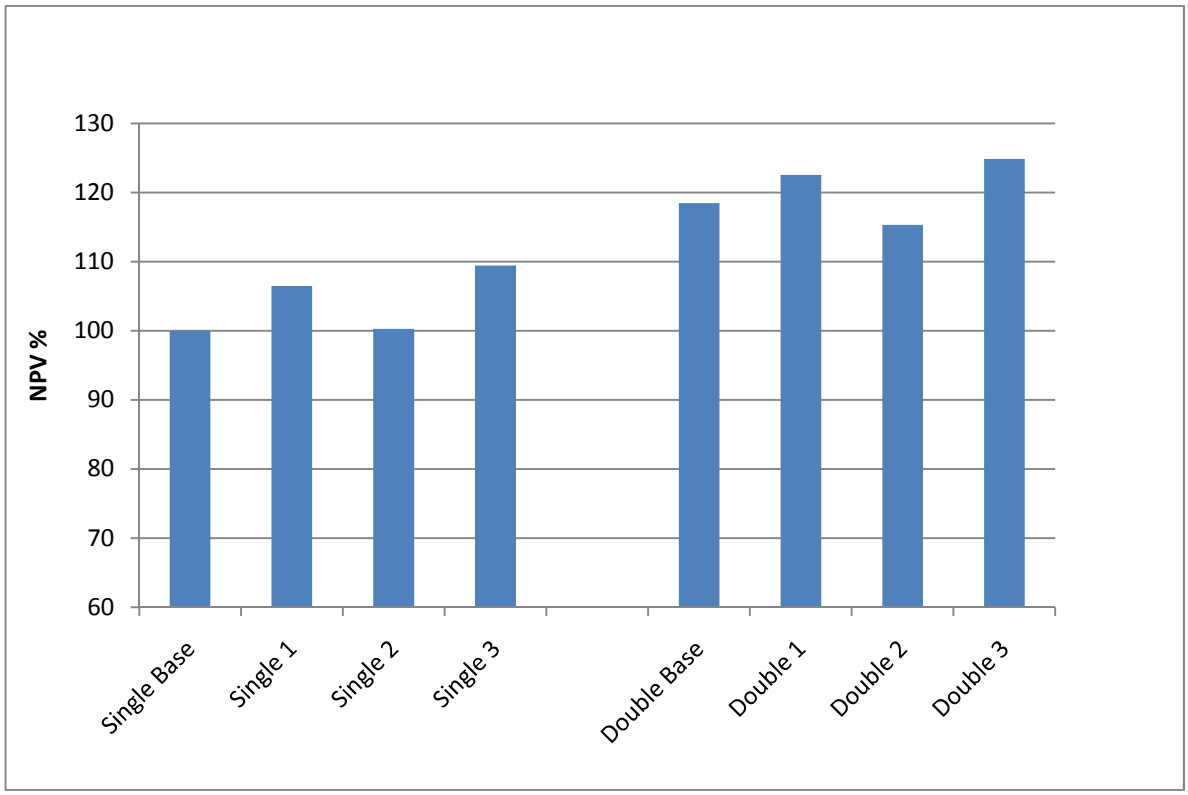

Figure 8.5 NPV Variation, decline rate scenario

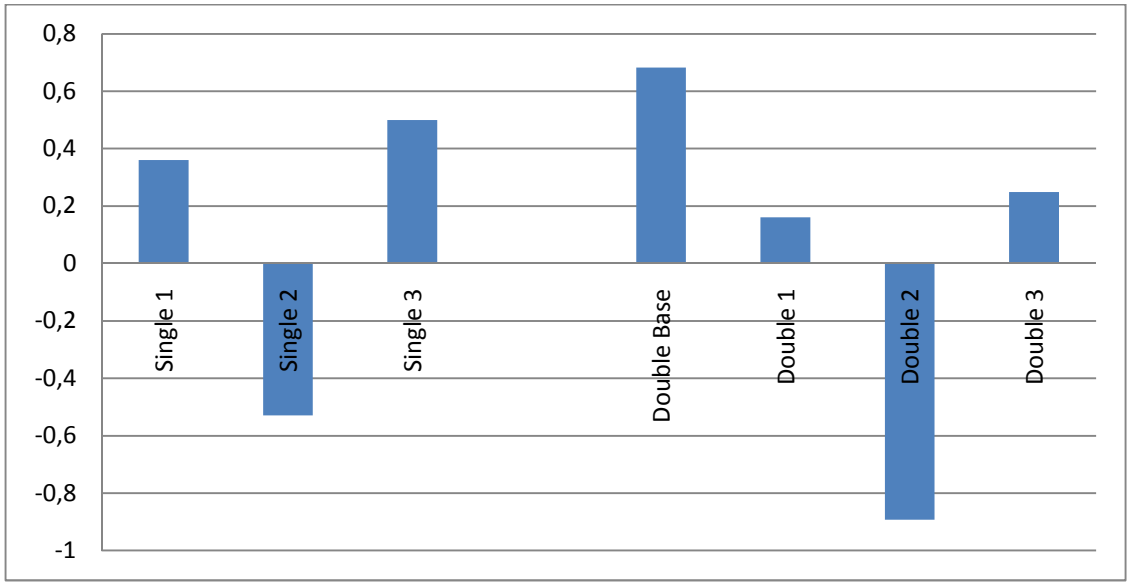

Figure 8.6 Solar Investment Efficiency, declination rate scenario.

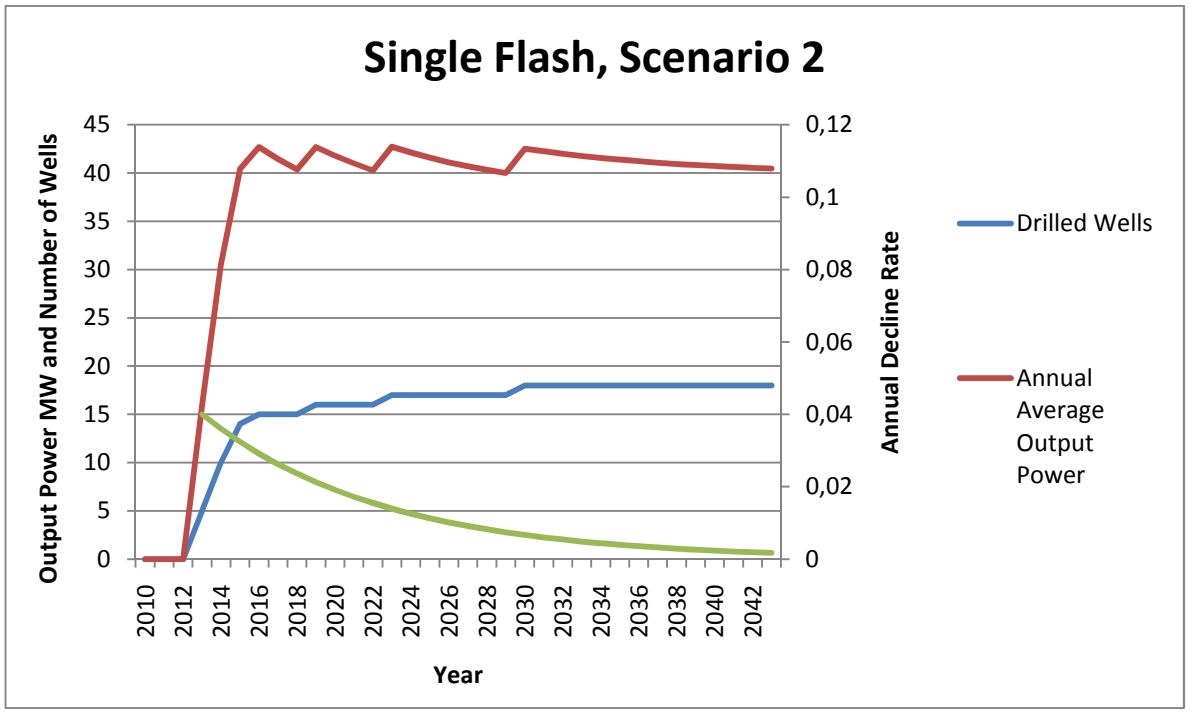

Figure 8.7 Single Flash, Scenario 2, lifetime behavior to ilutrate the reduced decline rate impact.

The results obtained in this scenario are interesting and show a new option that had not previously disclosed in this investigation. While the data are based on an assumption that has not been tested, they show an increase in the present value of project that supports the fact that it is possible to use solar energy to improve the performance of the geothermal field, using less geothermal resources to produce the same amount of energy.

The efficiency of the investment is also improved, but total amount invested is lower than the base case, due to the reduced cost of drilling, so the value ΔI results negative, while ΔNPV switches to positive, that's why the indicator remains negative.

9 Conclusions

As presented in the chapters, this research is framed in a World facing an energy crisis caused mainly by the burning fossil fuels, in a country where 71.3% of the primary energy comes from fossil fuels, most of which are imported. Under these conditions, the energy challenges that Chile and the world are facing are clear, to cut the GHG emissions and reduce the foreign energy resources dependency, especially of the Chilean energy system, as a matter of national security and also to benefit the local economy by finding and exploiting sources of energy that are local, sustainable over time and environmentally friendly to provide a reliable foundation for the development of society. In both respects, the results of this research are promising.

From a thermodynamic point of view, in the proposed cases the objectives for the operation of the hybrid power plant were achieved, both for the single and double flash technology. In all the cases, the simulation models can predict the thermodynamic behavior of the system and are an effective model tool based on basic thermodynamic principles.

With regard to operating strategies that were proposed, Strategy N°1, where the objective was to produce as much energy as possible while maintaining the operating conditions identical to the base case, achieved an increase on the energy production by 11.6% for the single flash technology when compared to its base case and 10.7% for the double flash technology, when compared to its base case. This increase in the amount of energy produced is exclusively caused by the use of solar energy and produces an output power profile with daily peaks, which roughly coincides with the hours of peak energy demand, raising the selling price of this energy in the spot market. The main advantage of this generation scheme is the simplicity of its operation, where geothermal components operate the same way they do in a conventional geothermal power plant, allowing the solar radiation to be the only system variable.

The objective of the strategy number 2 instead, was to use all the solar energy available to save geothermal resources, reducing the wells outflow and finally produce the same energy as in the base case, allowing a virtual increase in the life of the geothermal reservoir. In this case we reached reductions in the consumption of geothermal resources up to 10.4% and 10.8% for the single and double flash technology respectively when compared to their own base cases. While the goal was met, reducing geofluids consumption, the operation under this type of strategy requires constant monitoring of the production rate of productive wells based on the behavior of the solar field, which in practice is complex and has never been done before.

The geothermal reservoir's behavior is unknown when it is subjected to constant change of pressure and outflow rate. This gives the space for the hypothesis raised in section 8.4, where these constant changes increase the reservoir's internal irrigation system, reduce the decline rate, reduce the amount of productive wells needed to be drilled and improves the performance of the entire project.

One particular advantage of this production plan is an output power curve flat and constant, making it more attractive from a commercial standpoint.

The financial results show a revealing scene in terms of operational strategies proposed. With regard to Strategy N° 1, the results of the economic simulation for the lifetime of the project show an increase in the net present value for the single and double flash technology respectively compared with their corresponding base cases. But when it comes to the Strategy N° 2, the economic simulation, under the assumptions made, shows a destruction of the project value, but when the decline rate assumption is changed, the NPV of the project is increased. These results show that we cannot conclude rigorously about the convenience of using solar energy to reduce consumption of geothermal resources without having studied the impact of using geothermal resources with variable mass flow rate on the internal dynamics of the geothermal reservoir.

From our results we may conclude that there is a chance that we can prolong the reservoir lifetime using solar energy and even save money by having fewer wells to drill.

From the economic performance standpoint, it is convenient to harvest the maximum potential energy that can be obtained from the geothermal and solar energy working together, as proposed by Strategy N° 1, as long as the cost of the solar field and the energy selling price stay in between certain threshold determinate by the local markets.

A third strategy was studied, as the result of the union of the two strategies presented above, which operates the hybrid power plant at the optimum possible rate at all times, obtaining attractive results, both thermodynamic and economically, however, the level of complexity in this strategy is the same as the one discussed for Strategy N° 2, which requires further development of industry and knowledge about the behavior of the reservoir and the hybrid power plant, representing somehow a second developing stage for this type of electric generation.

For the Chilean electricity market, the geothermal solar hybrid generation represents a useful tool to meet the government energy targets, allowing to provide a emission-free and environmentally friendly base load energy, with a high capacity factor. Geothermal solar hybrid generation is an opportunity to harness the huge energy potential present in northern Chile, to meet local needs with domestic, reliable and clean energy source, making a contribution to the local economy, strengthening the national energy system expanding the energy source mix and reducing energy dependency from other countries.

The practical results of this study are valid only for the general area of Calama, Chile, however, several other geothermal fields in Chile and the world have similar climatic characteristics: the southwest of USA, the north of México, the northern part of Africa, Australia and some parts of Central America share similar atmospheric characteristics. Certainly, a specific study should be performed for each locality but,

according to the results obtained here, we recommend using solar geothermal hybrid energy when both resources are available given the synergies of bringing these technologies together.

Another important aspect in bringing geothermal solar hybrid generation is an opportunity for the development of solar energy industry. Solar thermal energy industry have been struggling to become a competitive source of electricity over the past years, now, solar geothermal hybrid generation presents an opportunity to broadening the range of utilization of the solar fields, since these hybrid power plants can be considered as an upgrade from regular geothermal power plants already in operation, a somewhat conversion kit can expand the market for solar fields stimulating markets to reduce solar field costs.

Some aspects that are revealed from this research and that require detailed studies to move toward the goal of making this hybrid technology happen are varied, one of the most important one is studying the impact of repeatedly vary the flow rate of extraction and injection on the behavior of the geothermal reservoir. Another important point is the quality of information available and in this sense, the quality of solar radiation data available for Chile are scarce and of dubious quality, it is important to have an extensive solar record both in time and locations in order to make a more complete and reliable study on climate variability as well as geographical variability and its impact on the thermodynamic and economic performance of this technology.

While this type of electricity generation is limited to the local availability of geothermal resources, and conditioned on a certain amount of solar radiation that support this type of hybrid generation, the results show a contribution aiming in the direction of the energy revolution that the world needs, presenting a clean and sustainable alternative energy source.

Solar geothermal hybrid generation is not the solution to all of the world's energy problems, but it is definitely a concrete contribution in the right direction. We hope to see in the near future this type of power plants operating all over the world.

REFERENCES

Abengoa Solar, T. C. (2007). *NREL CSP Technology Workshop, Panel 1 – Central Receivers PS 10 and PS 20 Power Towers in Seville, Spain.*

Academia Brasiliera de Ciências, Royal Society of Canada, Chinese Academy of Sciences, Academié des Sciences, Deutsche Akademie der Naturforscher, Indian National Science Academy, y otros. (2006). *Joint Science Academies' Statement: Global Response to Climate Change.*

Aravena, M. (2006). *Geothermal Energy: Contribution to the Country's Energy Security.* Santiago: Strategies for the development of geothermal industry in Chile.

Bloomquist, G. (2004). *Providing Incentives For and Reducing the Risk of Development* . Washington: United States Geothermal Policy.

Cardemil, J. M. (2006). *Modelación de Flujo Bimásico en un pozo geotérmico.* Santiago de Chile: PUC.

CEC, C. E. (2007). *Comparative Costs of California Station Electrcity Technologies.* California.

Chen, Y.-F., & Funke, M. (2010). *Global Warming and Extreme Events: Rethinking the Timing and Intensity of Enviromental Policy.* CESifo.

CNE. (2009). *Balance Nacional Energético 2008.* Santiago: CNE, Comision Nacional de Energia (Chile).

CNE. (2009). *Capacidad Instalada de Generación.* Santiago.

CNE. (2009). *Fijación de Precios Nudo Octubre de 2009 Sistema Ïnterconectado del Norte Grande, Informe Técnico Definitivo.* Santiago.

DiPippo, R. (2008). *Geothermal Power Plants; Principles, Applications, Case Studies and Enviromental Impact, Second Edition.* London: ELSEVIER.

DOE. (1997). *Renewable Energy Technology Characterizations.* Washington DC: U.S. Department of Energy.

Duffie, J. A., & Beckman, W. A. (1980). *Solar Engineering of Thermal Processes.* New York, USA: wiley & Sons INC.

GEO. (2008). *GEO, Geothermal Education Ofice*. Recuperado el September de 2009, de http://geothermal.marin.org/GEOpresentation/sld012.htm

Handal, S., Alvarenga, Y., & Recinos, M. (2008). *Solar Steam Booster in the Ahuachapán Geothermal Field.* El Salvador.

Hansen, J., Sato, M., Ruedy, R., Lo, K., Lea, D. W., & Medina-Elizade, M. (2006). *Global temperature change.* New York: Goddard Instutute for Space Studies, NASA.

Hesselgreaves, J. (2001). *COMPACT HEAT EXCHANGERS, SELECTION, DESIGN AND OPERATION.* London: Pergamon.

IEA, I. E. (2009). *Key World Energy Statistics 2009.* Paris: IEA.

IGA. (2009). *International Geothermal Association*. Recuperado el September de 2009, de http://www.geothermal-energy.org/226, installed_generating_capacity.html

IPCC. (2009). *IPCC.* Recuperado el 15 de Octubre de 2009, de Climate Change 2007: Synthesis Report: http://www.ipcc.ch/pdf/assessment-report/ar4/syr/ar4_syr.pdf

Lazard. (2008). *LEVELIZED COST OF ENERGY ANALYSIS Version 2.0.* Washington: NREL.

Lentz, & Almaza. (2003). *Parabolic troughs to increase the geothermal wells flow enthalpy.* Mexico.

Ley Corta I. (2004). *Ley numero19.940, ley corta I Regula sistemas de transporte de energía y regimen de tarifas.* Santiago: Congreso Nacional.

Ley Corta II. (2005). *Ley numero 20.018, ley corta II Modifica el Marco Normativo del Sector Electrico.* Santiago: Congreso Nacional.

Leyzerovich, A. (2005). *Wet-Steam Turbines for Nuclear Power Plants.* New York: PennWell.

Lira, I. (1992). *TERMOTECNIA, TEORIA Y METODOS EN TERMODINAMICA APLICADA.* Santiago: Ediciones PUC.

Lovekin, J. (2000). *GEOTHERMAL THE ECONOMICS OF SUSTAINABLE DEVELOPMENT.* Japan: Proceedings World Geothermal Congress.

McGee, M. (2010). *CO2 Now*. Recuperado el march de 2010, de http://co2now.org/

METEONORM. (2009). *Global Meteorological Database for Engineers, Planners and Education*. Recuperado el 2009, de http://www.meteonorm.com/pages/en/meteonorm.php

NREL. (2003). *Assessment of Parabolic Trough and Power Tower Solar Technology Cost and Performance Forecasts.* Washington DC.

NREL. (2009). *National Renewable Energy Laboratory*. Recuperado el 2009, de TroughNet, Parabolic Trough Solar Field Technology: http://www.nrel.gov/csp/troughnet/solar_field.html

Oreskes, N. (2004). *BEYOND THE IVORY TOWER: The Scientific Consensus on Climate Change.* Science Magazine.

Price, H., Lüpfert, E., Kearney, D., Zarza, E., Cohen, G., & Gee, R. (2002). *Advances in Parabolic Trough Solar Power Technology.* Journal of Solar Energy.

Sanyal, S. K., Butler, S. J., Brown, P. J., Goyal, K., & Box, T. (2000). *AN INVESTIGATION OF PRODUCTIVITY AND PRESSURE DECLINE TRENDS IN GEOTHERMAL STEAM RESERVOIRS.* Japan: Proceedings World Geothermal Congress.

Schott Solar. (2005). *Schott Solar*. Recuperado el 2009, de [http://www.schottsolar.com/us/products/concentrated-solar-power/schott-ptr-70-receiver.html]

SERNAGEOMIN, S. N. (2010). *Catastro de Concesiones de Energía Geotérmica actualizado a julio de 2010.* Santiago.

Smithsonian, N. M. (1994). *Global Volcanism Program*. Recuperado el March de 2010

Solar Energy Green Lifestyle for you. (2009). Recuperado el 2009, de http://www.solarenergygreenlifestyleforyou.com/2009/08/solarpros-yankovo-pv-power-plant-put.html

SolarShop. (2005). *Solar Shop*. Recuperado el 2009, de http://solarshop.org.uk/solar-powered-electric.htm

Stine, W., & Harrigan, R. (1985). *Solar Energy Systems Design.* John Wiley & Sons INC.

Therminol. (2009). *Therminol*. Recuperado el 2009, de www.therminol.com

UNEP. (2005). *Climate Neutral Network, United Nations Evironmental Programs*. Recuperado el 2009, de http://unep.org/climateneutral/Participants/Companies/CO2focus/tabid/237/Default.aspx

UNFCCC, U. N. (2008). *UNFCC*. Recuperado el March de 2010, de http://unfccc.int/kyoto_protocol/items/2830.php

United States National Academy of Sciences. (2008). *Undertanding and Responding to Climate Change.*

USGS. (2010). *USGS, United States Geological Survey*. Recuperado el 2010, de http://earthquake.usgs.gov/

Vaca, J. (2008). *Modelo de costeo de pozos geotérmicos aplicado para el caso del campo geotérmico de Cerro Prieto.* Ciudad de México: Geotermia, Revista Mexicana de Geoenergía vol. 21.

WHITE, B. (2006). *AN UPDATE ON GEOTHERMAL ENERGY IN NEW ZEALAND.* New Zealand: Geothermal Association.

World of renewables. (2010). Recuperado el 2010, de PV power stations: http://www.worldofrenewables.com/page.php?pageid=78

10 APPENDIX A: DIFFERENT WAYS TO ATTACH A SOLAR FIELD TO A GEOTHERMAL POWER PLANT

For this analysis we will consider the same productive well used for the main analysis and we will use three different productive points, as showed in figure 11.1, the objective is to test different ways to attach a solar field to a geothermal power plant in different mass flow rate conditions. We will use three different attachment alternatives for each productive condition. On each alternative we will add as much energy as possible, reaching 400 °C whenever possible.

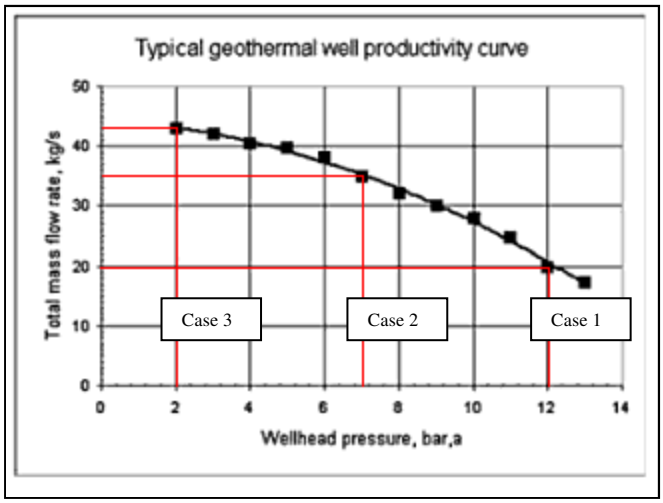

Mass flow rate $44.333 - 0.3363 \cdot P - 0.1357 \cdot P^2$ Kg/s

Figure 10.1Typical geothermal well productivity curve.

Case	Presión [MPa]	Flujo Másico [kg/s]
Case 1	1.2	20
Case 2	0.7	35
Case 3	0.2	42

Table 10.1 Case Values

10.1 Base Case

The base case consists on single flash power plant working under the operational conditions proposed in the different cases.

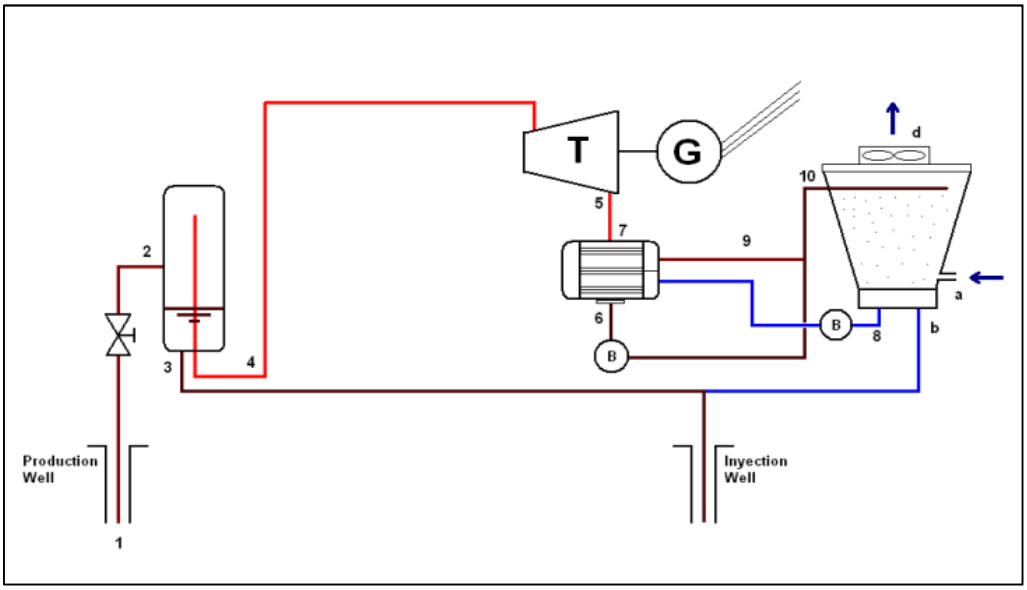

Figure 10.2 Appendix A, Base case diagram

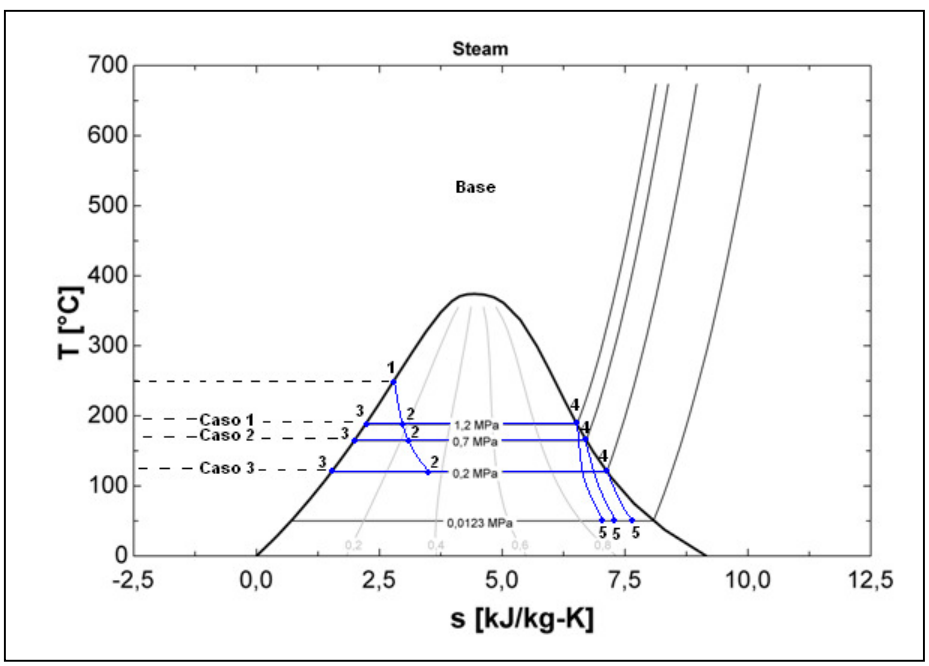

Figure 10.3 Appendix A, base case T-s Diagram

10.2 Alternative A

This alternative consists in using the solar field to evaporate all the fluids coming from the productive well, increasing the amount of steam in the turbine.

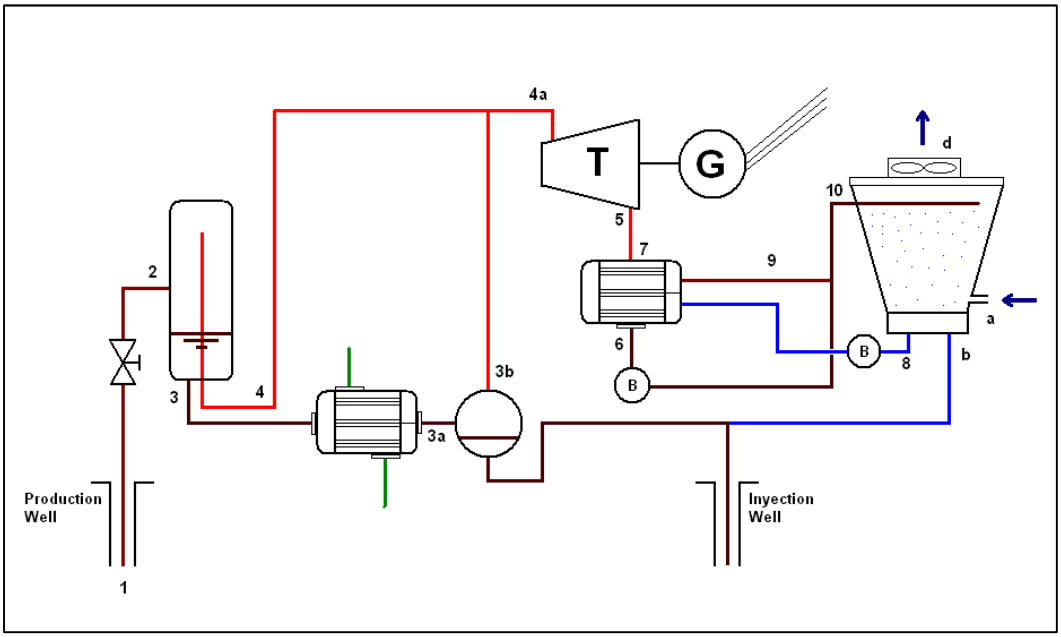

Figure 10.4 Appendix A, Alternative A Diagram

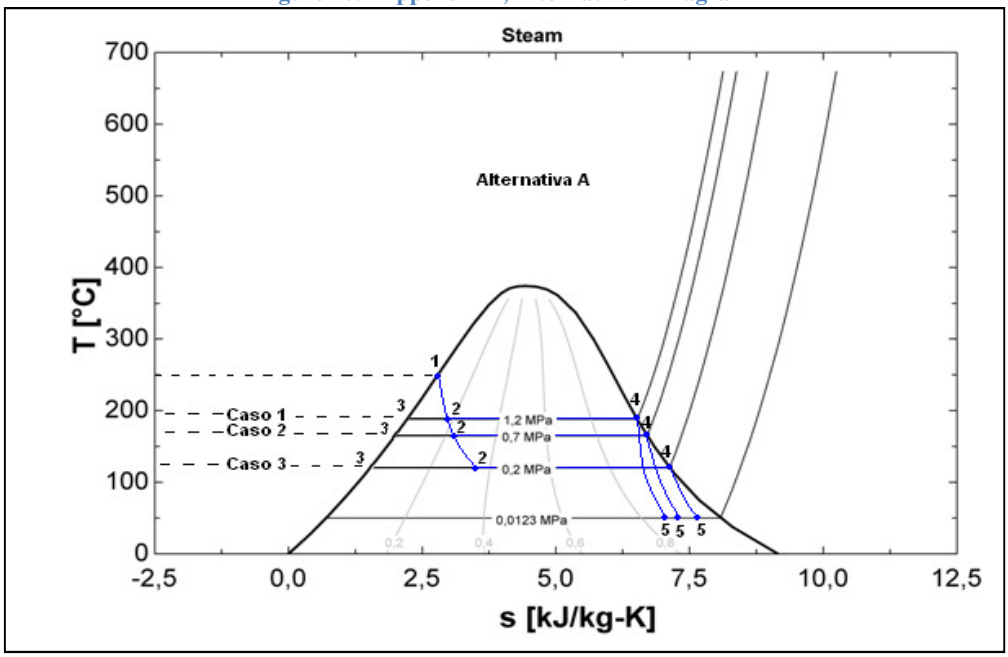

Figure 10.5 Appendix A, Alternative A T-s Diagram

10.3 Alternative B

In this alternative we use solar energy to overheat the steam naturally flowing from the productive well.

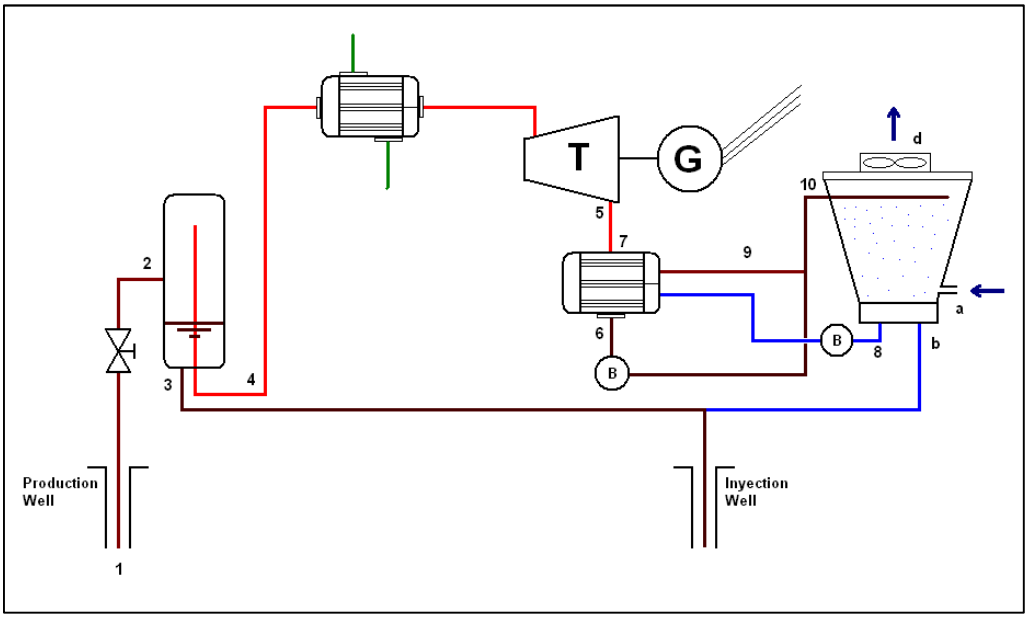

Figure 10.6 Appendix A, Alternative B Diagram

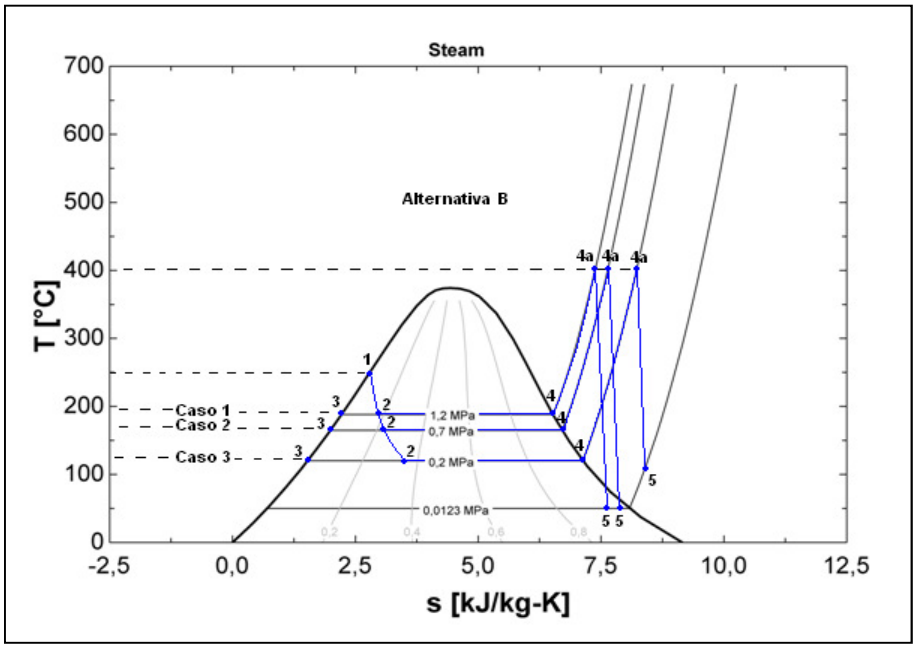

Figure 10.7 Appendix A, Alternative B T-s Diagram

10.4 Alternative C

This alternative overheats the main steam flow and then reheats it up to 400 °C.

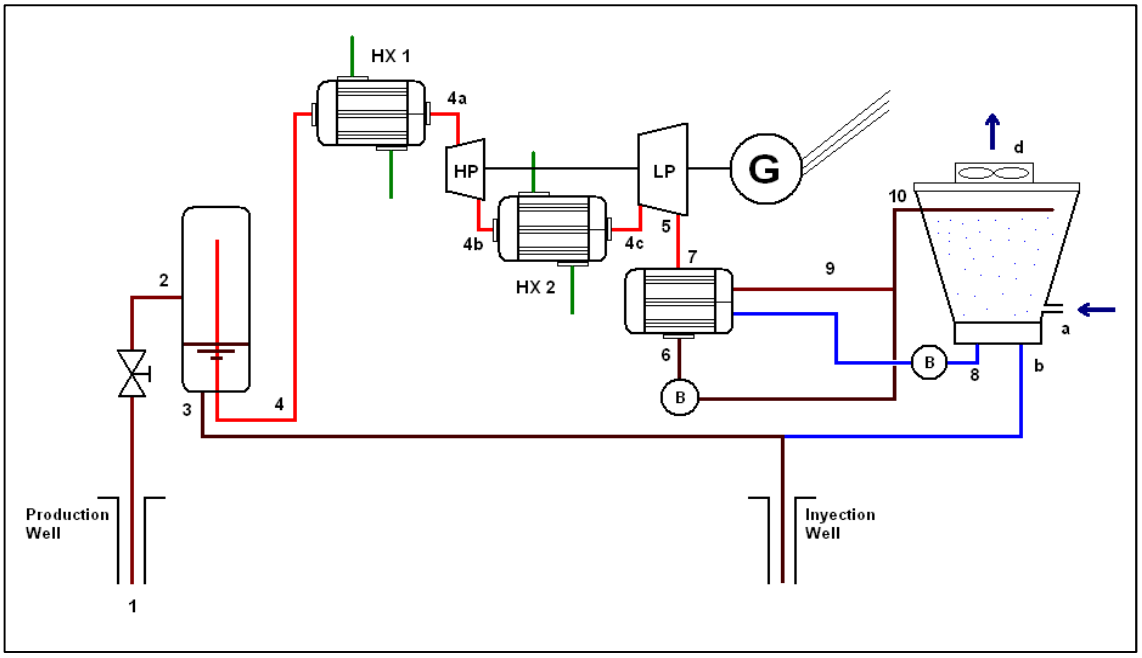

Figure 10.8 Appendix A, Alternative C diagram

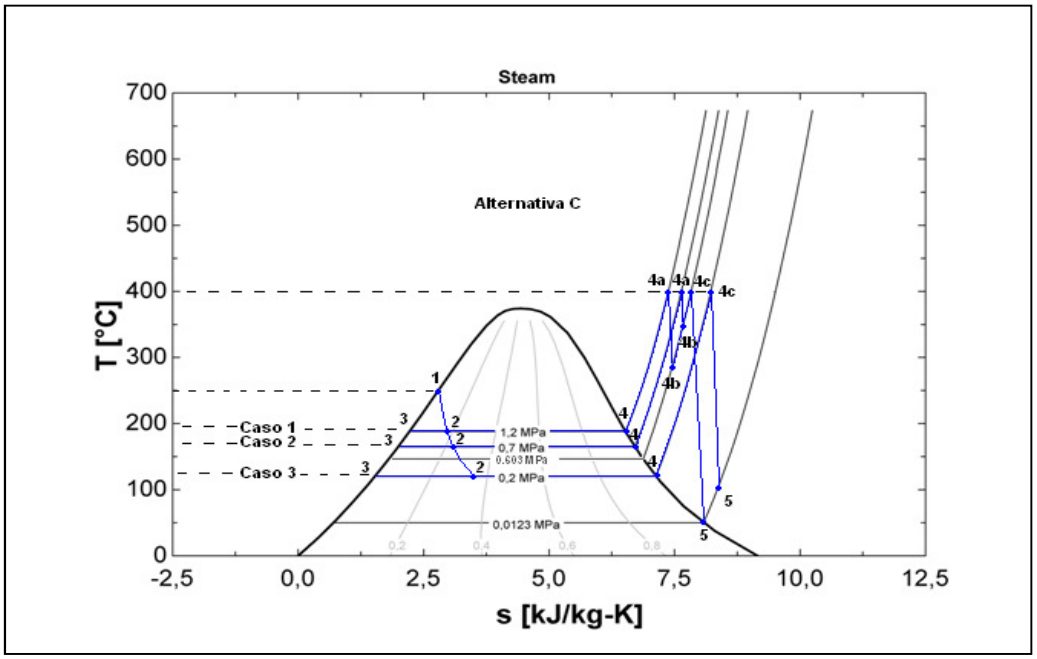

Figure 10.9 Appendix A, Alternative C T-s Diagram

10.5 Results

We will analyze de efficiency, both for the power plant and for solar energy. To do so we will use the energy efficiency defined by the first law of thermodynamics.

$$\eta_{planta} = \frac{\Delta h_t}{\Delta h_{fg} + \Delta h_t}$$

Where

Δh_t Is the enthalpy difference between the turbine inlet and outlet.. [kJ/kg]

Δh_{fg} Is the enthalpy difference between the turbine outlet and saturated liquid at the turbine's outlet pressure. [kJ/kg]

$$\eta_{solar} = \frac{\dot{m}_{steam} \cdot \Delta h_t - \dot{m}_{steam} \cdot \Delta h_{t,geo.}}{\dot{Q}_{solar}}$$

Where

$\dot{Q}_{solar}$ Is the total solar power delivered. [kW]

$\dot{m}_{steam}$ Is the total steam mass flow rate entering the turbine. [kg/s]

Δh_t Is the enthalpy difference between the turbine inlet and outlet.. [kJ/kg]

$\Delta h_{t,geo}$ Is the enthalpy difference between the turbine's outlet and saturated liquid at the turbine's outlet pressure assuming that no solar power was delivered i.e. using the same thermodynamic states as the base case. [kJ/kg]

Δh_{fg} Is the enthalpy difference between the turbine outlet and saturated liquid at the turbine's outlet pressure for each alternative. [kJ/kg]

	Case 1		Case 2		Case 3	
	η_{planta}	η_{solar}	η_{planta}	η_{solar}	η_{planta}	η_{solar}
Base	13.68%	--	19.09%	--	21.24%	--
Alternative A	13.68%	15.52%	19.09%	23.6%	21.24%	27.55%
Alternative B	17.64%	34.97%	22.83%	41.74%	25.06%	45.73%
Alternative C	17.64%	34.97%	24.09%	43.67%	26.95%	46.60%

Table 10.2 Appendix A, Summarized results for the efficiency analysis

10.6 Analysis

As is expected, the best results occur when the cycle temperature is kept as high as possible for the longest, obtaining for the alternative C consistently better results. According to this, the smartest way to use solar energy into a geothermal power cycle is to rice the cycle temperature to increase the efficiency of the cycle and to avoid a wet expansion whenever possible. This way, not only we use more efficiently the solar energy but we also get more energy from the geothermal resources.

11 APPENDIX B: HEAT EXCHANGER SIZING

Heat exchangers play a key role in the development of this thesis because they are the link between the concentrator solar field of and the geothermal cycle allowing the transfer of energy between them.

All models developed to simulate the performance of the hybrid power plants were done using ideal heat exchangers, without worrying about the actual size they can reach.

In this appendix we calculate the size the heat exchangers should have to ensure that the project is feasible to be built.

It should first be noted that, depending on the scenario chosen, the operating conditions of the heat exchanger vary considerably. In order to represent the worst case scenario, the temperature and mass flow rate will be chosen to obtain the maximum size of the heat exchanger.

As input data to size the heat exchangers it will be used a saturated steam flow rate of 10 kg/s, at a temperature of 110 °C and it will be heated to a temperature of 390 °C, on the side of the oil from the collector field is considered the maximum temperature that can reach the oil is 400 °C as the inlet temperature and a mass flow rate equal to 10 kg /s which are typical design values of our solar field collectors.

To size the heat exchanger, the logarithmic mean temperature difference (LMTD) method is used, which relates the input and output temperatures of both fluids with the overall heat transfer coefficient to obtain the total heat transfer area.

It is first necessary to make an energy balance to determine the temperature of the oil outlet, assuming that no heat is loss to the environment.

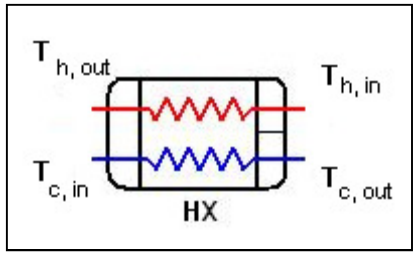

Figure 11.1 Heat Exchanger Diagram

$$\dot{m}_{oil} \cdot C_p \cdot \Delta T = \dot{m}_{steam} \cdot \Delta h$$

$$10\frac{kg}{s} \cdot 2.12\frac{KJ}{Kg°C} \cdot \left(400°C - T_{h,out}\right) = 10\frac{kg}{s} \cdot (3259 - 2724)\frac{kJ}{kg}$$

$$T_{h,out} = 147{,}6\ °C$$

Then following the LMTD procedure for counter flow (Lira, 1992), we obtain the logarithmic mean temperature difference, defined as:

$$\Delta T_{LM} = \frac{\Delta T_{in} - \Delta T_{out}}{ln\left(\frac{\Delta T_{in}}{\Delta T_{out}}\right)}$$

$$\Delta T_{LM} = 20.8\ °C$$

Now, to calculate the total heat transfer area, we use the following relation:

$$\dot{Q}_{HX} = U \cdot A_T \cdot \Delta T_{LM}$$

Where $\dot{Q}_{HX}$ represents the heat exchanger power, U represents the overall heat transfer coefficient and A_T represents the total heat transfer area.

To calculate the total heat transfer area is fist required to find the overall heat transfer coefficient, which depends on the characteristics of both fluids, and on the physical characteristics of the heat exchanger.

Without knowing the physical characteristics of the heat exchanger, we can only assume an overall heat transfer coefficient applications based recommendations for heat transfer between oil and gas. In our calculations we use a reference value of 60 W/m^2 K, (Lira, 1992).

Then, we finally obtain the total heat transfer area:

$$\dot{Q}_{HX} = \dot{m}_{oil} \cdot C_p \cdot \Delta T = \dot{m}_{steam} \cdot \Delta h = 5.350\ kW$$

$$A_T = 4.287\ m^2$$

To estimate the volume of the heat exchanger, it is required to know the density of transfer area per volume unit, which can reach more than 1600 m^2/m^3 (Hesselgreaves, 2001). In this calculation we will use:

$$\alpha = 400 \frac{m^2}{m^3}$$

Obtaining a total volume for the heat exchanger of:

$$Vol_{HX} = \frac{A_T}{\alpha} = 10{,}7\ m^3$$

Done this, it should be noted that these results give us only an idea of the magnitude of the heat exchangers and a detailed study must be conducted once the heat exchangers are determinate. Given the conservative values used in this analysis, it is likely that the actual size of the heat exchangers needed is smaller than the values obtained preliminarily.